The Astrophysical Journal Supplement Series, 281:20 (37pp), 2025 November https://doi.org/10.3847/1538-4365/adfc69

Search for the Optical Counterpart of Einstein Probe–discovered Fast X-Ray Transients from the Lulin Observatory

Amar Aryan[1], Ting-Wan Chen[1], Sheng Yang[2], James H. Gillanders[3], Albert K. H. Kong[4], S. J. Smartt[3,5], Heloise F. Stevance[3,5], Yi-Jung Yang[1], Aysha Aamer[5], Rahul Gupta[6,8], Lele Fan[2], Wei-Jie Hou[1], Hsiang-Yao Hsiao[1], Amit Kumar[7], Cheng-Han Lai[1], Meng-Han Lee[1], Yu-Hsing Lee[1], Hung-Chin Lin[1], Chi-Sheng Lin[1], Chow-Choong Ngeow[1], Matt Nicholl[5], Yen-Chen Pan[1], Shashi Bhushan Pandey[7], Aiswarya Sankar.K[1], Shubham Srivastav[3], Guanghui Sun[2], and Ze-Ning Wang[2]

[1] Graduate Institute of Astronomy, National Central University, 300 Jhongda Road, 32001 Jhongli, Taiwan; amar@astro.ncu.edu.tw, twchen@astro.ncu.edu.tw
[2] Henan Academy of Sciences, Zhengzhou 450046, Henan, People's Republic of China; sheng.yang@hnas.ac.cn
[3] Astrophysics Sub-department, Department of Physics, University of Oxford, Keble Road, Oxford, OX1 3RH, UK
[4] Institute of Astronomy, National Tsing Hua University, Hsinchu 300044, Taiwan
[5] Astrophysics Research Centre, School of Mathematics and Physics, Queen's University Belfast, Belfast BT7 1NN, UK
[6] Astrophysics Science Division, NASA Goddard Space Flight Center, Mail Code 661, Greenbelt, MD 20771, USA
[7] Aryabhatta Research Institute of Observational Sciences (ARIES), Manora Peak, Nainital, Uttarakhand, 263001, India
Received 2025 April 28; revised 2025 July 24; accepted 2025 August 14; published 2025 November 4

Abstract

The launch of the Einstein probe (EP) mission has revolutionized the detection and follow-up observations of fast X-ray transients (FXTs) by providing prompt and timely access to their precise localizations. In the first year of its operation, the EP mission reported the discovery of 72 high signal-to-noise FXTs. Subjected to the visibility in the sky and weather conditions, we search for the optical counterparts of 42 EP-discovered FXTs from the Lulin Observatory. We successfully detected the optical counterparts of 12 FXTs, and five of those were first discovered by us from the Lulin Observatory. We find that the optical counterparts are generally faint ($r > 20$ mag) and decline rapidly (>0.5 mag day^{-1}). We also find that 12 out of 42 FXTs show direct evidence of their association with gamma-ray bursts (GRBs) through significant temporal and spatial overlapping. Furthermore, the luminosities and redshifts of FXTs with confirmed optical counterparts in our observations are fully consistent with the faintest end of the GRB population. However, the nondetection of any associated optical counterpart with a significant fraction of FXTs suggests that EP FXTs are likely a subset of the so-called "dark FXTs," similar to "dark GRBs." Additionally, the luminosities of two FXTs with confirmed redshifts are also consistent with jetted tidal disruption events (TDEs). However, we find that the optical luminosities of FXTs differ significantly from typical supernova shock breakout or kilonova emissions. Thus, we conclude that a significant fraction of EP-discovered FXTs are associated with events having relativistic jets; either a GRB or a jetted TDE.

Unified Astronomy Thesaurus concepts: Transient sources (1851); High energy astrophysics (739); X-ray transient sources (1852); Optical identification (1167); Gamma-ray bursts (629)

1. Introduction

Fast X-ray transients (FXTs) are extragalactic bursts of soft X-rays (0.3–10 keV) lasting up to $\sim 10^1$–10^4 s (P. G. Jonker et al. 2013; A. Polzin et al. 2023; J. H. Gillanders et al. 2024; A. J. Levan et al. 2024a). The origin and nature of these FXTs, lasting from minutes to hours, still remain an intriguing mystery. However, numerous models have been proposed to unravel and quantify these enigmatic events. The supernova (SN) shock breakouts (SBO; A. M. Soderberg et al. 2008; G. Novara et al. 2020; D. Eappachen et al. 2024), binary neutron star mergers (Y. Q. Xue et al. 2019; S. Ai & B. Zhang 2021; D. Lin et al. 2022; D. Eappachen et al. 2024), tidal disruption events (TDEs) of white dwarfs on intermediate-mass black holes (P. G. Jonker et al. 2013; A. Glennie et al. 2015; J. A. Irwin et al. 2016; Z.-K. Peng et al. 2019; J. H. Gillanders et al. 2024), and low-luminosity long gamma-ray bursts (GRBs) or short GRBs (P. G. Jonker et al. 2013; A. Glennie et al. 2015; F. E. Bauer et al. 2017; J. H. Gillanders et al. 2024; A. J. Levan et al. 2024a; Y. Liu et al. 2024) are among the most favorable scenarios for producing FXTs. These are among the newest classes of transient objects first identified only about a decade ago in Chandra images of M86 (P. G. Jonker et al. 2013). Since then, intensive archival searches have resulted in the discovery of around 40 FXTs in Chandra, XMM-Newton images, and eROSITA (e.g., A. Glennie et al. 2015; F. E. Bauer et al. 2017; D. Alp & J. Larsson 2020; J. Quirola-Vásquez et al. 2022, 2023).

However, with the launch of the Einstein Probe (EP) mission (W. Yuan et al. 2018; W. Yuan et al. 2022) on 2024 January 9, the number of FXTs is significantly increasing. The EP mission is an innovative mission dedicated to scanning the sky in the soft X-ray band with high precision. The EP-Wide-field X-ray Telescope (EP-WXT) on board EP with a large field of view (FoV; $60^\circ \times 60^\circ$) systematically surveys and characterizes high-energy transients, while also monitoring variable objects with unprecedented sensitivity and frequency. Additionally, the EP mission also features a conventional narrow-field ($1^\circ \times 1^\circ$) EP-Follow-up X-ray Telescope (W. Yuan et al. 2022) for follow-up observations and precise

[8] NASA Postdoctoral Program Fellow.

localization of newly discovered transients. During the commissioning phase (until 2024 July 9), the EP mission has already provided several useful communications regarding the discovery of new FXTs on various platforms such as NASA's General Coordinates Network (GCN) Circulars,[9] GCN Notices,[10] and the Astronomer's Telegram (ATel).[11] The commissioning phase was completed on 2024 July 10. Now it is promptly providing publicly available alerts for transient objects, ensuring timely access to new discoveries.

In about 1 yr of its operation (2024 January 9 to 2025 January 9), the EP mission has reported the discovery of 72 high signal-to-noise ratio (SNR) FXTs. Figure 1 (top panel) shows the sky localization of those 72 FXTs. Similar to the GRBs, the occurrences of EP-discovered FXTs seem isotropic in nature, although the sample size currently is not very large. Currently, the EP-WXT provides the localization with an error circle of radius $\lesssim 3'$ for most of the detected FXTs. The localization improves significantly with the EP-Follow-up X-ray Telescope, which provides more precise localization with error circles having radii between $10''$ and $30''$ only. Such precise localization is ideal for enabling many narrow-field, large-aperture, follow-up telescopes to search for the multi-wavelength counterpart of any new FXT detection by the EP mission. Figure 1 (bottom panel) shows the distribution of angular offsets between the EP-WXT locations and the associated optical counterpart candidates. All identified counterparts fall within the EP-WXT error circles, indicating good positional consistency. Throughout this paper, we use the term FXTs specifically to refer to events detected by EP.

The groundbreaking first detection of multiwavelength counterparts (X-ray, optical, and radio) of EP 240315a has unlocked exciting new pathways for exploring the intriguing origins and nature of FXTs. Following J. H. Gillanders et al. (2024), A. J. Levan et al. (2024a), and Y. Liu et al. (2025), the role of the optical counterpart in deciphering the origin and nature of FXTs has proved essential. Additionally, early optical follow-up (within several hours post-discovery) helps us to probe the early evolution of the underlying FXT in its rest frame. The role of such follow-up is further amplified for high-redshift discoveries, where the observed frame optical evolution over a few days probes nearly the initial 24 hr of the FXT's rest-frame evolution. Similar to high-redshift GRBs, with detection up to $z \gtrsim 5$, FXTs demonstrate great potential for probing the early Universe (e.g., EP 240315a; $z = 4.859$). Based on the multiwavelength observations, several studies (J. H. Gillanders et al. 2024; A. J. Levan et al. 2024a; Y. Liu et al. 2025) infer EP 240315a to originate from a relativistic event with two possible scenarios: a long GRB or a jetted TDE, although the measured optical and radio luminosity in their analysis lies consistently with long GRBs. Recently, R. Ricci et al. (2025) presented the long-term radio monitoring of EP 240315a and reported evidence of a relativistic jet.

About a month after EP 240315a, the EP mission reported the discovery of FXT EP 240414a (T. Y. Lian et al. 2024b). Later, EP 240414a was also discovered with multiwavelength counterparts (J. S. Bright et al. 2024; H. Sun et al. 2025; J. N. D. van Dalen et al. 2025; S. Srivastav et al. 2025). Owing to the extremely blue spectrum in the early phase, J. N. D. van Dalen et al. (2025) linked the EP 240414a to luminous fast blue optical transients (LFBOTs). However, due to the nonthermal origin of the early phase followed by the decaying phase nicely explained by a power law, S. Srivastav et al. (2025) find evidence linking EP 240414a to GRBs. The prompt and afterglow phase investigations by H. Hamidani et al. (2025a) place EP 240414a between long GRBs and low-luminosity GRBs. Further, the late-time photometric and spectral evolutions of EP 240414a match Type Ic broad-lined (BL) supernovae (SNe) as presented in H. Sun et al. (2025) and also in J. N. D. van Dalen et al. (2025). Type Ic BL SNe are occasionally found to be associated with several long GRBs (M. Modjaz et al. 2016). Another study by J.-H. Zheng et al. (2025) proposes that EP 240414a could be the result of an off-axis view of a jet-cocoon system from an expanded helium progenitor star. Recently, elaborate analyses of EP 241021a displaying exceptional rebrightening also suggest a likely link between EP mission discovered FXTs and low-luminosity GRBs (M. Busmann et al. 2025). Detailed X-ray, optical, and radio analyses by S. Xinwen et al. (2025) indicate the launch of a relativistic jet for the case of EP 241021a, and later, M. Yadav et al. (2025) confirmed this relativistic jet launch scenario through radio observations. Similar to EP 240414a, G. Gianfagna et al. (2025) propose an off-axis jet and cocoon scenario for EP 241021a. Another detailed X-ray, optical, and radio analyses of EP 241021a by G.-L. Wu et al. (2025) suggest that it is an explosion-type event accompanied by a moderately relativistic jet. In early 2025 January, the EP mission reported the discovery of an interesting FXT EP 250108a (R. Z. Li et al. 2025a). Several studies report the Type Ic BL SN 2025kg to be associated with EP 250108a as its optical counterpart (R. A. J. Eyles-Ferris et al. 2025a; J. C. Rastinejad et al. 2025; G. P. Srinivasaragavan et al. 2025). Rigorous modeling of well-sampled multiwavelength light curves suggests a mildly relativistic outflow as the origin of this event (W. X. Li et al. 2025). The detailed analysis by R. A. J. Eyles-Ferris et al. (2025a) indicates that the observed X-ray and radio properties are consistent with a collapsar-powered low-energy jet that fails to break out of the dense material surrounding it. Additionally, they further suggest that the optical emissions possibly originate from a shocked cocoon resulting from the trapped jet. Further, a related work by J. C. Rastinejad et al. (2025) indicates similar results with the broadband data being consistent with a trapped or low-energy jet-driven explosion from a collapsar with a zero-age main-sequence (ZAMS) mass of 15–30 $M_{\odot}$. Finally, detailed analyses by G. P. Srinivasaragavan et al. (2025) strengthen the link of EP 250108a to low-luminosity GRBs.

Due to the limited number of available FXT detections, their collective origin and nature are poorly constrained. Moreover, the localization by EP-WXT allowed the rapid detection of optical and radio counterparts for EP 240315a, opening up new avenues to investigate these rather new transient events. Specifically, the early detection of the optical counterpart enables us to probe the early evolution of FXTs and put constraints on the origin of these enigmatic events.

In this paper, we report the results of our extensive search for the optical counterparts of the EP mission discovered FXTs in its first year of operation, utilizing Lulin Observatory[12] telescopes. In Section 2, we present the design and implementation of our follow-up observation campaign at the Lulin

[9] https://gcn.nasa.gov/circulars
[10] https://gcn.nasa.gov/docs/schema/v4.1.0/gcn/notices/einstein_probe
[11] https://astronomerstelegram.org
[12] https://www.lulin.ncu.edu.tw

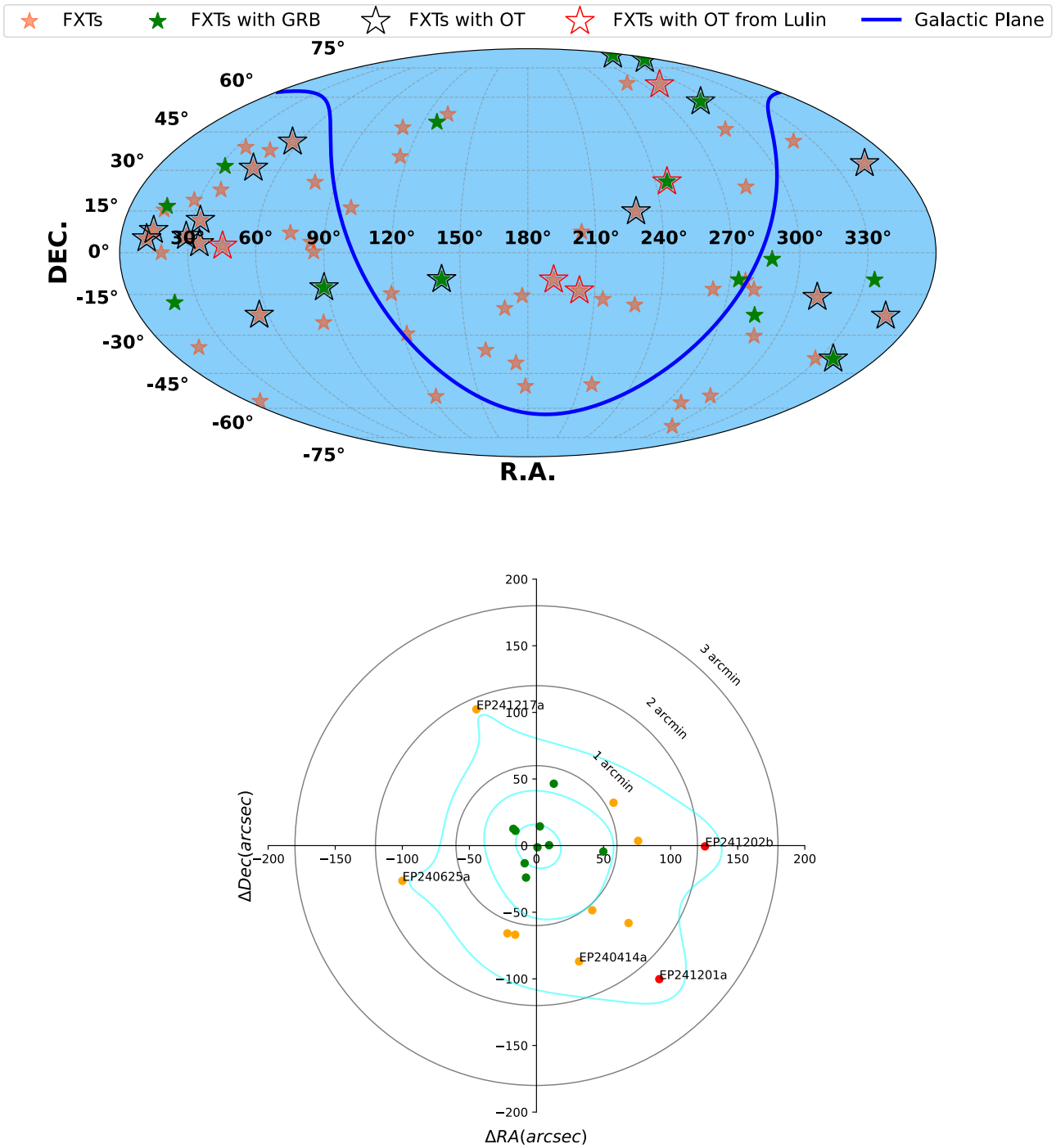

Figure 1. Top: the sky localizations of 72 high-SNR FXTs discovered by the EP mission in the first year of its operation. Within the context of the limited number of FXTs detected, the occurrences of FXTs seem to be isotropic in nature, similar to GRBs. The FXTs with associated GRBs, FXTs with corresponding OTs, and FXTs with respective OTs discovered from the Lulin Observatory are highlighted. Bottom: angular offset distribution between the EP-WXT candidates and their associated optical counterparts, plotted as ΔR.A. vs. Δdecl. in arcseconds. A point located at the center indicates perfect positional agreement between the EP-WXT detection and the corresponding OT. Black concentric circles mark angular separation radii of 1′, 2′, and 3′, corresponding to the typical positional uncertainty of the EP-WXT (∼3′). Each point represents a candidate, color coded by event group, with several labeled for clarity. Cyan contours denote the 1σ, 2σ, and 3σ levels of the event population density, illustrating the statistical spread in positional accuracy. This visualization highlights both the average localization precision of EP-WXT and the reliability of optical counterpart identification. The localization of the optical counterparts is adapted from GCN circulars.

Observatory. In Section 3, we present our observational results from the Lulin Observatory and emphasize the important role that meter- and submeter-class telescopes can play in the follow-up of sources discovered by the EP mission. Furthermore, in Section 4, we discuss the constraints of possible aspects on the nature and possible origin of FXTs following from our observations. Finally, in Section 5, we summarize our findings and provide concluding remarks based on the current study. Throughout the paper, we assume a ΛCDM cosmology in line with Planck Collaboration et al. (2016) with a Hubble

Table 1
Details of the FXTs with Their Optical Counterpart Observed from the Lulin Observatory

Name	WXT R.A. OT R.A.[a]	WXT Decl. OT Decl.	WXT Error Redshift	Ref.	FXT R.A.	Optical Counterpart Discoverer References	FXT Decl. OT Name	FXT Error	$\text{Time}_{\text{FXT-WXT}}$ $\text{Time}_{\text{OT-WXT}}$
EP 240315a	141.644	−9.547	3′	…	141.6483	…	−9.5335	10″	42 hr
(GRB 240315C)	141.64764	−9.53409	4.859	(1)	…	(10, 11)	AT 2024eju	…	1.1 hr
LXT 240402A	…	…	…	…	245.451	…	25.763	10″	…
(GRB 240402B)	245.45103	+25.76315	1.551	(2)	…	(12, 13,[b] 14)	…	…	1.28 days
EP 240414a	191.498	-9.695	3′	…	191.509	…	−9.718	10″	2 hr
	191.50695	−9.71913	0.41	(3)	…	(15)	AT 2024gsa	…	3.13 hr
EP 240416a	203.15	−13.612	3′	…	…	(14, 16)	…	…	…
	203.14381	−13.63029	…	…	…	(14, 17[c])	…	…	14.15 hr
EP 240801a	345.14	32.61	2.4′	…	345.163	…	32.5927	10″	180 sec
	345.16263	32.59386	1.673	(4)	…	(18)			2.24 hr
EP 241021a	28.852	5.957	2.4′	…	28.8483	…	5.9395	10″	36.5 hr
	28.84757	+5.93842	0.75	(5)	…	(19)	…	…	1.77 days
EP 241030a	343.013	80.449	2.4′	…	343.1426	…	80.4498	10″	21 hr
(GRB 241030A)	343.13988	+80.44997	1.411	(6)	…	(20)	…	…	−0.73 hr[a]
EP 241107a	…	…	…	…	35.0085	…	3.3329	10″	5 min
	35.01021	+3.33394	0.456	(7)	…	(21)	…	…	1.5 hr
EP 241201a	282.596	66.081	2.343′	…	282.4865	…	66.0693	10″	12 hr
	282.65866	+66.05316	…	…	…	(14, 22[c])	…	…	13.4 hr
EP 241202b	45.302	2.441	2.6′	…	…	…	…	…	…
	45.33693	+2.44084	…	…	…	(14, 23[c])	…	…	19.45 hr
EP 241217a	46.957	30.901	2.8′	…	46.9398	…	30.9299	20″	7.64 hr
	46.9425	+30.92942	4.59	(8)	…	(24)	…	…	2.5 hr
EP 250108a	55.623	-22.509	2.2′	…	Limit	…	Limit	Limit	22.2 hr
	55.61829	−22.50591	0.176	(9)	…	(25, 26)	SN 2025kg	…	31.5 hr

Notes.
[a] The coordinates (R.A. and decl.) of the OT are adopted from the relevant discovery of GCNs; while for EP 240315a, EP 240414a, EP 241021a, and EP 250108a, we adopted the Pan-STARRS updated coordinates.
[b] The OT was detected by Swift/UVOT shortly after the GRB trigger, and thus prior to the EP-WXT trigger time.
[c] Discovered by Lulin Observatory.
References. (1) A. Saccardi et al. (2024); (2) N. R. Tanvir et al. (2024); (3) P. G. Jonker et al. (2024); (4) J. A. Quirola-Vasquez et al. (2024f); (5) G. Pugliese et al. (2024); (6) W. Zheng et al. (); (7) J. Quirola-Vasquez et al. (2024a); (8) A. J. Levan et al. (2024c); (9) Z. P. Zhu et al. (2025a); (10) S. Srivastav et al. (2024b); (11) J. H. Gillanders et al. (2024); (12) A. J. Levan et al. (2024b); (13) S. Yang et al. (2024b), (14) this work; (15) A. Aryan et al. (2024g); (16) S. Srivastav et al. (2025); (17) T. W. Chen et al. (2024a); (18) S. Y. Fu et al. (2024c); (19) S. Y. Fu et al. (2024h); (20) N. J. Klingler et al. (2024); (21) M. Odeh et al. (2024a); (22) M. H. Lee et al. (2024b); (23) C. C. Ngeow et al. (2024); (24) A. J. Levan et al. (2024d); (25) R. Eyles-Ferris (2025); (26) R. A. J. Eyles-Ferris et al. (2025a).

constant of $H_0 = 67.7\ \text{km s}^{-1}\ \text{Mpc}^{-1}$, $\Omega_M = 0.309$, and $\Omega_\Lambda = 0.691$. All magnitudes are reported in the AB system, and time is in Coordinated Universal Time (UTC).

2. Lulin Observatory Search for the EP Mission–discovered FXTs

In about the first year of its operation (up to 2025 January 9), the EP mission reported the discovery of 72 high-SNR FXTs. Subject to their visibility from the Lulin Observatory and weather conditions, we triggered our telescopes to search for the optical counterparts of 42 out of 72 high-SNR FXTs reported by the EP mission. Tables 1 and 2 list the coordinates and error circle radii for the EP-WXT and the EP-Follow-up X-ray Telescope for 42 FXTs, observed from the Lulin Observatory.

The optical follow-up program of FXTs from the Lulin Observatory is a part of the Kilonova Finder (Kinder; T.-W. Chen et al. 2025) project. It primarily focuses on searching for kilonovae without relying on gravitational-wave triggers. Leveraging the advantageous geographic location of the Lulin Observatory, Taiwan (23°28′10.″0 N , 120°52′21.″5 E) and scheduling flexibility on the small telescopes, we are able to significantly contribute to capturing short-lived events and quickly respond to unique astronomical events. For example, Kinder observed the early light curve and color evolution of the nearby Type II SN 2024ggi, right when ATLAS first detected its explosion (T.-W. Chen et al. 2025).

We use both the 40 cm SLT and the Lulin One-meter Telescope (LOT) for imaging follow-ups. The SLT is an RC Optical Systems carbon 16 inch $f/8.4$ telescope with an Ascension 200HR mount. It is equipped with a CCD camera Andor 934 with a BEX2-DD chip (blue sensitive) with a gain of 1.088 electrons ADU^{-1}, a readout noise of 8.831 electrons rms, and a pixel scale of $0.″76\,\text{pixel}^{-1}$. The LOT is a Cassegrain $f/8$ telescope by APM Telescopes, equipped with a SOPHIA 2048B CCD camera, having a gain of 0.92 electrons ADU^{-1}, a readout noise of 7.27 electrons rms, and a pixel scale of $0.″34\,\text{pixel}^{-1}$. Both SLT and LOT have the same Astrodon photometric Sloan filters, providing excellent multi-band observational capabilities (see Figure D1 for the filter transmission curves[13]).

The Kinder workflow and observation steps, from receiving EP triggers to completing observations, analyzing the data, and

[13] The SDSS, Pan-STARRS, and SkyMapper filters' response curves are obtained from http://svo2.cab.inta-csic.es/theory/fps/, while the DESI Legacy Survey filter response curves are obtained from its DR10 website, https://www.legacysurvey.org/dr10/description/.

Table 2
Details of FXTs Having Optical Upper Limits from the Lulin Observatory

FXT	R.A. (deg, J2000)	Decl. (deg, J2000)	Error Circle Radius[a] EP-WXT/EP-Follow-up X-ray Telescope	T_0 (UTC)	EP-WXT Discoverer References
EP 240331a	169.414	−20.042	20′/−	2024-03-31T22:07:17	X. Pan et al. (2024a)
EP 240408a	158.840	−35.749	3′/−	2024-04-08T17:56:30	J. W. Hu et al. (2024d)
EP 240413a	228.794	−18.800	20′/30″	2024-04-13T14:39:37	T. Y. Lian et al. (2024c)
EP 240506a	213.978	−16.715	3′/−	2024-05-06T05:01:39	D. Y. Li et al. (2024b)
EP 240617a	285.030	−22.561	3′/−	2024-06-17T12:19:13	H. Zhou et al. (2024a)
EP 240618a	281.648	23.833	3′/30″	2024-06-18T05:43:43	H. Sun et al. (2024a)
EP 240625a	310.7308	−15.9760	2′/10″	2024-06-25T01:48:23	X. Pan et al. (2024b)
EP 240626a	263.0171	−13.0490	2′/30″	2024-06-26T06:28:28	H. Sun et al. (2024a)
EP 240702a	328.203	−38.980	3′/−	2024-07-02T00:50:05	W. Chen et al. (2024a)
EP 240703a	273.803	−9.681	3′/−	2024-07-03T00:38:40	Y. L. Wang et al. (2024a)
EP 240703c	289.264	−30.325	3′/−	2024-07-03T18:15:00	Y. J. Zhang et al. (2024a)
EP 240708a	345.9656	−22.8428	3′/10″	2024-07-08T23:28:23	Y. J. Zhang et al. (2024a)
NVSS J004348+342626[b]	10.955	34.428	2.′2/−	2024-07-17T03:13:01	S. Q. Jiang et al. (2024d)
EP 240802a	287.8070	−2.3125	1′.9/10″	2024-08-02T10:32:52	Y. L. Wang et al. (2024b)
EP 240908a	14.0031	8.0735	−/10″	2024-09-08T17:28:27	X. Mao et al. (2024b)
EP 240913a	16.681	16.750	2.′5/−	2024-09-13T11:39:33	D. Y. Li et al. (2024a)
EP 240918a	289.3937	46.1281	−/20″	2024-09-18T11:24:37	Z. J. Zhang et al. (2024b)
EP 240918b	258.66	66.739	2.′9/−	2024-09-18T15:40:00	Y. F. Liang et al. (2024d)
EP 240918c	281.338	−13.167	2.′3/10″	2024-09-18T18:06:47	Y. F. Liang et al. (2024d)
EP 240919a	334.2797	−9.7362	−/20″	2024-09-19T14:47:40	Y. F. Liang et al. (2024a)
EP 241026b	56.4058	41.0312	2′.9/10″	2024-10-26T18:14:30	T. Y. Lian et al. (2024a)
EP 241101a	37.7526	22.7175	2′.8/10″	2024-11-01T23:52:49	Y. F. Liang et al. (2024e)
EP 241104a	32.574	31.555	2.′7/−	2024-11-04T18:34:15	H. Zhou et al. (2024e)
EP 241109a	18.3599	0.0184	−/15″	2024-11-09T06:01:55	A. Li et al. (2024)
EP 241115a	19.416	−17.954	2.′6/−	2024-11-15T05:47:20	J. W. Hu et al. (2024b)
EP 241119a	84.1062	3.8404	2′.3/10″	2024-11-19T17:53:20	W. J. Zhang et al. (2024b)
EP 241125a	48.561	37.677	2.′65/−	2024-11-25T00:06:06	B. T. Wang et al. (2024d)
EP 241126a	33.7444	11.7013	2′.429/10″	2024-11-26T19:39:41	D. F. Hu et al. (2024)
EP 241206a	34.702	38.914	3.′78/−	2024-12-06T16:34:47	Y. H. I. Yin et al. (2024a)
EP 241208a	127.8303	49.0831	4′/10″	2024-12-08T16:36:13	Y. L. Wang et al. (2024c)

Notes.
[a] The error circle radius is at the 90% C.L. statistical and systematic.
[b] An FSRQ blazar within the EP-WXT localization error circle.

reporting, are outlined as follows: Initially, we notice new EP triggers through the EP internal Slack channel by collaborating with EP members, where they are discussed before the night begins at Lulin, prompting us to initiate follow-up observations. Primarily, our team relies on General Coordinates Network (GCN) Circulars from the EP team as the main source for receiving these triggers. Furthermore, we utilize the Kafka client provided by GCN notices to automatically retrieve alert notifications from EP. These alerts contain essential information such as trigger time (in UTC), localization, count rate, and significance. During nighttime, we automatically convert these alerts into a format compatible with the Astronomer's Control Panel Observatory Control Software used at the Lulin Observatory.[12] Each target is then marked with the highest priority ("first priority"), and visibility plots are generated. These steps allow the telescope operators in our control room to efficiently point the telescope directly toward the designated targets. During the daytime, we compile these alert notifications and generate visibility plots, which are then sent to our dedicated Slack channel for further discussion, enabling the team to decide if the target will be observed during the upcoming night. Additionally, the alerts and related information are automatically emailed to all members of our team, ensuring everyone stays promptly informed.

On-site observers or telescope operators then conduct follow-up observations, typically with long exposures (30 minutes for LOT and 2 hr for SLT), and upload the images in real time to Google Drive. After downloading the data to our lab studio, we process it using a custom-built pipeline,[14] which follows the standard procedure of bias, dark subtraction, and flat-field correction. We have deliberately disabled the cosmic-ray removal function to preserve faint and weak detections of optical counterparts.

We employ three methods to search for optical counterparts of EP events: First, we perform a catalog search by plotting the observed combined image using `DS9` and overlaying known catalog sources from the Sloan Digital Sky Survey (SDSS), USNO, and Gaia with region markers; any source that is not marked may be considered a candidate optical counterpart. Second, we visually compare the

[14] https://hdl.handle.net/11296/98q6x4

template image with the observed combined image using blink frames in DS9, a method that successfully led to the identification of five optical counterparts. Third, we apply template subtraction by subtracting the observed images from baseline images obtained from major survey projects (e.g., Pan-STARRS1, K. C. Chambers et al. 2016; SDSS, D. G. York et al. 2000; DESI Legacy Survey, A. Dey et al. 2019; and SkyMapper, C. Wolf et al. 2018) to reveal optical counterparts that may be obscured by the host galaxy's background. For template subtraction, we employ either the Kinder pipeline (S. Yang et al. 2021) using the "hotpants" algorithm (A. Becker 2015) or the Python-based package AutoPhOT (S. J. Brennan & M. Fraser 2022) with the "hotpants," "sfft" (L. Hu et al. 2022), or "Zogy" (B. Zackay et al. 2016) algorithms; any prominent residual in the difference image may be considered a candidate optical counterpart. In this paper, however, all subtractions are conducted using the Kinder pipeline to ensure a uniform analysis. Figure 2 displays the Kinder observed science images for the EP-Follow-up X-ray Telescope follow-up, along with the corresponding reference images and the resulting difference images by subtracting the reference from the science frames.

We provide a general overview of our Kinder pipeline below. The Kinder pipeline was specifically developed for the Kinder project and is based on the SNOoPY pipeline.[15] Similar to SNOoPY, the Kinder pipeline is a collection of Python scripts that interface with standard IRAF tasks via PyRAF, along with additional specialized analysis tools. These include "SExtractor" (E. Bertin & S. Arnouts 1996) for source extraction and star/galaxy classification, "DAOPHOT" (P. B. Stetson 1987) for point-spread function (PSF)-fitting photometry, and "hotpants" for image subtraction with PSF matching. Photometry is performed using PSF fitting, with the sky background first subtracted using a low-order polynomial fit to the surrounding regions. The PSF is constructed by averaging the profiles of isolated field stars automatically selected from the frame. After fitting and removing the optical transition (OT) from the original frame, a new local background is estimated, and the fitting procedure is iterated. Residuals from the PSF fit are visually inspected to validate the results. Photometric errors are estimated using artificial star experiments. A fake star, with brightness similar to that of the OT, is inserted near the OT position in the residual image. The PSF-fitting procedure is repeated multiple times at slightly different positions, and the dispersion in these measurements provides an estimate of the instrumental error. This is then combined in quadrature with the formal "DAOPHOT" error. If a suitable template image is available, the pipeline also allows for template subtraction using "hotpants" after PSF matching. In these cases, the OT magnitude is again measured via PSF fitting, which has been shown to be less sensitive to noise in the difference image. Once subtraction is completed, sources with Gaussian-like profiles are likely to be real, whereas non-Gaussian profiles often indicate artifacts caused by detector effects or poor subtraction. Although automatic real-bogus classification using image stamps is under development, the pipeline currently relies primarily on visual inspection for candidate validation.

[15] SNOoPy is a package for SN photometry using PSF fitting and/or template subtraction developed by E. Cappellaro. A description of the package can be found at http://sngroup.oapd.inaf.it/ecsnoopy.html.

2.1. Detection Limits for LOT and SLT

The top panel of Figure 3 helps one assess the detectability of the optical counterpart AT 2024gsa associated with EP 240414a. We analyze LOT observations obtained from 2024 April 14 to 17, where each individual frame has an exposure time of 300 s. To investigate the effect of the integrated exposure time on the depth of detection, we stack images with increasing total exposure times. For a target with magnitude 21.3, we find that a minimum integration of 900 s is required to achieve a detection above the 3σ level. With a total exposure time of 1800 s, the detection depth improves to approximately 23 mag. This demonstrates that even when the transient fades to fainter than 22 mag, it remains clearly detectable with LOT under similar observing conditions.

We also investigate the dependence of limiting magnitude on seeing conditions using the same data set in both the *r* and *i* bands; see Figure 3 (bottom panel). Adopting the method outlined in E. Brocato et al. (2018), we first measure the average full width at half-maximum of point sources in each frame and generate PSFs accordingly. Artificial stars with a range of magnitudes are randomly injected into the images. After performing image subtraction, we assess the recovery rate of these injected sources. The detection efficiency is defined as the ratio of recovered to injected stars, and the limiting magnitude is determined at the 50% recovery threshold. This analysis allows us to quantify the impact of seeing on our detection sensitivity in a systematic way.

3. Results

3.1. Kinder's Observational Contributions to the EP Follow-up

In this paper, we present a statistical study of the FXT sources detected by the EP mission and followed up by the Lulin Observatory during the first year of the EP mission, up to 2025 January 9. Out of the 72 high-SNR FXT detections by the EP mission, we have conducted follow-up observations for 42. Out of the 42 sources followed from the Lulin Observatory, 12 sources (namely, EP 250315a, LXT 240402A, EP 240414a, EP 240416a, EP 240801a, EP 241021a, EP 241030a, EP 241107a, EP 241201a, EP 241202b, EP 241217a, EP 250108a) have confirmed optical detections through our observations (see Figure 2), and for five of these, we were the first to report the discovery, while for the remaining 30, we have provided corresponding 3σ upper limits. If we include the optical follow-up observations throughout the world, then a total of 23 FXTs out of 72 (namely, EP250315a, LXT 240402A, EP 240414a, EP 240416a, EP 240420a, EP 240625a, EP 240708a, EP 240801a, EP 240804a, EP 240806a, EP 240908a, EP 241021a, EP 241025a, EP 241026a, EP 241026b, EP 241030a, EP 241107a, EP 241126a, EP 241201a, EP 241202b, EP 241217a, EP 250108a, EP 250109a) have shown confirmed optical counterparts. Thus, some fraction of FXTs also show optical counterparts.

Followed by their X-ray detection, most of the optical counterparts are discovered early; only four among those 23 are discovered 24 hr after their EP-WXT detection. In the direction of early optical follow-up observations, S. Wu et al. (2025) also performed rigorous searches utilizing the Burst Observer and Optical Transient Exploring System (BOOTES) telescope network (A. J. Castro-Tirado et al. 1999). The top panel of Figure 4 shows the earliest optical detections or upper limits reported publicly by the community. This figure

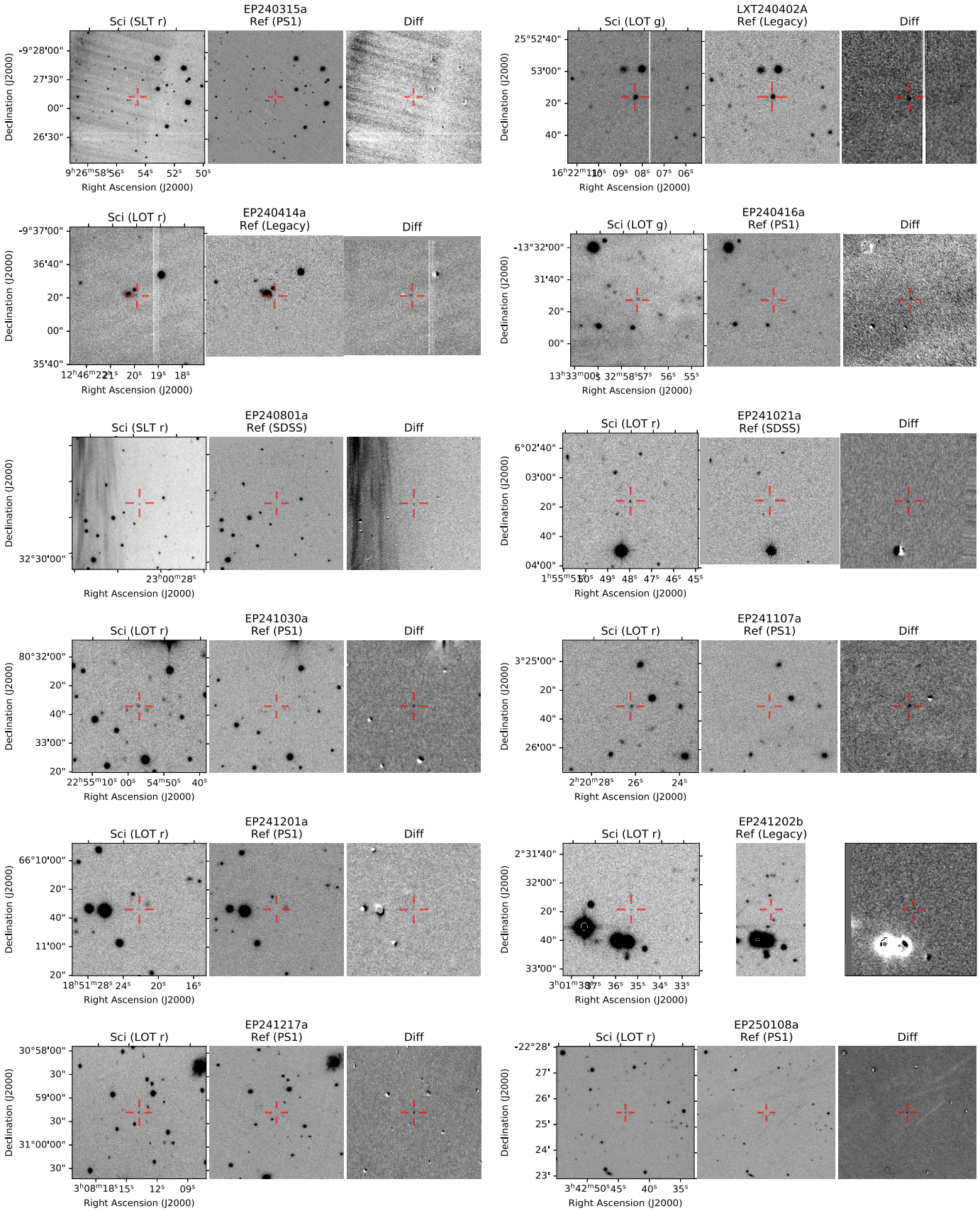

Figure 2. Kinder observations with Lulin SLT and LOT were carried out for EP-Follow-up X-ray Telescope follow-up. For 12 EP events, we detected optical counterparts, and for five of these, we were the first to report the discovery. In each panel, the EP event is labeled at the top. The left column shows stacked science frames obtained with the corresponding telescope and filter; the middle column presents reference images from various all-sky surveys; and the right column displays the difference frames produced by subtracting the reference images from the science frames.

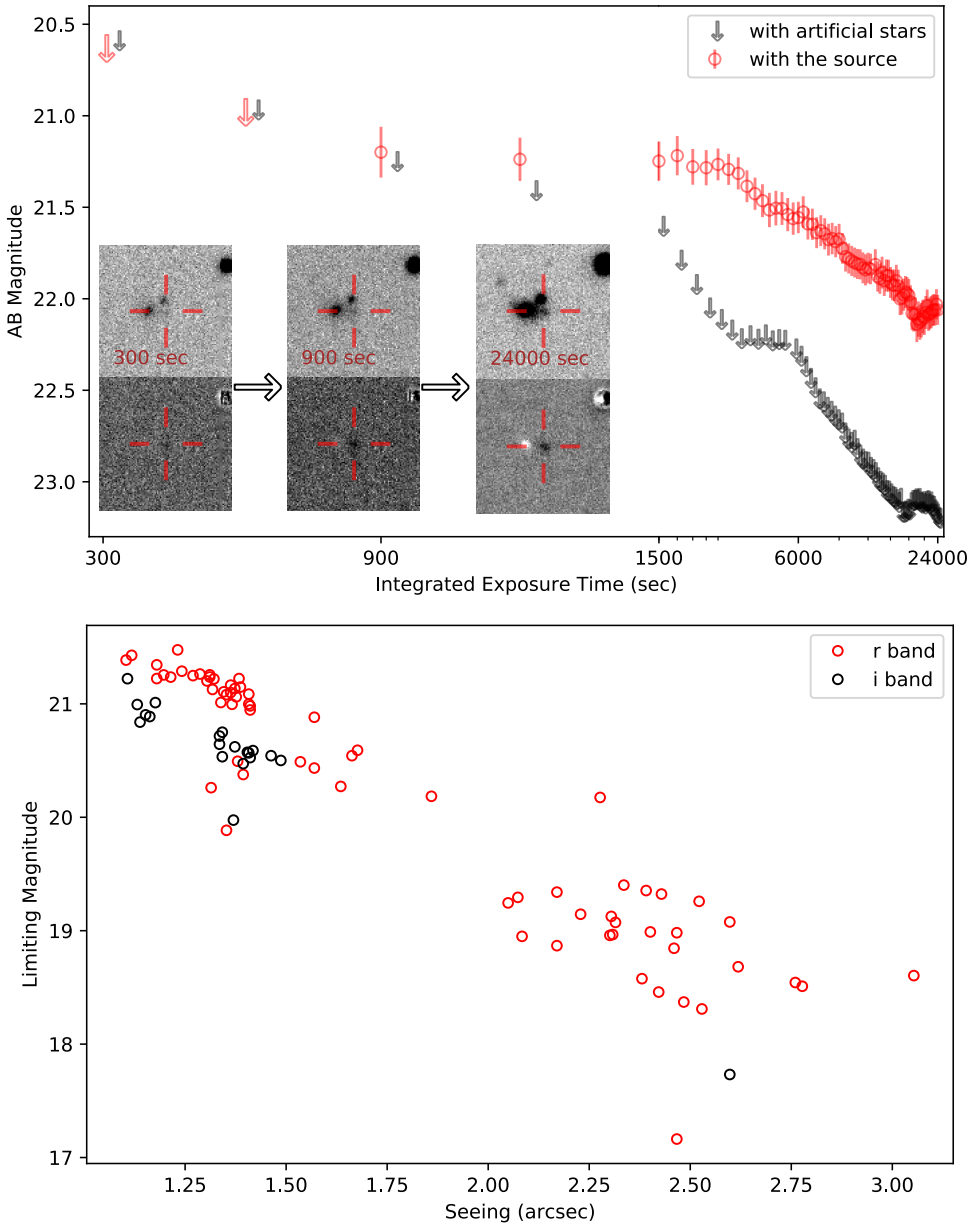

Figure 3. Top: integrated exposure time enhances the detectable magnitude depth. In the lower left panel, the top row displays images with increasing integrated exposure time, while the bottom row shows the corresponding template-subtracted results. The marker at the center indicates the location of the optical counterpart, AT 2024gsa, of EP 240414a. For a target at 21.3 mag, an integrated exposure time of 900 s is required to achieve a detection above 3σ. With a stacked exposure time of 1800 s, the detection depth reaches 22 mag, and can even reach 23 mag in some cases with better conditions. Typically, we use long exposures (30 minutes) for detections. Bottom: limiting magnitude as a function of seeing.

indicates that the optical counterparts are often bright ($\sim$15.5–21.5 mag) if discovered early within a few hours (with the exception of EP 240708a discovered with an r band of 24.0 ± 0.3 mag as reported in S. Q. Jiang et al. 2024b); however, the late discoveries (beyond $\sim$10 hr) are expected to be faint. As presented above, a total of 23 sources were discovered in optical bands, and 12 of them have also been detected from the Lulin Observatory. Thus, among the remaining 11 (out of 23) sources, four, namely, EP 240625a (late follow-up by us), EP 240708a (rapidly decaying faint optical counterpart), EP 240908a (late follow-up by us, faint OT with $r \sim 24$ mag, J. Quirola-Vasquez et al. 2024d), EP 241026b (late follow-up by us), EP 241126a (rapidly decaying faint optical counterpart), were followed from the Lulin Observatory, but the optical counterparts were not detected in observations; although the remaining six (namely, EP 240420a, EP 240804a, EP 240806a, EP 241025a, EP p;241026a, and EP 250109a) were visible from the Lulin Observatory, they were missed due to unfavorable weather conditions.

The bottom panel of Figure 4 shows our observations plotted over the publicly reported observations. In total, 41 GCN Circulars and one ATel have been issued for the EP follow-up by the Kinder project; three papers using Kinder data have been published: EP 240315a (J. H. Gillanders et al. 2024), EP 240414a/AT 2024gsa (S. Srivastav et al. 2025), EP 240801a (S.-Q. Jiang et al. 2025), and one under review: EP 250108a/SN 2025kg (the "kangaroo"; J. C. Rastinejad

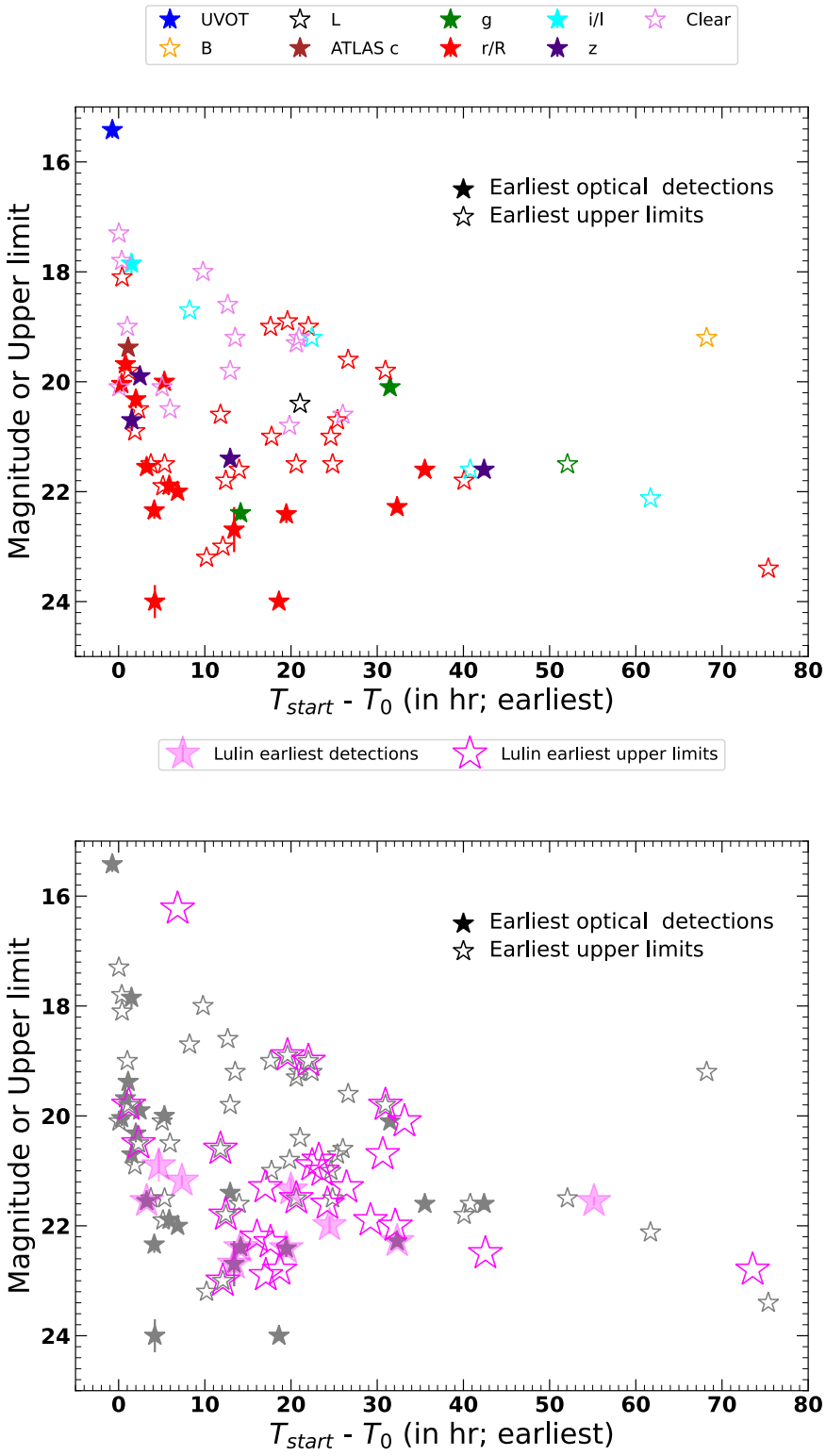

Figure 4. Top: earliest optical detections (or upper limits in case of nondetection of any optical counterpart) for the entire FXTs' sample reported in GCN Circulars. Out of 72 FXTs discovered by the EP, 23 showed corresponding optical counterparts. All reported times are in the observer frame, where $T_{\rm start}$ indicates the beginning of the observation, and T_0 refers to the trigger time of the EP-WXT detection. Bottom: comparison of $T_{\rm start} - T_0$ of Kinder/Lulin observations with other observations reported in GCNs. 12 out of 23 FXTs with optical counterparts were also detected from the Lulin Observatory. Further, five out of those 12 were first discovered by us. The Kinder optical detections for EP 241021a and EP 250108a were delayed and thus are not shown here. We had only obtained optical upper limits in their respective first epoch of observations; those upper limits have been included in this plot. The pre-EP discovery Swift-UVOT optical counterpart detection was for EP 241030a, which was associated with GRB 241030A (N. J. Klingler et al. 2024). The references for first detections or upper limits are credited in Appendix D.

Table 3
Photometric Observation Log for the Sources with Optical Counterpart Discovery/Follow-up from the Lulin Observatory

FXT	$T_{start} - T_0$ (hr)	$T_{mid} - T_0$ (hr)	MJD_{start}	Telescope	Total Exposure	Filter	Apparent Magnitude (AB mag)	$E(B-V)$
EP 240315a[a]	19.98	20.20	60385.673	SLT	6 × 300 s	*r*	21.34 ± 0.22	0.042
	43.22	43.67	60386.642	LOT	10 × 300 s	*i*	22.75 ± 0.23	…
	89.58	90.86	60388.573	SLT	29 × 300 s	*i*	>21.8	…
	89.92	91.34	60388.588	LOT	30 × 300 s	*i*	22.79 ± 0.36	…
	113.21	114.40	60389.558	LOT	20 × 300 s	*i*	>22.1	…
LXT 240402A	32.31	32.95	60403.713	LOT	12 × 300 s	*r*	22.28 ± 0.10	0.037
	33.70	34.10	60403.771	LOT	10 × 300 s	*g*	22.86 ± 0.09	…
EP 240414a[a]	3.25	3.97	60414.545	LOT	11 × 300 s	*r*	21.55 ± 0.08	0.033
	3.70	3.46	60414.564	LOT	12 × 300 s	*i*	21.40 ± 0.16	…
	8.02	8.25	60414.744	LOT	6 × 300 s	*g*	21.90 ± 0.12	…
	28.04	29.58	60415.578	LOT	19 × 300 s	*r*	22.05 ± 0.07	…
	28.61	28.79	60415.602	LOT	5 × 300 s	*i*	21.69 ± 0.23	…
	50.71	51.69	60416.523	LOT	20 × 300 s	*r*	22.05 ± 0.14	…
	52.76	53.51	60416.608	LOT	18 × 300 s	*i*	22.20 ± 0.15	…
	73.73	74.37	60417.482	LOT	11 × 300 s	*r*	21.06 ± 0.15	…
EP 240416a	14.15	15.40	60416.702	LOT	7 × 300 s	*g*	22.39 ± 0.12	0.056
	14.27	14.61	60416.707	LOT	7 × 300 s	*r*	22.08 ± 0.12	…
	14.36	14.94	60416.711	LOT	7 × 300 s	*i*	22.02 ± 0.16	…
	444.92	446.10	60434.651	SLT	7 × 300 s	*i*	>21.19	…
EP 240801a[a]	4.66	5.14	60523.573	SLT	12 × 300 s	*r*	20.90 ± 0.30	0.099
	6.25	6.73	60523.640	SLT	11 × 300 s	*r*	21.17 ± 0.11	…
	9.42	9.85	60523.772	SLT	11 × 300 s	*r*	21.36 ± 0.15	…
EP 241021a	31.15	32.17	60605.512	SLT	24 × 300 s	*r*	>19.6	0.048
	274.61	274.83	60615.656	LOT	6 × 300 s	*r*	22.06 ± 0.33	…
	325.21	325.69	60617.764	LOT	12 × 300 s	*r*	>22.75	…
EP 241030a	55.15	55.37	60615.571	LOT	6 × 300 s	*r*	21.55 ± 0.08	0.121
	55.68	55.90	60615.593	LOT	6 × 300 s	*g*	22.27 ± 0.12	…
	172.64	172.86	60620.466	LOT	6 × 300 s	*r*	>22.06	…
EP 241107a	24.47	24.68	60622.610	LOT	6 × 300 s	*r*	21.99 ± 0.16	0.044
EP 241201a	13.40	13.62	60646.434	LOT	6 × 300 s	*r*	22.69 ± 0.41	0.051
EP 241202b	19.45	19.67	60647.445	LOT	6 × 300 s	*r*	22.41 ± 0.16	0.085
	20.26	21.34	60647.478	SLT	24 × 300 s	*g*	>21.8	…
	21.36	21.58	60647.524	LOT	6 × 300 s	*r*	>22.9	…
EP 241217a	7.34	7.96	60661.539	LOT	15 × 300 s	*r*	21.18 ± 0.10	0.204
	8.68	8.99	60661.595	LOT	6 × 300 s	*g*	>21.88	…
	8.77	9.27	60661.599	LOT	6 × 300 s	*i*	19.31 ± 0.06	…
EP 250108a[b]	190.53	191.68	60691.460	SLT	24 × 300 s	*i*	>19.8	0.016
	190.69	190.77	60691.466	LOT	3 × 300 s	*r*	20.55 ± 0.21	…
	190.95	191.04	60691.478	LOT	3 × 300 s	*g*	20.83 ± 0.11	…
	215.90	217.62	60692.517	SLT	35 × 300 s	*i*	20.55 ± 0.21	…
	263.08	263.30	60694.483	LOT	6 × 300 s	*r*	20.24 ± 0.06	…
	263.98	265.61	60694.520	SLT	18 × 300 s	*g*	20.92 ± 0.24	…
	359.58	361.15	60698.504	SLT	36 × 300 s	*i*	20.36 ± 0.14	…
	982.28	982.50	60724.450	LOT	6 × 300 s	*r*	21.43 ± 0.10	…

Notes. The magnitudes in the table are not corrected for the expected foreground extinction following E. F. Schlafly & D. P. Finkbeiner (2011) in the direction of transients.
[a] The photometry for EP 240315a, EP 240414a, and EP 240801a is already published in J. H. Gillanders et al. (2024), S. Srivastav et al. (2025), and S.-Q. Jiang et al. (2025), respectively.
[b] The photometry for EP 250108a was published in J. C. Rastinejad et al. (2025).

et al. 2025). Furthermore, two works are in preparation for the events EP250226a (R.-Z. Li et al. 2025, in preparation) and EP250304a (L. Cotter et al. 2025, in preparation).

Tables 1 and 2 list the details of the Lulin observations for the FXTs, and Tables 3 and A1 list all photometry measurements.

3.2. Optical Counterparts Discovered by Kinder

In this section, we list five FXTs discovered by the EP mission, for which the optical counterparts were discovered from the Lulin Observatory as part of Kinder observations.

3.2.1. LXT 240402A

LXT 240402A was first detected by LEIA (C. Zhang et al. 2022; Z. X. Ling et al. 2023) at 2024-04-02T08:47:41 with sky coordinates of R.A. = 245.438 deg and decl. = 25.800 deg with an uncertainty of 1.′5 in radius (X. P. Xu et al. 2024). About 35 hr post-LEIA detection at 2024-04-03T19:45:00, the EP-Follow-up X-ray Telescope performed follow-up observations and detected the X-ray afterglow at sky coordinates of R.A. = 245.451 deg and decl. = 25.763 deg with an uncertainty of only 10″ in radius (S. M. Jia et al. 2024). Followed by the detection of an X-ray counterpart, we searched for any

associated optical counterpart and discovered clear evidence of an uncataloged source at R.A. = $16^{h}21^{m}48\overset{s}{.}225$ and decl. = $+25°45'47\overset{''}{.}57$ (S. Yang et al. 2024b) with an r-band magnitude of 22.28 ± 0.10 and a g-band magnitude of 22.86 ± 0.09 (S. Yang et al. 2024b). We independently discovered this optical counterpart candidate, although while drafting the GCN Circular, we noticed that it was also reported in A. J. Levan et al. (2024b).

The Gravitational wave high-energy Electromagnetic Counterpart All-sky Monitor[16] (GECAM)-C observations of the FXT field provided crucial insights into the nature of the transient event LXT 240402A. The time-averaged spectrum of the GECAM-C instrument revealed characteristics that were strongly indicative of a long GRB 240402B (W.-C. Xue et al. 2024). The GECAM-C localization of GRB 240402B was found to be consistent with the LEIA localization of LXT 240402A within the error (W.-C. Xue et al. 2024). The associated burst was also detected by Konus-Wind (A. Ridnaia et al. 2024). Further, M. Yadav et al. (2024) reported the detection of an X-ray source by Chandra with high significance at the location of the optical counterpart. The Glowbug gamma-ray telescope (J. E. Grove et al. 2020; R. S. Woolf et al. 2022), operating on the International Space Station, also reported the detection of LXT 240402A/GRB 240402B. The spectroscopic observations by the Very Large Telescope (VLT) X-shooter detected a weak continuum throughout the spectrum and claimed to have detected multiple emission lines due to [O II], Hβ, [O III], Hα, and Lyα at a common redshift of $z = 1.551$ (N. R. Tanvir et al. 2024). The authors proposed that these emission lines are associated with the host. Thus, in our work, we adopted a redshift of 1.551 for LXT 240402A.

3.2.2. EP 240414a/AT 2024gsa

EP 240414a was discovered by EP-WXT at the sky coordinates of R.A. = 191.498 deg and decl. = −9.695 deg with an uncertainty of 3′ in radius (T. Y. Lian et al. 2024b). The X-ray transient triggered the EP-WXT processing unit at 2024-04-14T09:50:12. Following the EP-WXT discovery of the X-ray transient, a search for the optical counterpart of EP 240414a began. About 2 hr after the EP-WXT trigger at 2024-04-14T11:50:01, the EP-Follow-up X-ray Telescope performed follow-up observations. The follow-up EP-Follow-up X-ray Telescope observations unambiguously detected an X-ray source at sky coordinates of R.A. = 191.509 deg and decl. = −9.718 deg with an uncertainty of 10″ in radius (J. Guan et al. 2024).

Followed by the EP-WXT discovery and EP-Follow-up X-ray Telescope follow-up observations, several telescopes were quickly triggered to search for the optical counterpart. Our Kinder observations from the LOT in the r band started about 3.13 hr after the EP-WXT trigger. We discovered an optical counterpart candidate at R.A. = $12^{h}46^{m}01\overset{s}{.}72$ and decl. = $-09°43'08\overset{''}{.}87$ (A. Aryan et al. 2024g) with an r-band magnitude of 21.52 ± 0.12. We registered it in the Transient Name Server with an IAU name AT 2024gsa (A. Aryan et al. 2024h). The optical counterpart candidate was associated with the galaxy SDSS J124601.99-094309.3, having an r-band magnitude of 19.04 mag in SDSS DR15 (D. S. Aguado et al. 2019). The spectroscopic observations of SDSS J124601.99-094309.3 showed unambiguous hydrogen and oxygen features at $z = 0.41$ (P. G. Jonker et al. 2024). After the optical counterpart discovery, several optical/near-infrared (NIR) follow-up observations also detected the optical counterpart candidate (V. Karambelkar et al. 2024; A. J. Levan et al. 2024e; W. X. Li et al. 2024k; S. Srivastav et al. 2024a; B. T. Wang et al. 2024a; D. Xu et al. 2024). Later, J. Bright et al. (2024) reported the radio detection from MeerKAT. Thus, EP 240414a was just the second FXT detected with X-ray, optical, and radio counterparts within a month after EP 240315a.

EP 240414a displays complex temporal evolution across X-ray, optical, and radio bands, with a red, nonthermal optical rebrightening and late-time SN emergence (H. Sun et al. 2025; J. S. Bright et al. 2025; S. Srivastav et al. 2025). Several theoretical interpretations have been proposed, including a weak relativistic jet associated with a Type Ic BL SN (H. Sun et al. 2025), afterglow emission from a mildly relativistic, possibly of f-axis or choked jet (J. S. Bright et al. 2025), jet breakout through an extended circumstellar medium (H. Hamidani et al. 2025b), cocoon-dominated emission viewed off-axis (J.-H. Zheng et al. 2025), and shock interactions analogous to LFBOTs (J. N. D. van Dalen et al. 2025).

3.2.3. EP 240416a

EP 240416a was discovered by EP-WXT at the sky coordinates of R.A. = 203.150 deg and decl. = −13.612 deg with an uncertainty of 3′ in radius while performing calibration observation (H. Q. Cheng et al. 2024). The EP-WXT detected this FXT at 2024-04-16T02:42:13. Following the EP-WXT discovery, several telescopes were triggered to search for the optical counterpart. Our observations from LOT in the g band started about 14.15 hr after the EP-WXT discovery. We discovered a plausible optical counterpart candidate at R.A. = $13^{h}32^{m}34\overset{s}{.}51$ and decl. = $-13°37'49\overset{''}{.}05$ (T. W. Chen et al. 2024a) with a g-band magnitude of 22.39 ± 0.12. Followed by the discovery of an optical counterpart candidate, several telescopes performed optical/NIR follow-up observations, but none of those observations reported any further detection (G. Antipov et al. 2024a; S. Belkin et al. 2024c; G. Mo et al. 2024; N. Pankov et al. 2024a; D. R. Xiong et al. 2024a). The reported upper limits were all later and also shallower than ours. Probably, due to these reasons, none of them detected the proposed optical counterpart in follow-up observations.

3.2.4. EP 241201a

The EP-WXT discovered EP 241201a at 2024-12-01T21:01:22. It was detected at sky coordinates of R.A. = 282.596 deg and decl. = 66.081 deg with an uncertainty of $2\overset{'}{.}343$ in radius (W. Chen et al. 2024e). About 12 hr after the EP-WXT discovery, a follow-up observation was performed using the EP-Follow-up X-ray Telescope, which detected an uncataloged X-ray source at R.A. = 282.4865 deg and decl. = 66.0693 deg with an uncertainty of 10″ in radius (W. Chen et al. 2024d). Followed by the EP-WXT discovery and EP-Follow-up X-ray Telescope follow-up observations, a few telescopes were triggered to search for the optical counterpart. The observations by V. Lipunov et al. (2024d) provided a shallow limit of about 19.0–19.5 mag in their four pointings. Our observations from LOT in the r band started about 13.40 hr after the EP-WXT discovery. We proposed a

[16] https://gecam.nssdc.ac.cn/

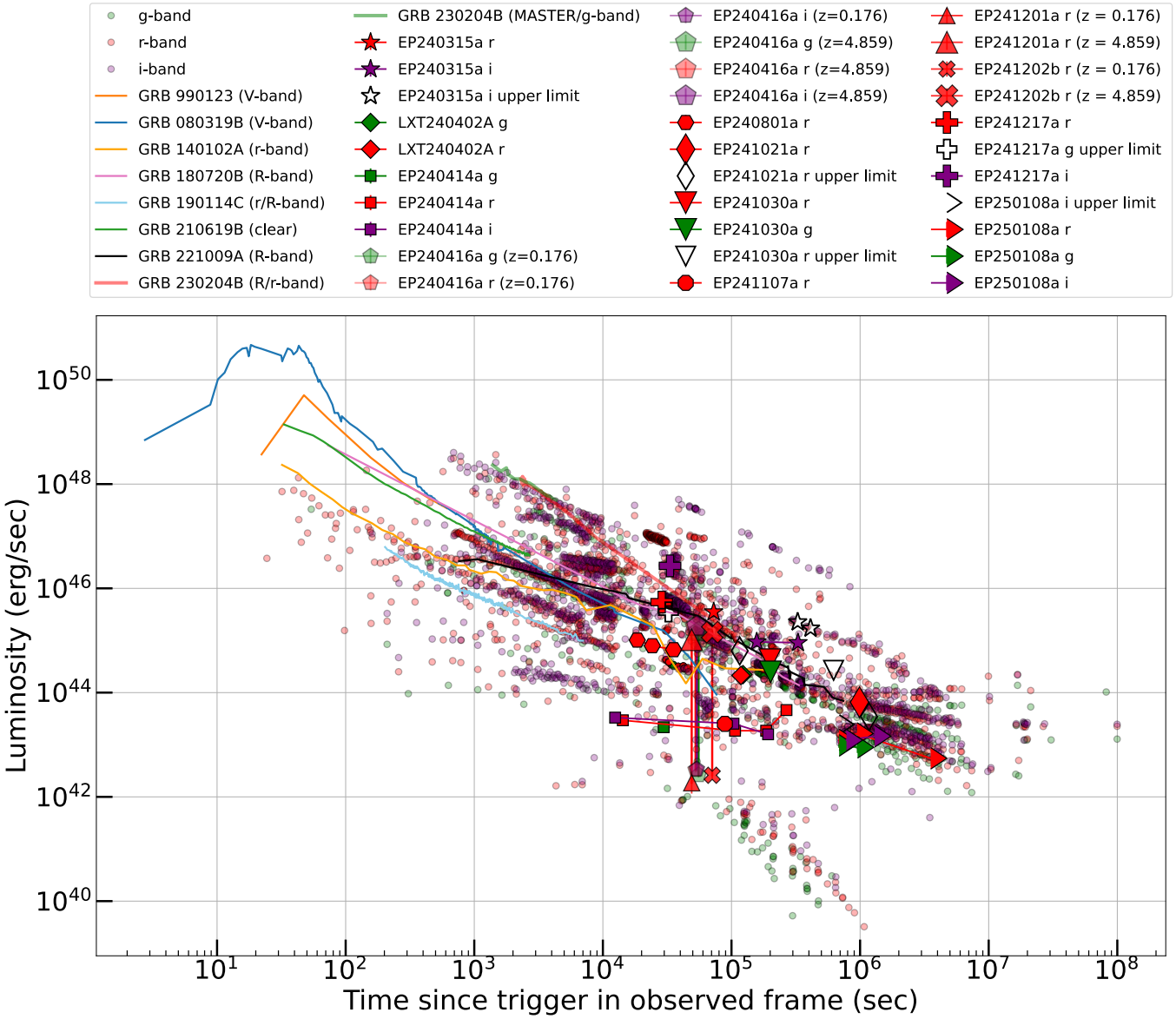

Figure 5. The comparison of the optical luminosity of FXTs in our study with a sample of 535 GRBs from M. G. Dainotti et al. (2024) in the *g*, *r*, and *i* bands (round markers). A few peculiar and bright GRBs are also shown and highlighted for comparison. The optical luminosities of FXTs are consistent with GRBs. The redshifts of EP 240416a, EP 241201a, and EP 241202b are unknown; however, the vertical lines joining the smaller and larger markers show the range of luminosities had they occurred within the known range of redshift for FXTs in our sample (i.e., $z = 0.176$ to 4.859). The sources of optical light curve of highlighted GRBs are as follows: GRB 990123 from C. Akerlof et al. (1999), GRB 080319B from J. L. Racusin et al. (2008), GRB 140102A from R. Gupta et al. (2021a), GRB 180720B from R. Gupta et al. (2021b), GRB 190114C from N. Jordana-Mitjans et al. (2020), GRB 210619B from G. Oganesyan et al. (2023), GRB 221009A from A. K. Ror et al. (2023), and GRB 230204B from R. Gupta et al. (2024).

plausible optical counterpart at R.A. = $18^{h}50^{m}38\overset{s}{.}079$ decl. = $+66°03'11\overset{''}{.}36$ with an *r*-band magnitude of 22.69 ± 0.41 mag (M. H. Lee et al. 2024b). The further optical follow-up observations from other facilities were either delayed or had shallower limits than ours. None of them found any evidence of the proposed optical counterpart (G. Du et al. 2024; X. Liu et al. 2024d; I. Perez-Garcia et al. 2024g).

3.2.5. EP 241202b

EP 241202b was first detected by EP-WXT at 2024-12-02T15:12:55 with the sky coordinates of R.A. = 45.302 deg and decl. = 2.441 deg with an uncertainty of $2\overset{'}{.}6$ in radius (C. Zhou et al. 2024). Followed by EP-WXT discovery, our observations utilizing LOT in the *r* band started about 19.45 hr later. We proposed a plausible optical counterpart candidate at R.A. = $03^{h}01^{m}20\overset{s}{.}862$ decl. = $+02°26'27\overset{''}{.}04$ with an *r*-band magnitude of 22.41 ± 0.16 mag (C. C. Ngeow et al. 2024). Only a few telescopes searched further to confirm the proposed optical counterpart. None of them detected the proposed optical counterpart as the limits were shallow (>19.5 mag in the *clear* band at ∼19.2 hr in W. Zheng et al. 2024h) and (>21.5 mag in the *clear* band at ∼14.4 hr in V. Lipunov et al. 2024b).

4. Discussion

4.1. Coincidences of FXTs with GRBs or Their Detection in Gamma-Ray Bands

We noticed that a few FXTs in our sample were associated with GRBs. EP 240315a was found coincident with GRB

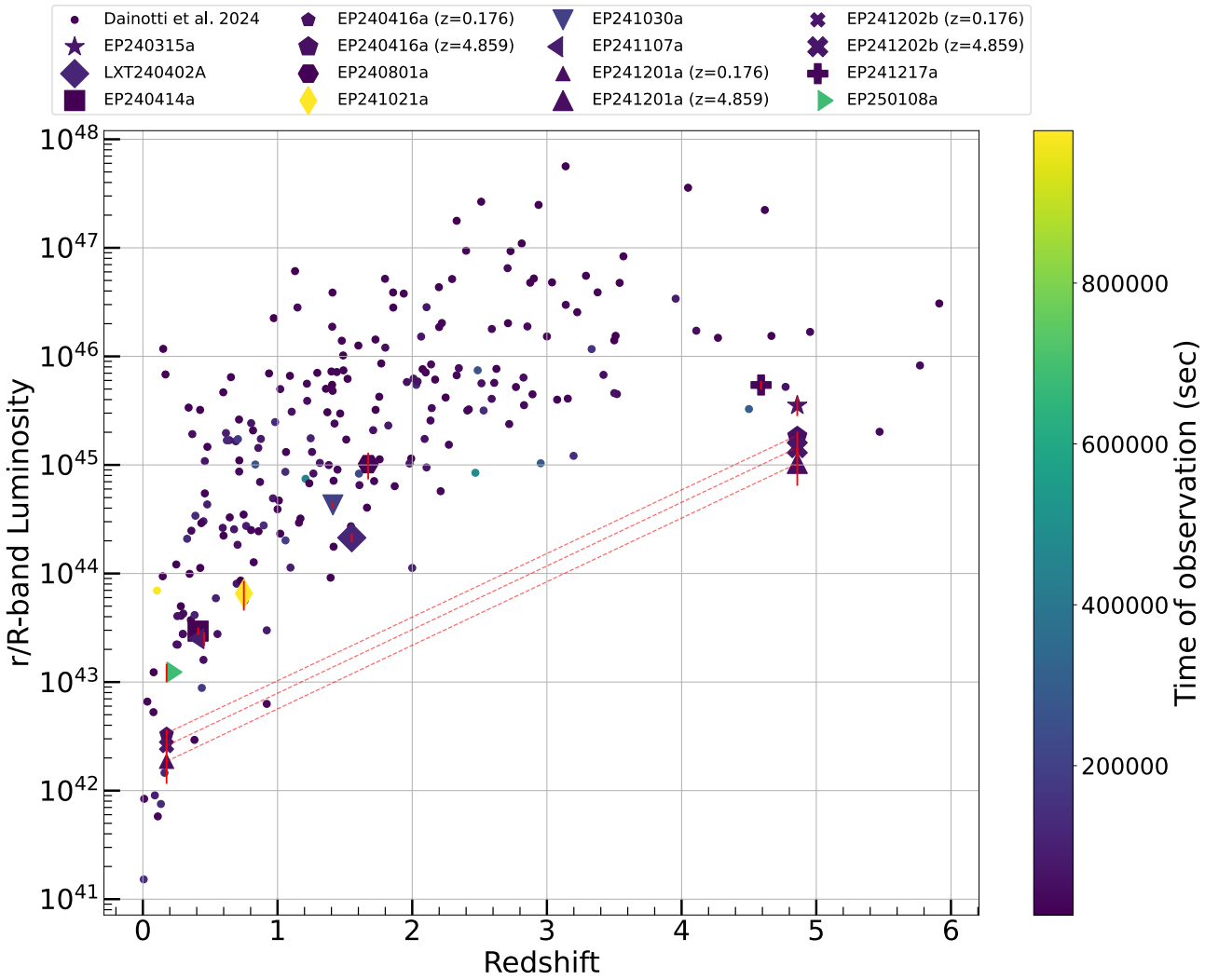

Figure 6. The redshift of the occurrence of the FXTs in our sample and their earliest *r*-/*R*-band luminosity compared with a sample of GRBs from M. G. Dainotti et al. (2024). Once again, the redshift and luminosity of FXTs are consistent with GRBs. The dashed lines show the range of luminosities of EP 240416a, EP 241201a, and EP 241202b, had they occurred within the observed redshift range of FXTs in our sample (i.e., $z = 0.176$ to 4.859). The luminosities of EP 240416a, EP 241201a, and EP 241202b lie toward the fainter limit had they occurred at high redshifts. They are more consistent with low-redshift GRBs. The redshifts of GRBs are compiled in R. Gupta et al. (2024).

240315C (see Section A.1.1), LXT 240402A was associated with GRB 240402B through significant coincidence (see Section 3.2.1), EP 240801a was also discovered by Fermi-GBM, and its multiwavelength properties resembled GRB 221009A (BOAT; E. Burns et al. 2023) under the assumption of a two-component jet model (see Section A.1.2), and EP 241030a was coincident with GRB 241030A (see Section A.1.4). Thus, among the sources having confirmed optical detections in our observations, four of those showed their direct association with GRBs either through coincidence or through direct detection in gamma-ray bands.

Among the source with upper limits in our observations, eight FXTs, namely, EP 240617a (a weak gamma-ray transient was discovered within EP-WXT localization, see Section A.2.5), EP 240703a (coincident with GRB 240703A, see Section A.2.10), EP 240802a (coincident with GRB 240802A, see Section A.2.14), EP 240913a (coincident with GRB 240913C, see Section A.2.16), EP 240919a (coincident with GRB 240919A, see Section A.2.20), EP 241104a (coincident with GRB 241104A, see Section A.2.23), EP 241115a (coincident with GRB 241115D, see Section A.2.25), and EP 241208a (coincident with a long and soft transient discovered by SVOM-ECLAIRS, see Section A.2.30) provided strong evidence of their association with GRBs through significant spatial and temporal coincidences.

Thus, in our sample of 42 FXTs followed from the Lulin Observatory, 12 of them showed strong evidence of their association with GRBs either through spatial and temporal coincidences or through direct detection in gamma-ray bands.

4.2. FXTs with No/Faint Optical Counterparts and the Context of "Dark FXTs"

For a subset of FXTs, specifically EP 240413a, EP 240918b, EP 240918c, EP 241104a, EP 241115a, EP 241125a, EP 241206a, EP 241201a, EP 241202b, and EP 241208a, the optical follow-up was limited, with only one to three telescopes triggering after the EP-WXT detection. This limited response was primarily due to either significant delays in the release of EP detection GCN alerts (exceeding 10 hr postdetection), or the timing of the alerts coinciding with weekends. Except for EP 241201a and EP 241202b (with

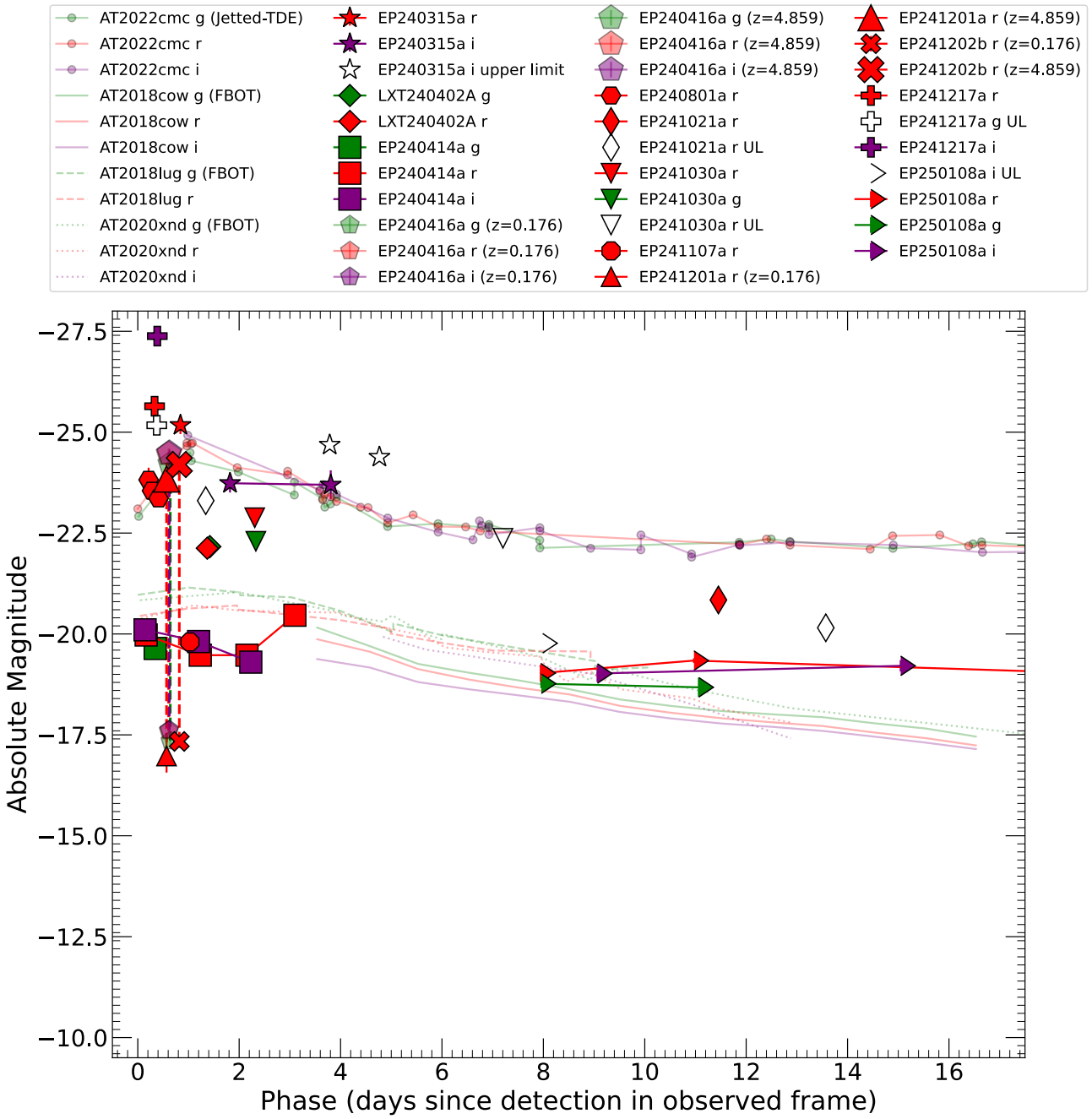

Figure 7. The comparison of the absolute optical magnitudes of the FXTs in our sample with the only confirmed jetted TDE, AT 2022cmc. The optical data for AT 2022cmc are obtained from I. Andreoni et al. (2022). Besides matching the GRBs, FXTs EP 240315a and EP 240801a are also consistent with jetted TDE. It also shows the comparison with the FBOT events AT 2018cow, AT 2018lug, and AT 2020xnd. The dashed, vertical lines show the range of optical absolute magnitudes had EP 240416a, EP 241201a, and EP 241202b occurred within the range of known redshift for FXTs in our sample ($z = 0.176$ to 4.859). The sources of optical data are: AT 2018cow (S. J. Prentice et al. 2018); AT 2018lug (A. Y. Q. Ho et al. 2020); and AT 2020xnd (D. A. Perley et al. 2021). The dashed lines show the range of optical absolute magnitudes if EP 240416a, EP 241201a, and EP 241202b had occurred within the range of known redshift for FXTs in our sample ($z = 0.176$ to 4.859).

reported optical counterparts fainter than ∼22.4 mag), no others were detected in optical bands.

We notice that the majority (49 out of a total of 72) of FXTs were not detected with any associated optical counterpart. In our sample of 42 FXTs, 30 were not detected in optical bands. As presented in Table A1, 11 FXTs (namely, EP 240408a, EP 240413a, EP 240506a, EP 240617a, EP 240625a, EP 240626a, EP 240802a, EP 240908a, EP 240913a, EP 241026b, EP 241115a) were followed $\gtrsim$24 hr from the Lulin Observatory, after their detection in X-ray by EP-WXT. Among these, EP 240625a (a weak and ambiguous candidate reported with $z = 20.7 \pm 0.2$ at 1.52 hr, S. Y. Fu et al. 2024b), EP 240908a (very faint optical counterpart with an r-band magnitude of ∼24 mag at ∼18.6 hr, J. Quirola-Vasquez et al. 2024d), and EP 241026b (late discovery of an optical counterpart with $r = 21.6$ mag discovered at 35.52 hr although Galactic origin of the source could not be completely ruled out, A. Rossi et al. 2024) had optical counterpart, but missed by us either due to their faintness or late trigger of telescopes. However, we notice that despite early follow-up from other

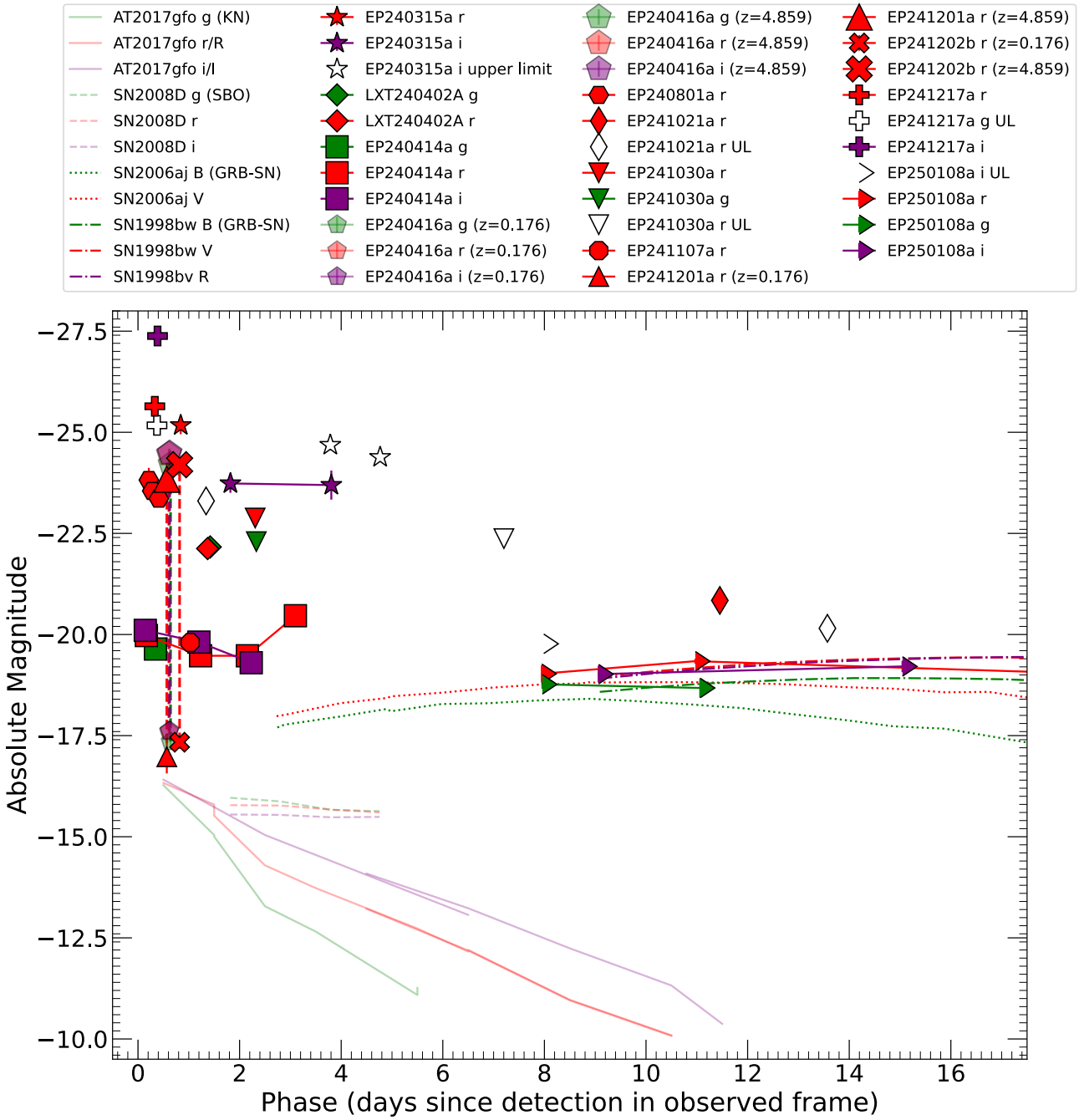

Figure 8. The comparison of the absolute magnitudes in the optical bands of the FXTs in our sample with the kilonova event AT 2017gfo. The absolute magnitudes are also compared with the early SBO component of SN 2008D, a weak X-ray flash event followed by an early optical detection (P. A. Mazzali et al. 2008). SN 2008D proves to be a possible link between X-ray transients and the SBO phenomena. Additionally, the comparison with GRB-SNe 1998bw (data from A. Clocchiatti et al. 2011) and 2006aj (data from P. Ferrero et al. 2006) is also shown. The dashed, vertical lines show the range of optical absolute magnitudes if EP 240416a, EP 241201a, and EP 241202b had occurred within the range of known redshift for FXTs in our sample ($z = 0.176$ to 4.859).

telescopes, no credible optical counterpart candidates in the following sources were found: EP 240413 (GOTO *L*-band limit of >20.4 mag at ∼21 hr, K. A. Pall'e et al. 2024), EP 240626a (KAIT optical upper limit of >19.0 mag in the *clear* band at 1.01 hr, W. Zheng et al. 2024i), EP 240802a (KAIT optical upper limit of >21.0 mag in the *clear* band at ∼17.8 hr, W. Zheng et al. 2024e), EP 240913a (JinShan optical upper limits of >21.9 mag in the *r* band at 5.1 hr, Z. P. Zhu et al. 2024b), and EP 241115a (Global MASTER-Net upper limit of 18.6 mag in the *clear* band at ∼12.7 hr, V. Lipunov et al. 2024c). Thus, (a) delayed trigger of telescopes to search for the optical counterpart, (b) intrinsically faint nature of the associated optical counterpart, and/or (c) optical counterpart being intrinsically absent, could be the possible reasons for their nondetection.

The intrinsically faint nature of the associated optical counterpart and/or optical counterpart being intrinsically absent despite their detection in X-ray bands suggests that a major fraction of FXTs could be "dark FXTs" similar to "dark GRBs" (J. U. Fynbo et al. 2001; P. Jakobsson et al. 2004; J. Greiner et al. 2011; R. Gupta et al. 2022; A. J. Castro-Tirado et al. 2024). Originally, the term "dark GRB" was coined for

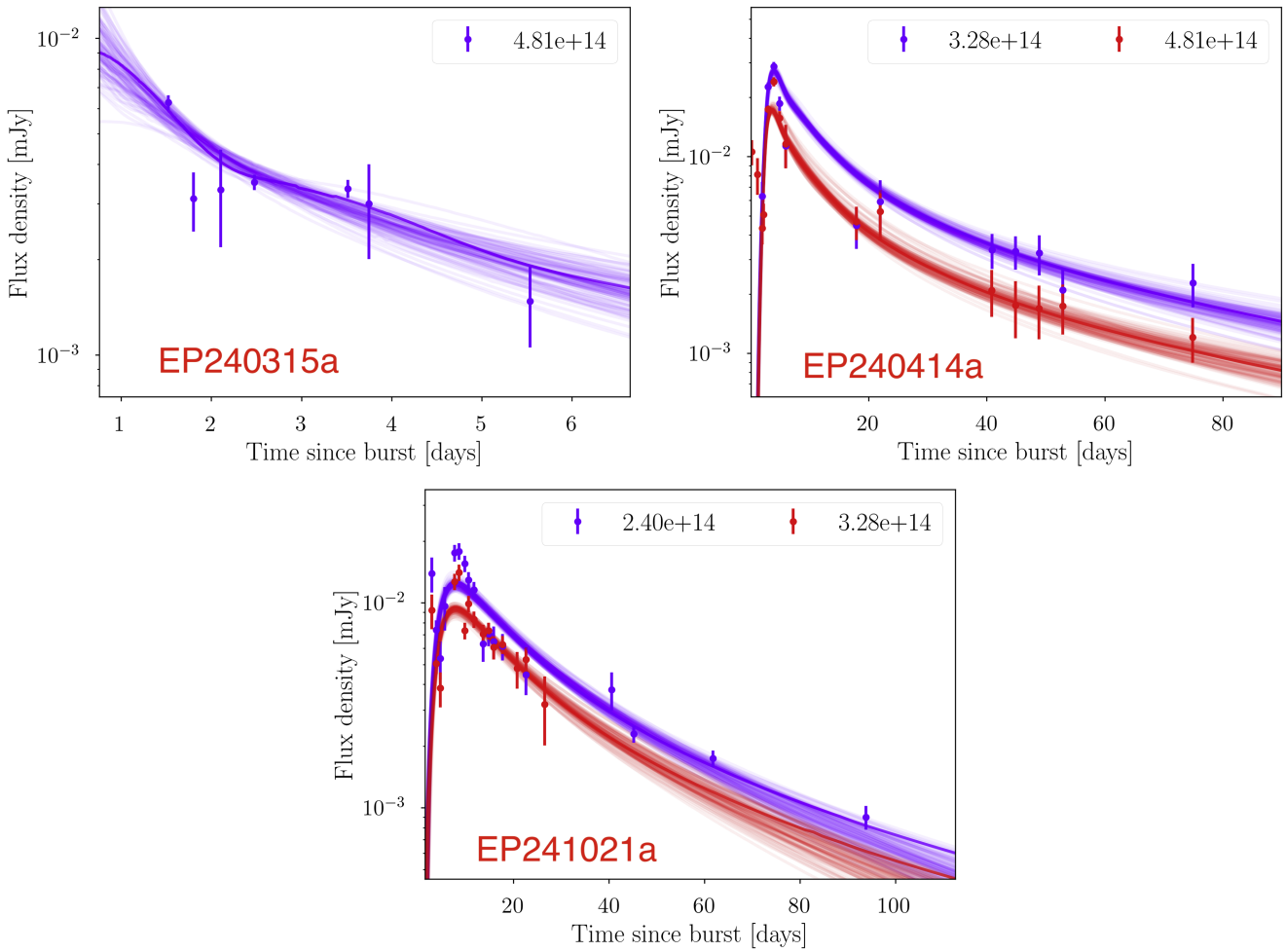

Figure 9. Outcomes of the broadband afterglow (assuming the "gaussiancore" model) fitting using REDBACK (N. Sarin et al. 2024) to the *i*- (4.81×10^{14} Hz), *z*- (3.28×10^{14} Hz), and *J*-band (2.40×10^{14} Hz) light curves of well-studied FXTs. The top-left panel shows the fitting to the *i*-band light curve of EP 240315a; the top-right panel shows the fittings to the *z*- and *i*-band light curves of EP 240414a, and the bottom panel shows the fittings to the *J*-band and *z*-band light curves of EP 241021a. Sources of light curves: EP 240315a (J. H. Gillanders et al. 2024), EP 240414a (S. Srivastav et al. 2025), and EP 241021a (M. Busmann et al. 2025). To avoid the problem of Lyα leaking, only bands redder than the *i* bands are used. The best-fit parameters are listed in Table B1.

the GRBs that were detected in X-rays but without an optical counterpart (J. U. Fynbo et al. 2001). Following this analogy, the FXTs with no optical counterparts should be classified as "dark FXTs." Later, the nomenclature of "dark GRBs" was made more specific by adding a time and brightness limit, e.g., $R > 23$ mag at 1–2 days of the burst (S. G. Djorgovski et al. 2001). These constraints on the time and brightness limit will still make several FXTs even with optical counterparts from categorizing them as "dark FXTs" since they are usually fainter than 23 mag in optical bands (Figure 4) at 1–2 days after their discovery in X-ray bands. A more advanced and robust condition of optical-to-X-ray spectral index of $\beta_{\rm OX} < 0.5$ was proposed by P. Jakobsson et al. (2004). The estimation of $\beta_{\rm OX}$ for the sources with optical detection is beyond the scope of this paper, although we quote the $\beta_{\rm OX}$ for a few FXTs available from the literature. While performing the multiwavelength afterglow fitting for EP 240315a, Y. Liu et al. (2024) reported a spectral index of $-0.93-0.04+0.04$, consistent with EP250315a falling under the category of "dark FXTs." For EP 240414a, S. Srivastav et al. (2025) fit a single power law to the optical and X-ray data points, and measure a spectral index of -0.76 ± 0.05. With $\beta < 0.5$ for the optical and X-ray data, EP 240414a also falls under the category of "dark FXTs." Further, for EP 241021a, M. Busmann et al. (2025) estimated the optical-to-IR spectral index ($\beta_{\rm OIR}$) of $-1.09-0.06+0.05$, and the extrapolation of the OIR spectral index to X-ray data was consistent. Thus, EP 241021a fell under the category of "dark FXTs." With these results, we conclude that the majority of FXTs are "dark FXTs" due to the nondetection of any associated optical counterpart. Although several FXTs have optical counterpart detection, those can still fall under the category of "dark FXTs" due to $\beta_{\rm OX} < 0.5$.

4.3. Comparison of GRBs, TDEs, FBOTs, SBO, and Kilonova

First, we compare the optical luminosity of FXTs with GRBs. To estimate the optical luminosity from the observed magnitudes, we proceed as follows. The apparent magnitude m is first converted to absolute magnitude M using the formula

$$M = m - 5\log_{10}\left(\frac{D_{\rm L}}{10\ {\rm pc}}\right) + 2.5\log_{10}(1+z) - A_\lambda,$$

where $D_{\rm L}$ is the luminosity distance derived from the redshift z assuming a flat ΛCDM cosmology, and A_λ represents the Galactic extinction. We ignored the host galaxy extinction as the FXTs appear mostly hostless or far from the host. The term

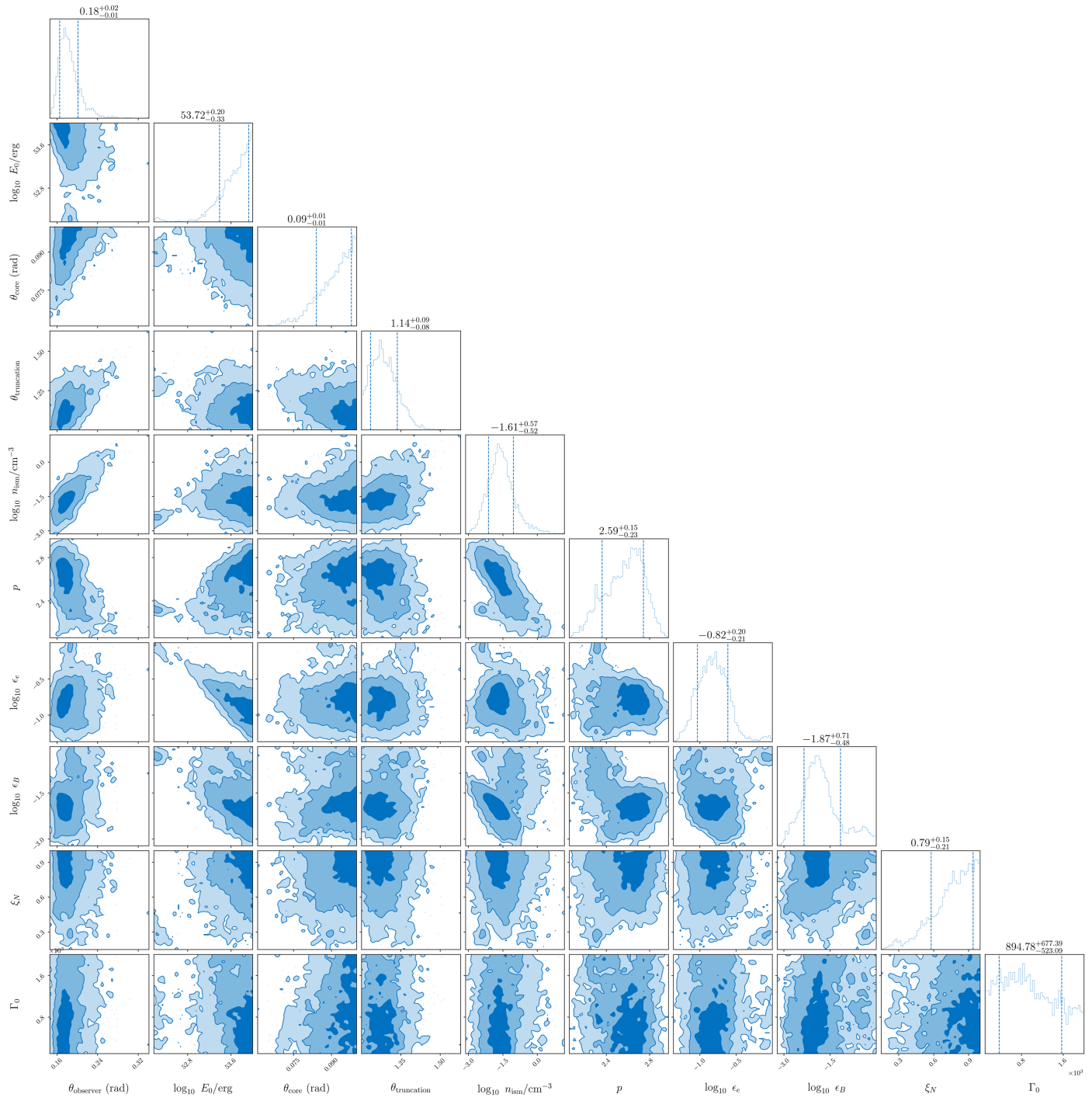

Figure 10. The corner plot of the posteriors for the "gaussiancore" afterglow model using REDBACK for EP 241021a.

$2.5\log_{10}(1+z)$ serves as an approximate k-correction to account for the redshifted spectral energy distribution. The absolute magnitude is then converted to monochromatic luminosity (in erg s^{-1} Hz^{-1}) via

$$L = 3.0128 \times 10^{35} \times 10^{-0.4M},$$

where the zero-point 3.0128×10^{35} erg s^{-1} Hz^{-1} corresponds to $M = 0$. This approach yields an estimate of the rest-frame luminosity that incorporates both distance and an approximate k-correction.

The top panel of Figure 4 shows the earliest optical detections (upper limits in case of nondetections) for the sample of FXTs reported in GCNs. There are 23 out of 72 FXTs that are detected with optical counterparts. The sources with confirmed optical detections have a mean (median) optical magnitude of 20.89 mag (21.48 mag), with a standard deviation of 1.81 mag. Further, the mean (median) time of optical detection following the X-ray discovery is 10.92 hr (4.76 hr), with a standard deviation of 12.74 hr. The earliest mean (median) r-/R-band magnitude of GRBs estimated from M. G. Dainotti et al. (2024) is 19.10 mag (19.23 mag) with a

standard deviation of 2.50 mag. Additionally, the mean (median) time of the first r-/R-band observations is 9.70 hr (1.79 hr) with a standard deviation of 26.54 hr. The earliest mean (median) r-/R-band magnitude of GRBs appears brighter than FXTs because a large number of GRBs are discovered in optical bands much earlier in time when compared to the discovery of FXTs, as shown in Figure 5. For the sources with upper limits, the mean (median) upper limits in the optical bands are 20.32 mag (20.5 mag), respectively, with a standard deviation of 1.44 mag. Additionally, the mean (median) time of first upper limit is 18.87 hr (13.98 hr) since detection, respectively, with a standard deviation of 17.63 hr.

Figure 5 shows the comparison of the optical luminosities of FXTs in our analysis with a sample of 535 GRBs from M. G. Dainotti et al. (2024). A few peculiar and bright GRBs are also highlighted. The optical luminosities of FXTs are very well consistent with GRBs. The redshifts of EP 240416a, EP 241201a, and EP 241202b are unknown; however, the vertical lines joining the smaller and larger markers show the range of luminosities, had they occurred within the known range of redshift for FXTs in our sample (i.e., $z = 0.176$ to 4.859). The optical luminosities of all the FXTs in our sample with confirmed optical counterparts are consistent with the luminosities of GRBs, no matter how early or late after the X-ray detections their optical counterparts have been discovered.

Figure 6 shows the redshifts of the occurrences of the FXTs with confirmed optical counterparts in our sample and their luminosity beyond 14,300 s since detection compared with a sample of GRBs from M. G. Dainotti et al. (2024). The choice of a cutoff of 14,300 s is made since our earliest r-band detection is at 14,292 s for EP 240414a. For the rest of the FXTs in our sample, their detections are beyond 14,292 s. The dashed lines show the range of luminosities of EP 240416a, EP 241201a, and EP 241202b, had they occurred within the observed redshift range of FXTs (i.e., $z = 0.176$ to 4.859) in our sample. Once again, we find that the redshifts and luminosities of FXTs are consistent with GRBs. In particular, for a given redshift, the FXTs seem to lie toward the faint end of GRB populations.

Figure 7 shows the comparison of the absolute magnitudes of the FXTs having confirmed optical counterparts in our sample with the only confirmed jetted TDE event AT 2022cmc. The optical data for AT 2022cmc are obtained from I. Andreoni et al. (2022). The dashed lines show the range of optical absolute magnitudes if EP 240416a, EP 241201a, and EP 241202b had occurred within the range of known redshifts for FXTs in our sample ($z = 0.176$ to 4.859). Besides being consistent with GRBs, the optical luminosities of FXTs EP 240315a and EP 240801a are also consistent with the jetted TDE event. However, EP 240315a is confirmed to be associated with GRB 240315C (Y. Liu et al. 2025), which diminishes the probability of EP 240315a having a jetted TDE origin. Recently, S.-Q. Jiang et al. (2025) reported the detection of EP 240801a by Fermi-GBM. Further, the detailed multiwavelength analysis by S.-Q. Jiang et al. (2025) showed the resemblance of EP 240801a to GRB 221009A (BOAT; E. Burns et al. 2023) under the assumption of two-component jet models. Thus, EP 240801a was probably another off-axis jet or intrinsically weak GRB. Among the sources with unknown redshifts, the optical luminosities of EP 240416a, EP 241201a, and EP 241202b are also consistent with jetted TDE if we consider them to occur at the highest known redshift for FXTs. None of the other FXTs produce luminosities consistent with the jetted TDE event.

In the case of EP 240414a, the entire optical evolution was divided into three phases (H. Sun et al. 2025; J. N. D. van Dalen et al. 2025). Followed by the first blue peak in the optical bands, the source luminosity reduced slowly with time. It then reached the second peak with a fast rise rate, and the light curve subsequently faded rapidly thereafter. Such fast optical evolution resembled the evolution of LFBOTs. The observations by J. N. D. van Dalen et al. (2025) associated the progenitors of typical long GRBs with some FXTs even in the absence of a detected GRB, and found a possible connection between FXTs and LFBOTs. Additionally, several FXTs have detection with corresponding radio counterparts. Thus, we find it reasonable to compare the luminosities of FXTs with FBOTs. Figure 7 also shows the comparison of the absolute magnitudes in the optical bands of the FXTs in our sample with luminous and radio-loud FBOT events (A. Y. Q. Ho et al. 2023), including AT 2018cow (S. J. Prentice et al. 2018), AT 2018lug (A. Y. Q. Ho et al. 2020), and AT 2020xnd (D. A. Perley et al. 2021). The dashed lines show the range of optical absolute magnitudes had EP 240416a, EP 241201a, and EP 241202b occurred within the range of known redshift for FXTs in our sample ($z = 0.176$ to 4.859). Besides EP 240314a in its early phases and EP 250108a in its late stages, none of the other FXTs have luminosities comparable to these FBOTs.

To compare the optical bands' absolute magnitudes of FXTs in our sample with a neutron star–neutron star (NS–NS) merger event in Figure 8, we use the only confirmed kilonova source AT 2017gfo. The kilonovae are a robust indicator of binary merger (NS–NS or neutron star–black hole (NS–BH)) events (B. D. Metzger et al. 2010), and they are among the rapidly evolving transients. The g-, r-/R-, and i-/I-band data are obtained from E. Pian et al. (2017), S. J. Smartt et al. (2017). The light curves are corrected for Galactic extinction using the NASA/IPAC Extragalactic Database. Additionally, following J. Hjorth et al. (2017), we use a redshift of 0.009783 for AT 2017gfo. The detection of SN 2008D, preceded by the first discovery in the X-ray band, suggested a possible link between X-ray transients and SBO events. Figure 8 also shows the comparison of the absolute magnitudes in the optical bands of the FXTs in our sample with SN 2008D SBO. The g-, r-, and i-band data are obtained from A. M. Soderberg et al. (2008). Following P. A. Mazzali et al. (2008), we correct the light curves of SN 2008D for a total extinction, $E(B - V)$ of 0.65 mag. Further, following L.-X. Li (2008), we adopt a redshift of 0.006494 for SN 2008D while estimating the absolute magnitudes. As displayed in this figure, the FXTs' absolute magnitudes seem much brighter than the SBO and kilonova events. The emergence of the SN component in the last evolutionary stages of EP 240414a (S. Srivastav et al. 2025; H. Sun et al. 2025) and EP 250108a (W. X. Li et al. 2025; J. C. Rastinejad et al. 2025; G. P. Srinivasaragavan et al. 2025) is well established; thus, we also show the comparison of the FXTs in our sample with the GRB-SNe events, SN 1998bw and SN 2006aj. SN 1998bw was the first GRB-SN event (T. J. Galama et al. 1998). The intrinsic BVR data for SN 1998bw are taken from A. Clocchiatti et al. (2011). The total extinction-corrected B- and V-band data (subjected to host-flux

correction too) for SN 2006aj are obtained from P. Ferrero et al. (2006). The FXT EP 250108a appears similarly luminous as GRB-SN events.

Overall, we find that the properties of FXTs with optical counterparts in our sample align well with low-luminosity GRBs. Thus, we utilize REDBACK (N. Sarin et al. 2024) to model the broadband afterglow, incorporating the "gaussiancore" structured jet model to fit the optical light curves of three best studied and best followed FXTs in the literature, i.e., EP 240315a, EP 240414a, and EP 241021a. This model has been successful in explaining the GRB afterglows (e.g., R. Gupta et al. 2024). To avoid the problem of Lyα leaking, only bands $\geqslant i$ bands are used in fitting. The "gaussiancore" structured jet model is parameterized by a normalization E_0, a width $\theta_{\rm core}$, and a truncation angle $\theta_{\rm truncation}$ outside of which the energy is initially zero. $\theta_{\rm observer}$ is the viewing angle, ϵ_B is the fraction of thermal energy in the magnetic field, and a fraction ξ_N of the electron population is shock-accelerated electrons with a fraction ϵ_e of thermal energy. The model is explicitly discussed in G. Ryan et al. (2020). We used the default range of parameters specified in REDBACK. Figure 9 shows that barring the initial decline after the first detection, the rest of the luminosities could be nearly produced by the afterglow model (for examples on GRB afterglows, see R. Sari et al. 1998, 1999; R. Gupta 2023). The details of the posterior distribution for each of the sources are mentioned in Table B1. The "corner" plot displaying the posteriors from fitting for EP 240414a is shown in Figure 10. These results further favor the FXT-GRB link.

5. Conclusions

Following the detection of the optical counterpart of EP 240315a, a growing number of telescopes have initiated prompt and systematic follow-up observations whenever the EP mission reports a new FXT. This increased attention from the astronomical community has led to a surge in the follow-up observations of FXTs, aiming to capture and analyze these transient events across different wavelengths. In this study, we have conducted an extensive search for the optical counterparts of FXTs discovered by the EP mission during its first year of operation, utilizing the 40 cm SLT and 1 m LOT telescopes at the Lulin Observatory as a part of the Kinder project. We were able to observe the fields of 42 FXTs. Out of these, 12 FXTs were clearly detected in our observations. For five out of these 12, we discovered the optical counterpart candidates. There were a total of 30 remaining FXTs for which we did not detect any optical counterpart in our observations from the Lulin Observatory. We reported upper limits across various optical bands for such FXTs. Additionally, we utilized the valuable communications available on the GCN and ATel platforms to derive significant insights and conclusions:

1. EP sources with detected optical counterparts are typically identified within 7 hr after the EP-WXT discovery. These counterparts often exhibit relatively bright early-time magnitudes (16–18 mag), followed by a rapid fading trend typically declining to between 22 and 24 mag, with most counterparts clustering around 20 mag. In cases where the counterpart is discovered more than 10 hr post-trigger, the observed brightness is generally fainter, around 22 mag. We find that the sources with confirmed optical detections have a mean (median) optical magnitude of 20.89 mag (21.48 mag), with a standard deviation of 1.81 mag. Further, the mean (median) time of the optical detection after the X-ray discovery is 10.92 hr (4.76 hr), with a standard deviation of 12.74 hr. When compared with GRBs, the earliest mean (median) r-/R-band magnitude of GRBs appears brighter than FXTs because a large number of GRBs are discovered in optical bands much earlier (and hence brighter than FXTs) in time, when compared to FXTs.
2. The EP sources with nondetection in the optical bands are reported with a mean (median) limiting magnitude of 20.32 mag (20.50 mag), with a standard deviation of 1.44 mag. The average (median) delay in reporting the first upper limits is 18.87 hr (13.98 hr), with a standard deviation of 17.63 hr. Hence, we conclude that the following three causes for the nondetection of the optical counterparts for a major fraction of FXTs: (a) delayed trigger of the telescopes to search for optical counterparts, (b) the optical counterparts are intrinsically very faint, and (c) there are no optical counterparts at all, similar to many GRBs.
3. The redshift and luminosity distributions of FXTs observed in our study closely match those of GRBs, especially at the faint end. For a given redshift, the FXTs lie toward the faint end of the GRB populations. Additionally, only 23 out of the 72 high-SNR FXTs discovered by the EP mission show optical afterglows, and the remaining 49 are not detected in optical wavelengths. The nondetection in optical wavelengths supports the interpretation that a major fraction of EP mission discovered FXTs represents a population of "dark FXTs," similar to "dark GRBs."
4. The multiband optical luminosities of EP 240315a and EP 240801a were also consistent with jetted TDE events. However, the direct association of EP 240315a with GRB 240315A ruled out the possibility of it being linked to the jetted TDE event. The detection of EP 240801a by Fermi-GBM ruled out the possibility of it being a TDE. Additionally, EP 240416a, EP 241201a, and EP 241202b were consistent with the jetted TDE event had they been high-redshift ($z = 4.859$) events.
5. We notice that for a few FXTs, namely, EP 240413a, EP 240918b, EP 240918c, EP 241104a, EP 241115a, EP 241125a, EP 241206a, EP 241201a, and EP 241202b, EP 241208a, only one, two, or three telescopes were triggered to search for their optical counterparts. For these sources, either the EP detection GCNs are delayed ($>$10 hr since detection) or the GCNs are on weekends. Hence, automated follow-up observations and a wide, time-zone-distributed observational network are crucial for improving the detection rate of optical counterparts.

These findings highlight the critical role of prompt optical follow-up in unveiling the nature of FXTs. Their high-energy origins are likely associated with GRBs, particularly at the faint end of the luminosity distribution. The large fraction of EP mission discovered FXT events are detected without optical counterparts, which supports the interpretation that many EP FXTs constitute a population of "dark FXTs," analogous to the so-called "dark GRBs." While TDEs remain a

possible origin for some events, our sample disfavors SN SBOs and kilonovae as dominant contributors. Continued rapid-response observations will be essential for building a statistically significant sample and advancing our understanding of these energetic transients. Future efforts combining multiwavelength and spectroscopic follow-up will be crucial to further constrain their physical properties and explosion mechanisms.

Acknowledgments

We thank the anonymous referee for providing constructive comments that further improved the manuscript significantly. We acknowledge the EP team for their great work and useful communication. A.A. and T.-W.C. thank Ed Hsing-Wen Lin for useful discussions.

A.A. and T.-W.C. acknowledge the Yushan Young Fellow Program by the Ministry of Education, Taiwan, for the financial support (MOE-111-YSFMS-0008-001-P1). T.-W.C. acknowledges funding from the National Science and Technology Council, Taiwan (NSTC grant 114-2112-M-008-021-MY3) to support GREAT Lab. S.Y. acknowledges the funding from the National Natural Science Foundation of China under grant No. 12303046, the Startup Research Fund of Henan Academy of Sciences No. 242041217, and the Joint Fund of Henan Province Science and Technology R&D Program No. 235200810057. S.J. S. acknowledges funding from STFC Grants ST/T000198/1, ST/Y001605/1, a Royal Society Research Professorship, and the Hintze Charitable Foundation. H.F.S. is supported by Schmidt Sciences. A.A. is supported by the European Research Council (ERC) under the European Union's Horizon 2020 research and innovation program (grant agreement No. 948381). R.G. was sponsored by the National Aeronautics and Space Administration (NASA) through a contract with ORAU. The views and conclusions contained in this document are those of the authors and should not be interpreted as representing the official policies, either expressed or implied, of NASA or the US Government. The US Government is authorized to reproduce and distribute reprints for government purposes, notwithstanding any copyright notation herein. M.N. is supported by ERC under the European Union's Horizon 2020 research and innovation program (grant agreement No. 948381). Y.C.P. is supported by the National Science and Technology Council (NSTC grant 112-2112-M-008-026-MY3).

This publication has made extensive use of data collected at the Lulin Observatory, partly supported by the TAOVA grants NSTC 112-2740-M-008-002 and NSTC 113-2740-M-008-005. We are thankful to the Lulin Observatory observing staff for promptly conducting our ToO observations. We are also thankful to the PIs of the accepted proposals for LOT to facilitate smooth ToO observations from the Lulin Observatory.

Facilities: LO:1m, Swift (XRT and UVOT).

Software: `IRAF` (D. Tody 1986, 1993), astropy (Astropy Collaboration et al. 2013, 2018), `SExtractor` (E. Bertin & S. Arnouts 1996), `hotpants` (A. Becker 2015), `SciPy` (P. Virtanen et al. 2020), `NumPy` (C. R. Harris et al. 2020), `matplotlib` (J. D. Hunter 2007), `ChatGPT`.[17]

[17] ChatGPT serves as a grammar checker and a paraphrasing tool (Introducing ChatGPT, https://openai.com/blog/chatgpt).

Appendix A
Follow-up Description

A.1. Summary: Sources with Confirmed Detection

In this section, we discuss the observational details of the remaining FXTs whose optical counterparts were also detected from the Lulin Observatory, but that we were not the first to discover.

A.1.1. EP 240315a

EP 240315a was discovered at 2024-03-15T20:10:44 by the EP-WXT while performing a calibration observation. In the J2000 epoch, the reported X-ray transient had a R.A. = +141.644 deg and a corresponding decl. = −9.547 deg with an uncertainty of 3′ in radius (W. J. Zhang et al. 2024a). Soon after the EP-WXT discovery, S. Srivastav et al. (2024b) noticed that the normal survey mode observations from ATLAS[18] had serendipitously visited the EP-WXT localization of this FXT multiple times. Thus, a careful examination of the field resulted in the detection of an optical counterpart candidate AT 2024eju within the EP-WXT localization error circle. This candidate was detected just 1.1 hr after the EP-WXT discovery of EP 240315a, at coordinates R.A. = 141.64763 deg and decl. = −9.53401 deg ($09^{h}26^{m}35\overset{s}{.}43, -09°32'02\overset{''}{.}4$) with an ATLAS *cyan*-band magnitude of 19.38 ± 0.08 (J. H. Gillanders et al. 2024). After the serendipitous optical counterpart detection by ATLAS, we were the first to perform the follow-up observations using the 40 cm SLT in the *r* band. The details of our photometry are presented in Table 3. Later, J. H. Gillanders et al. (2024) reported the first-ever discovery of optical and radio counterparts for an FXT. Thus, EP 240315a was the first FXT with detection in X-ray, optical, and radio bands.

Several studies were undertaken to explore the nature and origin of EP 240315a. A consistent pattern emerged across all these studies, leading to the compelling conclusion that EP 240315a had a GRB origin (J. H. Gillanders et al. 2024; A. J. Levan et al. 2024a; Y. Liu et al. 2024; R. Ricci et al. 2025). For instance, the timing and spatial localization of EP 240315a, when cross-referenced with GRB 240315C, revealed a strong correlation indicating its GRB origin (Y. Liu et al. 2024; R. Ricci et al. 2025). Additionally, models simulating the evolution of EP 240315a under the assumption of a GRB origin have successfully reproduced key observational features (R. Ricci et al. 2025). Moreover, the temporal and spectral characteristics of EP 240315a closely matched those typically associated with GRBs (A. J. Levan et al. 2024a; Y. Liu et al. 2024). We saw that the "gaussiancore" structured-jet model could provide good fits to its optical light curves, strenghtening its association with GRBs. The details of the posterior distribution are mentioned in Table A1.

A.1.2. EP 240801a

EP 240801a was first detected by EP-WXT at the sky coordinates of R.A. = 345.140 deg and decl. = +32.610 deg with an uncertainty of 2′.4 in radius (H. Zhou et al. 2024c). The EP-WXT trigger began at 2024-08-01T09:06:03. The EP-Follow-up X-ray Telescope trigger started autonomously 180 s after the EP-WXT detection. The follow-up observations from

[18] https://atlas.fallingstar.com

Table A1
Posterior Distribution of the "Gaussiancore" Structured Jet Model from REDBACK Fittings for Three of the Best Studied FXTs in the Literature, i.e., EP 240315a, EP 240414a, and EP 241021a

Parameters	Range	Nature of Priors	EP 240315a	EP 240414a	EP 241021a
$\theta_{\rm observer}$ (rad)	[0, 1.5707963267948966]	Sine	$0.21-0.07+0.04$	$0.30-0.03+0.03$	$0.18-0.01+0.02$
$\log_{10} E_0$ (erg)	[44, 54]	Uniform	$53.57-0.43+0.29$	$53.44-0.40+0.35$	$53.72-0.33+0.20$
$\theta_{\rm core}$ (rad)	[0.01, 0.1]	Uniform	$0.08-0.02+0.01$	$0.09-0.01+0.00$	$0.09-0.01+0.01$
$\theta_{\rm truncation}$	[1, 8]	Uniform	$5.73-2.10+1.33$	$2.47-0.13+0.30$	$1.14-0.08+0.09$
$\log_{10} n_{\rm ism}$ ($\rm cm^{-3}$)	[−5, 2]	Uniform	$0.02-1.97+1.22$	$-2.80-0.32+0.40$	$-1.61-0.52+0.57$
p	[2, 3]	Uniform	$2.49-0.30+0.32$	$2.95-0.06+0.03$	$2.59-0.23+0.15$
$\log_{10} \epsilon_e$	[−5, 0]	Uniform	$-0.44-0.38+0.24$	$-0.90-0.28+0.30$	$-0.82-0.21+0.20$
$\log_{10} \epsilon_B$	[−5, 0]	Uniform	$-1.13-1.17+0.78$	$-0.18-0.29+0.13$	$-1.87-0.48+0.71$
ξ_N	[0.0, 1.0]	Uniform	$0.64-0.35+0.27$	$0.33-0.16+0.26$	$0.79-0.21+0.15$
Γ_0	[100, 2000]	Uniform	$1029.39-640.11+659.87$	$1105.85-657.46+608.00$	$894.78-523.09+677.39$

Note. We used the default range of parameters specified in REDBACK.

the EP-Follow-up X-ray Telescope detected an uncataloged X-ray source at the sky coordinates of R.A. = 345.1630 deg and decl. = +32.5927 deg with an uncertainty of 10″ in radius (H. Zhou et al. 2024c). Recently, S.-Q. Jiang et al. (2025) reported its detection by Fermi-GBM, thus indicating EP 240801a also had a GRB link.

Followed by the EP-WXT discovery and EP-Follow-up X-ray Telescope confirmation, several telescopes searched for the optical counterpart candidate associated with EP 240801. The optical observations by S. Y. Fu et al. (2024c) proposed the detection of an optical counterpart at R.A. = $23^{\rm h}00^{\rm m}39\overset{\rm s}{.}019$ decl. = +32°35′37″.20 with an R-band magnitude of 20.32 ± 0.16. The proposed candidate optical counterpart was further confirmed by multiple observations (J. An et al. 2024d; A. Aryan et al. 2024e; R. Z. Li et al. 2024b; D. B. Malesani et al. 2024c; A. Moskvitin et al. 2024; A. S. Moskvitin et al. 2024b; L. Moretti et al. 2024; A. S. Moskvitin et al. 2024c; N. Pankov et al. 2024b; I. Pére-z-Fournon et al. 2024a; N. Pankov et al. 2024f, 2024g; D. Turpin et al. 2024; W. Zheng et al. 2024j; Z. P. Zhu et al. 2024c). Our observations in the r band using SLT started about 4.66 hr after the EP-WXT discovery (A. Aryan et al. 2024e). The details of our photometry are presented in Table 3. GTC spectroscopy of the proposed optical counterpart candidate detected a well-defined continuum over a wavelength range of 5100–10000 Å (J. Quirola-Vásquez et al. 2024g). The presence of several absorption lines in the GTC spectrum was interpreted to originate from Mg II and Fe II ions, indicating a common redshift of 1.673 for EP 240801a. Later, the Keck/LRIS spectroscopic observations by W. Zheng et al. (2024a) also confirmed the GTC proposed redshift. The detailed multiwavelength analysis by S.-Q. Jiang et al. (2025) showed the resemblance of EP 240801a with GRB 221009A (BOAT; E. Burns et al. 2023) under the assumption of two-component jet models. Thus, EP 240801a was probably another off-axis jet or intrinsically weak GRB.

A.1.3. EP 241021a

The EP-WXT discovered EP 241021a at 2024-10-21T05:07:56. It was detected at sky coordinates of R.A. = 28.852 deg and decl. = 5.957 deg with an uncertainty of 2.′4 in radius (J. W. Hu et al. 2024c). A follow-up observation using the EP-Follow-up X-ray Telescope was also performed about 36.5 hr after the EP-WXT discovery. The EP-Follow-up X-ray Telescope follow-up observation detected an uncataloged X-ray source at R.A. = 28.8483 deg and decl. = 5.9395 deg with an uncertainty of 10″ in radius (Y. Wang et al. 2024a).

Followed by the EP-WXT discovery and EP-Follow-up X-ray Telescope follow-up observations, several telescopes were triggered to search for the optical counterpart. Some early observations with shallow limits did not detect any optical counterpart (B. P. Gompertz et al. 2024; V. Lipunov et al. 2024j). However, about 1.77 days after the EP-WXT discovery, S. Y. Fu et al. (2024h) proposed a plausible candidate at R.A. = $01^{\rm h}55^{\rm m}23\overset{\rm s}{.}41$ decl. = +05°56′18″.01 with a z-band magnitude of 21.60 ± 0.11. The proposed optical counterpart candidate was rigorously followed in several observations (A. Bochenek & D. A. Perley 2024a; M. Busmann et al. 2024b, 2024c; J. Freeburn et al. 2024c; S. Y. Fu et al. 2024g; J. J-Jin et al. 2024; A. Kumar et al. 2024a; W. X. Li et al. 2024a, 2024b; A. S. Moskvitin et al. 2024d, 2024e; A. K. Ror et al. 2024; W. Zheng et al. 2024o; J. Freeburn & I. Andreoni 2024; B. Schneider & C. Adami 2024b).

About 6.8 days after the EP-WXT discovery, J. A. Quirola-Vasquez et al. (2024f) reported the rebrightening of the optical counterpart. The optical rebrightening was further confirmed by several other observations (A. Bochenek & D. A. Perley 2024b; J. Freeburn et al. 2024a; N. Klingler et al. 2024; A. S. Moskvitin et al. 2024a; Y. Pan et al. 2024; B. Schneider & C. Adami 2024a).

The optical spectroscopy using VLT/FORS2 detected the presence of a strong emission line of [O II] at 3728 Å and Mg II doublet absorption feature at 4897 Å around a common redshift of $z = 0.75$ (G. Pugliese et al. 2024). This redshift was also confirmed by I. Pérez-Fournon et al. (2024c) and W. Zheng et al. (2024c). Thus, we adopt a redshift $z = 0.75$ in the current work.

The first epoch of observations from the 40 cm SLT in the r band started about 1.3 days after the EP-WXT discovery; however, we did not detect the proposed optical counterpart up to a limit of 19.6 mag (S. Yang et al. 2024a). Although during the rebrightening episode of the FXT, we detected the optical counterpart. Our observations during the rebrightening episode using the 1 m LOT in the r band started about 11.44 days after the EP-WXT trigger (A. Aryan et al. 2024a). The details of our photometry are presented in Table 3.

About 3 days after the EP-WXT trigger, e-MERLIN radio observations did not reveal any significant radio source (G. Gianfagna et al. 2024). Interestingly, a significant radio

counterpart was detected in ATCA radio observation about 8.4 days after the EP-WXT trigger (R. Ricci et al. 2024a). Thus, EP 241021a was the third FXT in our sample with X-ray, optical, and radio counterparts. Later, the radio counterpart was also detected by F. Carotenuto et al. (2024) and G. Schroeder et al. (2024). About 65 days after the EP-WXT trigger, Submillimeter Array radio observations at 235 GHz did not reveal any significant source up to an upper limit of 0.8 mJy (A. Aryan et al. 2025).

Elaborative analysis of EP 241021a displaying exceptional rebrightening suggested a likely link between EP-discovered FXTs and low-luminosity GRBs (M. Busmann et al. 2025). Detailed multiwavelength analyses by S. Xinwen et al. (2025) indicated the launch of a relativistic jet, which was further confirmed by M. Yadav et al. (2025) through radio observations. The study by G. Gianfagna et al. (2025) proposed an of f-axis jet and cocoon scenario. Another multiwavelength analysis of EP 241021a by G.-L. Wu et al. (2025) suggested it to be an explosion-type event accompanied by a moderately relativistic jet.

A.1.4. EP 241030a

EP 241030a was discovered by EP-WXT at the sky coordinates at 2024-10-30T06:33:18 with R.A. = 343.013 deg and decl. = 80.449 deg having an uncertainty of 2.′4 in radius (H. Z. Wu et al. 2024) and was found coincident with GRB 241030A (Fermi-GBM team 2024a). About 2.8 days after the EP-WXT discovery, EP-Follow-up X-ray Telescope follow-up observations also detected the afterglow in X-ray (Y. F. Liang et al. 2024f).

Soon after the EP-WXT discovery, several telescopes were triggered to search for the optical counterpart. The optical counterpart of GRB 241030a/EP 241030a was first discovered by N. J. Klingler et al. (2024) at R.A. = $22^{h}52^{m}33\overset{s}{.}57$ and decl. = $+80°26'59\overset{''}{.}9$ in Swift-UVOT with an estimated magnitude of 15.42 ± 0.14 (quoted error was 1σ). The optical counterpart was confirmed in several other observations (M. Busmann et al. 2024a, A. Moskvitin & V. P. Goranskij 2024; Y. S. Yan et al. 2024; C. Adami & B. Schneider 2024; A. Reguitti et al. 2024).

The spectroscopic observations of the optical counterpart showed the presence of numerous narrow absorption lines, including Mg II doublets at redshifts of 0.456, 0.862, and 1.411 (W. Zheng et al. 2024b). Further spectroscopic follow-up observations by R. Z. Li et al. (2024a) revealed a strong absorption line of Al II at 1671 Å, along with weaker absorption lines of Fe II at 2374, 2383, 2587, and 2600 Å, Mg II at 2800 Å, and Mg I at 2852 Å. All these metal features indicated a common redshift of around 1.4, consistent with W. Zheng et al. (2024b). Thus, we adopt $z = 1.411$ for EP 241030a in the present work. Our observations from 1 m LOT in the *r* band started about 2.30 days after the EP-WXT discovery (A. Aryan et al. 2024a). The details of our photometry are presented in Table 3.

A.1.5. EP 241107a

EP 241107a was discovered by EP-WXT at 2024-11-07T14:10:23. About 5 minutes later, an autonomous observation by EP-Follow-up X-ray Telescope also discovered an X-ray source at R.A. = 35.0085 deg and decl. = 3.3329 deg with an uncertainty of 10″ in radius (H. Zhou et al. 2024d).

Followed by EP-WXT and EP-Follow-up X-ray Telescope observations, several telescopes were quickly triggered to search for the optical counterpart. Only about 90 minutes after the EP-WXT trigger, M. Odeh et al. (2024b) reported the discovery of a bright optical counterpart candidate at R.A. = $02^{h}20^{m}02\overset{s}{.}45$ decl. = $+03°20'02\overset{''}{.}2$ in the *Ic* band with 17.85 ± 0.18 mag. The proposed optical counterpart was confirmed in several optical/NIR follow-up observations (W. X. Li et al. 2024c; M. Odeh et al. 2024a; W. Zheng et al. 2024k, SVOM/C-GFT Team et al. 2024; Mohan et al. 2024c; M. Bussman et al. 2024d; C. Adami et al. 2024a). Our observations from the 1 m LOT in the *r* band started about 1.02 days after the EP-WXT trigger (A. K. H. Kong et al. 2024a). The details of our photometry are presented in Table 3.

A radio follow-up observation using the Very Large Array (VLA) revealed a point radio source at a location consistent with the optical counterpart (A. Balasubramanian et al. 2024). Thus, EP 241107a is the fourth source in our sample having X-ray, optical, and radio counterparts.

A.1.6. EP 241217a

The EP-WXT discovered EP 241201a at 2024-12-17T05:36:03. It was discovered at sky coordinates of R.A. = 46.957 deg and decl. = 30.901 deg with an uncertainty of 2.′8 in radius (H. Zhou et al. 2024b). Followed by EP-WXT discovery, an EP-Follow-up X-ray Telescope follow-up observation was also performed, which detected an uncatalogued X-ray source at R.A. = 46.9398, decl. = 30.9299 deg with an uncertainty of about 20″ in radius (H. Zhou et al. 2024b). The Fermi-GBM observations in a time interval of −50 to +500 s from the EP-WXT trigger did not reveal any GRB-like detection coinciding with the EP 241217a spatially and temporally. However, between a time interval of T_0+24.2 to T_0+25.7 ks, the Swift-X-Ray Telescope (XRT) detected an uncatalogued source consistent with the EP-Follow-up X-ray Telescope localization (M. A. Williams et al. 2024).

Quickly after the EP-WXT discovery, several telescopes were triggered to search for any associated optical counterpart. Approximately 2.5 hr after the EP-WXT discovery, observations by A. J. Levan et al. (2024d) discovered a candidate optical counterpart at R.A. = $03^{h}07^{m}46\overset{s}{.}20$ and decl. = $+30°55'45\overset{''}{.}9$ with a *z*-band magnitude of ∼19.9. The candidate optical counterpart was confirmed in several other follow-up observations (A. Bochenek & D. A. Perley 2024c; D. Liu et al. 2024; L. Izzo & D. B. Malesani 2024a; J. Jin et al. 2024; T. Mohan et al. 2024b; Z. P. Zhu et al. 2024d).

The spectroscopic observations of the optical counterpart by A. J. Levan et al. (2024c) detected a bright continuum with a strong break at ∼6820 Å, along with several narrow absorption lines of Si II, C II, weak C IV, Fe II, and Al II, all at a common redshift of $z = 4.59$. Thus, in the present work, we adopted a redshift of 4.59 for EP 241217a. Our observations from 1 m LOT in the *r* band started about 7.34 hr after the EP-WXT discovery. We clearly detected the optical counterpart candidate (L. L. Fan et al. 2024a). The details of our photometry are presented in Table 3.

The field of EP 241217a was also scanned by a few radio telescopes. About 2.45 days after the EP-WXT discovery, the e-MERLIN radio observations at 5 GHz did not reveal any significant radio source down to 96 μJy (R. Ricci et al. 2024b). However, about 3.81 days after the EP-WXT discovery, the

VLA observations detected a point radio source consistent with EP 241217a having 20 ± 6.6 μJy at 3 GHz, 58 ± 4 μJy at 6 GHz, and 99.3 ± 4.1 μJy at 10 GHz (T. An et al. 2025a). Thus, EP 241217a is the fifth source in our sample having X-ray, optical, and radio counterparts.

A.1.7. EP 250108a

EP 241201a was discovered by EP-WXT at 2024-12-17T05:36:03 with the sky coordinates of R.A. = 55.623 deg and decl. = −22.509 deg with an uncertainty of $2\farcm2$ in radius (R. Z. Li et al. 2025a). Followed by EP-WXT discovery, an EP-Follow-up X-ray Telescope follow-up observation was also performed about 22.2 hr later, but no X-ray counterpart was detected (R. Z. Li et al. 2025b).

Followed by the EP-WXT discovery and EP-Follow-up X-ray Telescope follow-up observations, several telescopes were triggered to search for any associated optical counterpart candidate. About 31.5 hr after the EP-WXT discovery, R. Eyles-Ferris (2025) proposed an optical counterpart candidate at R.A. = $03^{\rm h}42^{\rm m}28\fs38$ decl. = $-22°30'\,21\farcs1$ with a g'-band magnitude of 20.10 ± 0.06. The proposed optical counterpart candidate was confirmed by several follow-up observations (A. Kumar et al. 2025a; A. J. Levan et al. 2025a; L. Izzo 2025; D. B. Malesani et al. 2025; A. S. Moskvitin et al. 2025; F. F. Song et al. 2025; Z. P. Zhu et al. 2025b; X. Zou et al. 2025). The spectroscopic observations by Z. P. Zhu et al. (2025a) detected a bright and blue continuum. Emission lines from H_α, [O II] 3727/29 Å, faint [O III] 5007 Å, (narrow) absorption from Ca II H and K were detected at a common redshift of $z = 0.176$. Thus, we adopted a redshift of 0.176 in the present work for EP 250108a.

About 10.3 days after the EP-WXT trigger, R. A. J. Eyles-Ferris et al. (2025b) claimed to observe the rebrightening episode, which was confirmed in further follow-up observations (A. J. Levan et al. 2025b; A. K. Ror et al. 2025; D. Xu et al. 2025). Additionally, the spectroscopic follow-up observations during the rebrightening episode revealed consistent features matching Type Ic BL SNe (A. J. Levan et al. 2025b; D. Xu et al. 2025). SNe Type Ic BL are typically associated with collapsar origin GRBs. Our observations from 1 m LOT in the r band started about 7.95 days after the EP-WXT discovery. We clearly detected the optical counterpart candidate. The details of our photometry are presented in Table 3. No significant radio counterpart was detected (T. An et al. 2025b; F. Carotenuto et al. 2025; G. Schroeder et al. 2025).

The optical counterpart of the X-ray transient EP 250108a was identified as SN 2025 kg, a Type Ic BL SN (R. A. J. Eyles-Ferris et al. 2025a; J. C. Rastinejad et al. 2025; G. P. Srinivasaragavan et al. 2025). Analysis of the well-sampled light curves by W. X. Li et al. (2025) pointed toward a mildly relativistic outflow as the likely origin of the event. R. A. J. Eyles-Ferris et al. (2025a) found that the observed X-ray and radio properties were consistent with a low-energy jet, likely produced by a collapsar, that probably failed to penetrate the surrounding dense material. They further proposed that the optical emission might originate from a cocoon of shocked material surrounding the trapped jet. Supporting this scenario, J. C. Rastinejad et al. (2025) indicated similar results with the broadband data being consistent with a trapped or low-energy jet-driven explosion from a collapsar with a ZAMS mass of 15–30 $M_\odot$. Additionally, G. P. Srinivasaragavan et al. (2025) further reinforced the connection of EP 250108a with low-luminosity GRBs.

A.2. Summary: Sources with Upper Limits

This section presents a summary of FXTs followed from the Lulin Observatory that do not have confirmed optical detections in our observations, and we only provide optical upper limits.

A.2.1. EP 240331a

EP 240331a was discovered by EP-WXT at 2024-03-31T22:07:17. It was detected at sky coordinates of R.A. = 169.414 deg and decl. = −20.042 deg with an uncertainty of $20'$ in radius (X. Pan et al. 2024a). The large uncertainty in localization was attributed to the incomplete calibration of the detector. Followed by the EP-WXT discovery of EP 240331a, a few telescopes started the search for the optical counterpart of EP 240331a within a day. None of these observations detected any optical counterpart (M. Freeberg et al. 2024; P. Groot et al. 2024; V. Lipunov et al. 2024a). Our observations from 1 m LOT in the r band started about 17.62 hr after the EP-WXT trigger. We also utilized the 40 cm SLT for the g-band observations. For our observations, we used four different pointings in each band to significantly cover the entire error circle of localization. In the r band, each pointing had a total exposure time of 4×300 s, while in the g band, three pointings had an exposure time of 4×300 s, while one had an exposure time of 3×300 s. We find no evidence of a new source in any of the four pointings for each band. The upper limits in different bands are presented in Table B1. We provided the deepest upper limits that further confirmed the nondetection of any significant optical counterpart associated with EP 240331a. Our preliminary photometry was reported in T. W. Chen et al. (2024b).

A.2.2. EP 240408a

EP-WXT detected EP 240408a at 2024-04-08T17:56:30. It was detected at the sky coordinates of R.A. = 158.840 deg and decl. = −35.749 deg with an uncertainty of $3'$ in radius (J. W. Hu et al. 2024d). Besides the EP mission, Swift-XRT follow-up observations also confirmed the new FXT EP 240408a, about 33 hr after the EP-WXT discovery (J. W. Hu et al. 2024e). None of the follow-up observations in optical bands detected any optical counterpart within the specified EP-WXT error circle (G. Antipov et al. 2024b; W. X. Li et al. 2024l; I. Perez-Garcia et al. 2024b). Although A. Rau (2024) suggested a potential counterpart detection in the NIR J and H bands, they noted that the identified source was also there in the z-band data from the Legacy survey DR10.[19]. The 10th Legacy survey data were released in 2023 September (much earlier than EP 240408a was detected); thus, it was difficult to constrain whether the detected NIR counterpart candidate was actually associated with EP 240408a. About 42.38 hr after the EP-WXT discovery, our observations from 1 m LOT started in the r band for a total exposure time of 26×180 s. Also, the i-band follow-up observations using the 40 cm SLT began at 42.74 hr after the EP-WXT discovery for a total exposure time of 15×300 s.

[19] https://www.legacysurvey.org/

The upper limits in different bands for our follow-up observations are presented in Table B1.

A.2.3. EP 240413a

The EP team reported the detection of EP 240413a by EP-WXT at 2024-04-13T14:39:37. The sky coordinates of this source were R.A. = 228.794 deg and decl. = −18.800 deg with an uncertainty of 20′ in radius (T. Y. Lian et al. 2024c). The big uncertainty in the localization, compared to the usual value, was due to the incomplete calibration of the EP-WXT module. Followed by the EP-WXT discovery, the EP-Follow-up X-ray Telescope also performed the follow-up observations. The EP-Follow-up X-ray Telescope unambiguously detected an X-ray source at R.A. = 228.815 deg and decl. = −18.503 deg with an uncertainty of 30″ in radius (C. K. Li et al. 2024). Followed by the EP-WXT discovery and EP-Follow-up X-ray Telescope follow-up observations of EP 240413a, a few telescopes searched for the possible optical counterpart associated with the FXT. None of them found any optical counterpart (K. A. Pall'e et al. 2024; D. R. Xiong et al. 2024a). Our observations from 1 m LOT started about 73.55 hr after the EP-WXT trigger for a total exposure time of 6×300 s in the r band. The upper limit in the r band is presented in Table B1.

A.2.4. EP 240506a

EP 240506a was discovered by EP-WXT at 2024-05-06T05:01:39 while performing the calibration tests. The sky coordinates of the EP source were R.A. = 213.978 deg and decl. = −16.715 deg with an uncertainty of 3′ in radius (D. Y. Li et al. 2024b). Several telescopes were triggered to search for the possible optical counterpart associated followed by the EP-WXT discovery. However, none of them found any detection within reported EP-WXT localization (J. J. Jin et al. 2024; N. Pankov et al. 2024e; I. Perez-Garcia et al. 2024c; S. Tinyanont et al. 2024a). Our observations from the 40 cm SLT started about 32.10 hr after the EP-WXT trigger with a total exposure time of 30×300 s in the r band. The upper limits in different bands are presented in Table B1. Our preliminary photometry was reported in A. Aryan et al. (2024i). Further, N. Chang et al. (2024) did extensive archival radio searching. They found one radio detection in the Rapid ASKAP Continum Survey (RACS; C. L. Hale et al. 2021) data within the EP-WXT localization error circle. The radio fluxes of the specified source showed a power-law spectral index of −1.47. This radio source was found to be 2′ away from a variable star, SDSS J141557.82-164317.2. On inspecting the ALLWISE[20] source catalog further, they found WISEA J141556.28-164124.4 to be only 2″ away from the RACS source, ultimately concluding that the detected radio source in archival radio images could be a background galaxy.

A.2.5. EP 240617a

EP 240617a was discovered by EP-WXT at 2024-06-17T12:19:13. It was detected at sky coordinates of R.A. = 285.030 deg and decl. = −22.561 deg with an uncertainty of 3′ in radius (H. Zhou et al. 2024a). Followed by the EP-WXT discovery of EP 240617a, J. Yang et al. (2024) reported the discovery of a weak, untriggered gamma-ray transient in Fermi-GBM[21] data within the EP 240617a occurrence time interval. The location of the Fermi-GBM-detected transient aligned with the EP-WXT localization. Based on the spatial and temporal coincidence of EP 240617a, J. Yang et al. (2024) concluded it to be a GRB event. About 77 hr after the EP-WXT discovery, H. Sun et al. (2024b) reported a weak X-ray signal from Swift-XRT consistent with the EP-WXT localization. Several telescopes were also triggered to search for the optical counterpart, but none of them detected any candidate (I. Perez-Garcia et al. 2024d; A. Santos et al. 2024). Our observations from the 40 cm SLT started about 30.95 hr after the EP-WXT trigger with a total exposure time of 6×300 s in the r band. The upper limits in different bands are presented in Table B1.

A.2.6. EP 240618a

The EP team reported the EP 240618a detection by EP-WXT discovered at 2024-06-18T05:43:43. The sky coordinates of this source were R.A. = 281.627 deg and decl. = +23.820 deg with an uncertainty of 3′ in radius (H. Sun et al. 2024a). About an hour after the EP-WXT discovery, the EP-Follow-up X-ray Telescope also began follow-up observations, and unambiguously detected an X-ray source at R.A. = 281.648 deg and decl. = +23.833 deg with an uncertainty of 30″ in radius (H. Sun et al. 2024a). About 58 hr after the EP-WXT discovery of EP 240618a, Swift-XRT also observed the EP-Follow-up X-ray Telescope localization. However, no significant X-ray counterpart was detected within the EP-Follow-up X-ray Telescope localization error circle with a radius of 30″ (W. Chen et al. 2024b). Additionally, exploring the Fermi-GBM data, M. E. Ravasio & P. G. Jonker (2024) also reported the nondetection of any significant gamma-ray source. Several optical/NIR follow-up observations were also triggered after the EP-WXT and EP-Follow-up X-ray Telescope detections of EP 240618a. However, none of those observations found any strong evidence of a counterpart candidate (C. Adami et al. 2024b; D. Akl et al. 2024b; W. X. Li et al. 2024d; X. Liu et al. 2024b, 2024c; N. Pankov et al. 2024c; S. Tinyanont et al. 2024b; S. Y. Wu et al. 2024). Our observations from the 40 cm SLT started about 11.81 hr after the EP-WXT trigger for a total exposure time of 10×300 s in the r band. We did multiepoch follow-up observations but did not detect any optical counterpart. The upper limits in different bands are presented in Table B1.

A.2.7. EP 240625a

EP 240625a was discovered by EP-WXT at 22024-06-25T01:48:23. The sky coordinates of this source were R.A. = 310.760 deg and decl. = −15.966 deg with an uncertainty of 2′ in radius (X. Pan et al. 2024b). Following the EP-WXT discovery, the EP-Follow-up X-ray Telescope performed follow-up observations about an hour after the EP-WXT discovery. The EP-Follow-up X-ray Telescope clearly detected a slowly fading X-ray source at R.A. = 310.7308 deg and decl. = −15.9760 deg with an uncertainty of 10″ in radius (X. Pan et al. 2024c). Followed by the EP-WXT and EP-Follow-up X-ray Telescope detection, a few telescopes were triggered to search for the possible optical counterpart. S. Y. Fu et al. (2024b) proposed a marginally detected source within the EP-Follow-up X-ray Telescope localization error circle as the optical counterpart candidate for EP 240625a;

[20] https://wise2.ipac.caltech.edu/docs/release/allwise/

[21] https://fermi.gsfc.nasa.gov/science/instruments/gbm.html

however, they could not completely rule out the possibility of their detection being a background fluctuation. The observations reported by D. Akl et al. (2024a) also did not find any optical counterpart candidate. We began our observations from the 40 cm SLT about 40.99 hr after the EP-WXT trigger with a total exposure time of 10×300 s in the i band. The upper limits in different bands are presented in Table B1.

A.2.8. EP 240626a

The EP team reported the EP 240626a detection by EP-WXT at 2024-06-26T06:28:28. The sky coordinates of this source were R.A. = 263.023 deg and decl. = −13.051 deg with an uncertainty of 2′ in radius (Q. Y. Wu et al. 2024a). Following the EP-WXT discovery, the EP-Follow-up X-ray Telescope also performed follow-up observations about an hour after the EP-WXT discovery. The EP-Follow-up X-ray Telescope clearly detected a faint X-ray source at R.A. = 263.0171 deg and decl. = −13.0490 deg with an uncertainty of 30″ in radius (Q. Y. Wu et al. 2024b). Several telescopes were triggered to search for the optical counterpart of EP 240626a. None of those observations claimed to have optical counterpart detection (S. Leonini et al. 2024a; I. Perez-Garcia et al. 2024f; W. Zheng et al. 2024i). Our observations from the 40 cm SLT started about 33.16 hr after the EP-WXT trigger with a total exposure time of 6×300 s in the r band. The corresponding upper limit is presented in Table B1.

A.2.9. EP 240702a

EP 240702a was discovered by EP-WXT at 2024-07-02T00:50:05. It was detected at sky coordinates of R.A. = 328.203 deg and decl. = −38.980 deg with an uncertainty of 3′ in radius (W. Chen et al. 2024a). Followed by the EP-WXT discovery of EP 240702a, a few telescopes were triggered to search for the optical counterpart. None of them found any traces of a new uncatalogued source in their observations (W. X. Li et al. 2024e; S. Tinyanont et al. 2024c). Our observations from the 40 cm SLT started about 16.05 hr after the EP-WXT trigger in the r band with a total exposure time of 35×300 s. The upper limit in the r band is presented in Table B1. Additionally, Swift-XRT follow-up observations about 8 hr after the EP-WXT discovery did not reveal any significant X-ray source within the EP-WXT localization error circle.

A.2.10. EP 240703a

The EP team reported the detection of EP 240703a by EP-WXT at 2024-07-03T00:38:40. It was detected at sky coordinates of R.A. = 273.803 deg and decl. = −9.681 deg with an uncertainty of 3′ in radius (Y. L. Wang et al. 2024a). Only ∼2 s before the EP-WXT discovery of EP 240703a, Konus-Wind[22] detected the long GRB 240703A. Owing to the temporal and spatial coincidence of EP 240703a and GRB 240703A, D. Frederiks et al. (2024) claimed EP 240703a to be the GRB 240703A counterpart. Followed by the EP-WXT and Konus-Wind detection, Swift-XRT also triggered for follow-up observations; however, Q. C. Shui et al. (2024) claimed to have no significant X-ray source detection within the EP-WXT localization of EP 240703a. Further, several telescopes were also triggered to search for the optical counterpart, but none of those claimed to have any significant detection (J. An et al. 2024c; A. Bochenek & D. A. Perley 2024d; E. Fernandez-Garcia et al. 2024; S. Tinyanont et al. 2024d; A. Volnova et al. 2024; W. Zheng et al. 2024l). Our observations from 1 m LOT started about 12.43 hr after the EP-WXT trigger in the r band with a total exposure time of 3×300 s. The upper limits in different bands are presented in Table B1. Our preliminary photometry was reported in A. Aryan et al. (2024j).

A.2.11. EP 240703c

EP 240703c was discovered by EP-WXT at 2024-07-03T18:15:00. It was detected at sky coordinates of R. A. = 289.264 deg and decl. = −30.325 deg with an uncertainty of 3′ in radius (Y. J. Zhang et al. 2024a). A previously known high proper motion star, LP 924-17, was found to be lying within the EP-WXT localization error circle. Although they suggested that the detected EP transient was not a stellar flare based on its X-ray light curve and spectrum. However, they did not completely rule out this possibility. We investigated the quick-look data from Swift-Target of Opportunity (ToO) observations of the EP-WXT localization region proposed by the EP team that constrained a relatively softer spectrum from the Swift-XRT data. Additionally, the high proper motion star is clearly detected in the Swift-UVOT V band with a magnitude of 17.76 ± 0.21 in the AB system (Y. J. Yang et al. 2024b). Followed by EP-WXT discovery of the EP 240703c, our observations from the 40 cm SLT started about 20.61 hr after the EP-WXT trigger in the r band with a total exposure time of 16×300 s. We did not detect any new and uncatalogued optical counterpart candidate. However, the high proper motion star was also clearly detected in our observations. We noticed no significant brightness enhancement for LP 924-17 through our observations. The average magnitude was found to be 16.88 ± 0.05 mag in the r band (Y. J. Yang et al. 2024b). The upper limit in the r band for our SLT observations is presented in Table B1.

A.2.12. EP 240708a

The EP team reported the EP 240708a detection by EP-WXT at 2024-07-08T23:28:23. The sky coordinates of this source were R.A. = 345.963 deg and decl. = −22.840 deg with an uncertainty of 3′in radius (W. Chen et al. 2024c). Following the EP-WXT discovery, the EP-Follow-up X-ray Telescope also performed follow-up observations about 4 hr later. The EP-Follow-up X-ray Telescope clearly detected a faint X-ray source at R.A.=345.9656 deg and decl. = −22.8428 deg with an uncertainty of 10″ in radius (J. W. Hu et al. 2024a).

Further, the EP team also obtained Swift-XRT observations about 17 hr after the EP-WXT trigger, but they did not detect any evidence of a new X-ray source within the EP-WXT localization (J. W. Hu et al. 2024a; J. Quirola-Vásquez et al. 2024c). A number of telescopes were also triggered for the search for any possible optical counterpart. None of them detected any evidence of a new and uncatalogued source within the EP-WXT localization error circle (S. Q. Jiang et al. 2024b; W. X. Li et al. 2024f; C. Wu et al. 2024; W. Zheng et al. 2024m). Our observations from the 40 cm SLT in the r band started about 18.52 hr after the EP-WXT trigger with a total exposure time of 36×300 s. We also utilized the 1 m LOT in the r band and g band to search deeper, but we did not

[22] http://www.ioffe.ru/LEA/kw/index.html

find any evidence of an optical counterpart. The upper limits in different bands are presented in Table B1. We reported our preliminary photometry in C. H. Lai et al. (2024a).

A.2.13. NVSS J004348+342626

The EP team reported the detection of the X-ray brightening of blazar NVSS J004348+342626 by EP-WXT at 2024-07-17T03:13:01. The sky localization for the EP-WXT-detected point source was R.A. = 10.955 deg and decl. = +34.428 with an uncertainty of 2.′2 in radius (S. Q. Jiang et al. 2024d). There were several X-ray sources within the EP-WXT localization error circle. The Swift-XRT observations about 1.5 days after the EP-WXT trigger detected an X-ray source at R.A. = 10.9534 deg and decl. = +34.4401 with an uncertainty of only 3.″8, consistent with the spatial localization of blazar NVSS J004348+342626, confirming the EP-WXT trigger to be associated with this blazar (S. Q. Jiang et al. 2024d).

It was the very first time that the flat-spectrum radio quasar (FSRQ) NVSS J004348+342626 was detected in the X-ray band. About 1.5 days after the EP-WXT trigger, Swift-XRT also detected an X-ray source spatially consistent with the FSRQ position. Thus, EP-WXT and Swift-XRT confirmed the triggers to be associated with NVSS J004348+342626. The X-ray detection of this FSRQ for the very first time, along with its earlier detections in the radio band (J. J. Condon et al. 1998) and in gamma rays (S. Abdollahi et al. 2020), makes it an interesting source. Followed by EP-WXT discovery, we triggered the 40 cm SLT at the Lulin Observatory and detected the FSRQ probably in its flaring stage with an *r*-band magnitude of 18.38 ± 0.05. An archival search in the optical bands by S. Garrappa et al. (2024) at two epochs (one at ∼3 days and another at ∼10 months) prior to the EP-WXT and Swift-XRT triggers indicated capturing the quiescent phase of the FSQR with an unfiltered magnitude of 18.93 ± 0.09 mag at both epochs. Our observations from the 40 cm SLT in the *r* band started about 39.55 hr after the EP-WXT trigger with a total exposure time of 12 × 300 s. We reported the preliminary magnitude and corresponding upper limit from the observed field in M. H. Lee et al. (2024a). The left-hand panel of Figure D1 shows the FoV of this flaring-blazar event.

A.2.14. EP 240802a

EP 240802a was first detected by EP-WXT at 22024-08-02T10:32:52. The sky coordinates of this source were R.A. = 287.802 deg and decl. = −2.354 deg with an uncertainty of 1.′9 in radius (Y. L. Wang et al. 2024b) in radius. Following the EP-WXT discovery, EP-Follow-up X-ray Telescope also performed follow-up observations about 14 hr after the EP-WXT discovery. The EP-Follow-up X-ray Telescope clearly detected an uncatalogued X-ray source at R.A. = 287.8070 deg and decl. = −2.3125 deg with an uncertainty of 10″ (Y. L. Wang et al. 2024b) in radius.

Followed by the EP-WXT discovery and EP-Follow-up X-ray Telescope follow-up observation, several telescopes were triggered in search of the possible optical counterpart. About 29.22 hr after the EP-WXT trigger, we observed the field of EP 240802a and noticed the temporal coincidence of EP 240802a with GRB 240802A (G. Waratkar et al. 2024). This FXT triggered EP-WXT at 2024-08-02T10:32:52 and lasted for more than 500 s, while the long GRB 240802A was observed to display its strongest peak at 2024-08-02T10:34:04.5, clearly overlapping with EP 240802a. Till the start of our observations for EP 240902a, there was no spatial position information available for GRB 240802A; however, we reported the temporal overlapping in A. Aryan et al. (2024b). Later, the 3σ error region by the IPN triangulation[23] confirmed the positional coincidence of EP 240802a with GRB 240802A (A. S. Kozyrev et al. 2024b; N. Ruocco et al. 2024). Further, the SVOM/Gamma Ray Burst Monitor (GRM) team et al. (2024a) also suggested the association of these two events. Thus, EP 240802a was another FXT showing its association with a long GRB. A number of telescopes triggered after the EP-WXT and EP-Follow-up X-ray Telescope trigger; however, none of them found any evidence of an optical counterpart candidate (S. Leonini et al. 2024b; U. Quadri et al. 2024; W. Zheng et al. 2024e). The earliest upper limit since the EP-WXT trigger was reported in W. Zheng et al. (2024e), that too was at ∼0.74 days after the EP-WXT trigger. Thus, there was a probability of the optical counterpart of EP 240802a fading without being noticed. About 6 days after the EP-WXT discovery, we again triggered the LOT in the hope of discovering the SN component (an incidence similar to EP 240414a), although we did not find any evidence (Y. J. Yang et al. 2024a). The multiepoch upper limits in the *r* band from our observations are presented in Table B1.

A.2.15. EP 240908a

EP 240908a was discovered by EP-WXT at 2024-09-08T17:28:27 at the spatial position with R.A. = 13.992 deg and decl. = 8.089 deg, having an uncertainty of 2.′7 in radius. The EP-Follow-up X-ray Telescope also performed a follow-up observation about 1.34 hr after the EP-WXT discovery and detected an uncataloged X-ray source at R.A. = 14.0031, decl. = 8.0735 (J2000) with an uncertainty of about 10″ (X. Mao et al. 2024b, 2024a) in radius.

After the EP-WXT discovery, followed by the EP-Follow-up X-ray Telescope automated observations, several ground-based telescopes were triggered to search for any associated optical counterpart of EP 240908a. S. Y. Fu et al. (2024d) reported an upper limit of ∼21.6 mag in the *R* band. Some shallow limits were also reported by V. Lipunov et al. (2024k) in the *clear* (unfiltered) band. J. Quirola-Vasquez et al. (2024d) proposed a very faint optical counterpart (*r*-band AB magnitude ∼24) through their observations from the Gemini-North telescope at an epoch of 0.777 days since EP-WXT discovery. They further confirmed the proposed counterpart through additional observations about 2.19 days postdetection (J. Quirola-Vasquez et al. 2024e). Due to the very faint nature of the optical counter, no other telescopes could capture the optical counterpart. The observations by N. Pankov et al. (2024d) reported an upper limit of 23.5 mag in the *R* band at an epoch of ∼1 day after the EP trigger. About 24.22 hr after the EP-WXT trigger, our observations from the 40 cm SLT started in the *r* band with a total exposure time of 12 × 300 s. We also only obtained an upper limit in the *r* band as presented in Table B1.

A.2.16. EP 240913a

The EP-WXT detected EP 240913a at 2024-09-13T11:39:33 with R.A. = 16.681 deg and decl. = 16.750 deg having an

[23] http://ssl.berkeley.edu/ipn3/index.html

uncertainty of 2.′5 in radius (D. Y. Li et al. 2024a). Soon after its EP-WXT discovery, EP 240913a was classified as a GRB event (Y.-H. I. Yin et al. 2024b) due to its positional and temporal coincidence with GRB 240913C, which was further supported by several other observations (A. Dasgupta et al. 2024; A. S. Kozyrev et al. 2024a; D. Pawar 2024; Y. Zhang et al. 2024). Swift-XRT also detected an X-ray source within the EP-WXT error circle, which was proposed to be the counterpart of EP 240913a (S. Q. Jiang et al. 2024e). No optical/NIR counterpart was reported by any of the follow-up observations (L. Asquini et al. 2024; Z. P. Zhu et al. 2024b,2024a; W. Zheng et al. 2024n; B. Schneider et al. 2024; V. Lipunov et al. 2024l; X. Zou et al. 2024b; S. Belkin et al. 2024a). Our observations from 1 m LOT in the *r* band started about 26.44 hr after the EP-WXT trigger with a total exposure time of 3×300 s. We also only obtained upper limits in the *r* band and *g* band, as mentioned in Table B1.

A.2.17. EP 240918a

EP 240918a was first detected by EP-WXT at 2024-09-18T11:24:37, and a subsequent autonomous observation started by the EP-Follow-up X-ray Telescope 2 minutes later. The EP-Follow-up X-ray Telescope localization coordinates of this source were R.A. = 289.3937 deg and decl. = 46.1281 deg with an uncertainty of 20″ in radius (Z. J. Zhang et al. 2024b).

Followed by the EP-WXT discovery and autonomous EP-Follow-up X-ray Telescope follow-up observations, several telescopes were triggered. No optical counterpart was detected in any of the observations (B. T. Wang et al. 2024c; T.-R. Sun et al. 2024b; S. Y. Fu et al. 2024f; V. Lipunov et al. 2024m; J. Zhang et al. 2024; SVOM/Visible Telescope (VT) commissioning team et al. 2024a), even though some observations were as early as $\sim$ 2 hr after the EP-WXT discovery and had upper limits as deep as $\sim$22.8 mag. A Swift-XRT follow-up observation was conducted by J. Quirola-Vasquez et al. (2024b) about 10.7 hr after the EP-WXT discovery, but no X-ray counterpart was detected. Our observations from the 40 cm SLT in the *r* band started about 2.30 hr after the EP-WXT trigger with a total exposure time of 16×300 s. We also conducted a further follow-up observation using 1 m LOT in the *r* band with a total exposure time of 6×300 s. We only obtained upper limits in the *r* band, as mentioned in Table B1. We reported our preliminary photometry in A. K. H. Kong et al. (2024b).

A.2.18. EP 240918b

EP-WXT discovered the EP 240918b at 2024-09-18T15:40:00 with R.A. = 258.66 deg and decl. = 66.739 deg having an uncertainty of 2.′9 in radius (Y. F. Liang et al. 2024d). About 20 hr after the EP-WXT discovery, the FXT was not detected in the follow-up observations by the EP-Follow-up X-ray Telescope (M. J. Liu et al. 2024).

Followed by the EP-WXT discovery and EP-Follow-up X-ray Telescope follow-up observations, we triggered the 40 cm SLT at the Lulin Observatory to search for the optical counterpart. No other telescope trigger had been reported on any platform. Our observations from the 40 cm SLT in the *r* band started about 22.02 hr after the EP-WXT trigger with a total exposure time of 7×300 s. We did not find evidence of any candidate counterpart down to a limit of 19 mag. We had reported our preliminary photometry in C. H. Lai et al. (2024d). The details of the photometry are presented in Table B1.

A.2.19. EP 240918c

EP 240918c was first detected by EP-WXT at 2024-09-18T18:06:47 with R.A. = 281.338 deg and decl. = −13.167 deg, having an uncertainty of 2.′3 in radius (Y. F. Liang et al. 2024d). Two follow-up observations by the EP-Follow-up X-ray Telescope were performed by EP-WXT starting at 2024-09-19T12:40:28 and 2024-09-24T13:01:28, respectively. Two X-ray sources were identified within the specified EP-WXT error circle region in each observation. First, EP J184515.3-131115 was reported at R.A. = 281.3138 deg and decl. = −13.1875 deg with an uncertainty of 10″ in radius. Second, EP J184516.2-130819 at R.A. = 281.3187 deg and decl. = −13.1371 deg (J2000) with an uncertainty of 10″ in radius, which was consistent with the position of the star TYC 5704-6-1 (M. J. Liu et al. 2024). Although no rapid dimming was reported for the two detected sources.

Followed by the EP-WXT discovery and EP-Follow-up X-ray Telescope follow-up observations, we triggered the 1 m LOT at the Lulin Observatory to search for the optical counterpart. Similar to EP 240918b, no other telescope trigger was reported on any platform. Our observations in the *r* band started about 19.59 hr after the EP-WXT trigger with a total exposure time of 5×300 s. We only obtained an upper limit in the *r* band of 18.9 mag, as presented in Table B1. We reported our preliminary photometry in C. H. Lai et al. (2024d).

A.2.20. EP 240919a

EP 240919a was discovered by EP-WXT at 2024-09-19T14:47:40 with a subsequent autonomous follow-up observation by the EP-Follow-up X-ray Telescope after 10 minutes. An uncataloged source was detected by the EP-Follow-up X-ray Telescope at the spatial position with R.A. = 334.2790 deg and decl. = −9.7361 deg, having an uncertainty of 10″ in radius (Y. F. Liang et al. 2024a, 2024b).

Only about 80 s after the EP-WXT discovery of EP 240919a, an event was also discovered in the Fermi-GBM. The discovered transient was consistent with EP 240919a in both timing and position, leading it to be also classified as a GRB event GRB 240919A (Y.-F. Liang et al. 2024c; O. J. Roberts et al. 2024). The burst was also weakly detected by SVOM-GRM (SVOM/GRM team et al. 2024b). A high-energy counterpart detection was reported by INTEGRAL SPI-ACS (J. Rodi et al. 2024), and interestingly, a radio counterpart of this event was also detected, as reported by A. Gulati et al. (2024). No plausible optical or NIR counterpart was discovered by any of the telescopes (S. Q. Jiang et al. 2024a; A. Kumar et al. 2024b; D. B. Malesani et al. 2024b; V. Lipunov et al. 2024n; W. Zheng et al. 2024f; R. Brivio et al. 2024; S. Belkin et al. 2024b; SVOM/VT commissioning team et al. 2024b). Our observations from the 40 cm SLT in the *r* band started about 1.27 hr after the EP-WXT trigger with a total exposure time of 11×300 s. Although we were quick to search for the optical counterpart, we also only obtained upper limits down to 19.8 mag in as mentioned in Table B1. We reported our preliminary photometry in A. Aryan et al. (2024f).

A.2.21. EP 241026b

EP 241026b was first detected by EP-WXT at 2024-10-26T18:14:30 with R.A. = 56.403 deg and decl. = 41.031 deg, having an uncertainty of 2.′9 in radius. Followed by the EP-WXT discovery, a follow-up observation was performed using the EP-Follow-up X-ray Telescope about 9 hr later. An uncatalogued X-ray source was reported with R. A. = 56.4058 deg and decl. = 41.0312 deg, having an uncertainty of 10″ in radius (T. Y. Lian et al. 2024a).

Followed by the EP-WXT discovery and EP-Follow-up X-ray Telescope follow-up observations, several telescopes were triggered to search for the optical counterpart of EP 241026b. V. Lipunov et al. (2024o), D. B. Malesani et al. (2024d), and T. Mohan et al. (2024a) did not find any optical counterpart. However, about 1.48 days after the EP-WXT trigger, A. Rossi et al. (2024) reported an obvious optical rebrightening transient at R.A. = $03^{h}45^{m}37\overset{s}{.}55$ and decl. = $+41°01'51\overset{''}{.}9$ that brightened by about 1.9 mag among their two epochs (first epoch reported in D. B. Malesani et al. 2024d) of observations. Later, A. Bochenek & D. A. Perley (2024e) also claimed to have marginally detected the proposed optical counterpart about 4.31 days after the EP-WXT trigger. The Keck-LRIS spectroscopic observation of this transient displayed a well-detected continuum in the range of 3400–10,200 Å, which put an upper limit of 1.8 for the redshift of EP 241026b (W. Zheng et al. 2024c). Our observations from the 1 m LOT in the r band started about 142.08 hr after the EP-WXT trigger with a total exposure time of 12×300 s. We did not find any evidence of any optical counterpart candidate down to 23.5 mag. The deeper limit was favored by an excellent observing condition with seeing of $\sim 1''$ and a median air mass of ~ 1. We reported our preliminary photometry in A. Aryan et al. (2024a).

A.2.22. EP 241101a

EP 241101a was discovered by EP-WXT at 2024-11-01T23:52:49 with R.A. = 37.763 deg and decl. = 22.731 deg, having an uncertainty of 2.′8 in radius (Y. F. Liang et al. 2024e). Followed by the EP-WXT discovery, an autonomous observation by the EP-Follow-up X-ray Telescope was also performed about 45 minutes later, but no counterpart was detected. Further analysis of the data during the EP-Follow-up X-ray Telescope's slew to the target before the observation started revealed an uncataloged X-ray source at R. A. = 37.7526 deg and decl. = 22.7175 deg with an uncertainty of 10″ in radius (Q. Y. Wu et al. 2024c).

Followed by the EP-WXT discovery and autonomous follow-up observations from the EP-Follow-up X-ray Telescope, many telescopes triggered in the direction of the transient to search for the optical counterpart. I. Perez-Garcia et al. (2024h), V. Lipunov et al. (2024r), and B. Grossan et al. (2024) reported only upper limits. However, C. Adami (2024) proposed a candidate optical counterpart at R.A. = $02^{h}30^{m}53\overset{s}{.}09$, decl. = $+22°43'48\overset{''}{.}11$ with an r-band magnitude of 22.8 ± 0.5. Later, M. Busmann et al. (2024e) also proposed another plausible candidate at R.A. = $02^{h}31^{m}10\overset{s}{.}85$, decl. = $+22°44'54\overset{''}{.}75$ coinciding with a variable source, PSO J037.7952+22.7485 in the Pan-STARRS1 catalog. The two sources proposed above were also marked as candidates by N. Pankov et al. (2024h). However, we notice that the source proposed by C. Adami (2024) was already present in the SDSS DR12 (SDSS J023053.10+224348.0) images, as well as in the DESI Legacy Survey images. Our observations from 1 m LOT in the r band started about 17.08 hr after the EP-WXT trigger with a total exposure time of 6×300 s. We reported the preliminary photometry in A. Aryan et al. (2024c). The upper limits from our observation in the r band and g band are presented in Table B1.

A.2.23. EP 241104a

The EP-WXT first detected EP 241104a at 2024-11-04T18:34:15 with R.A.= 32.574 deg and decl. = 31.555 deg, having an uncertainty of 2.′7 in radius (H. Zhou et al. 2024e).

EP 241104a was found spatially and temporally coincident with GRB 241104A (Fermi-GBM team 2024b) as indicated by H. Zhou et al. (2024e). Followed by the EP-WXT discovery of EP 241104a, no optical follow-up observations were reported for the optical counterpart. Our observations from 1 m LOT in the r band started about 18.68 hr after the EP-WXT trigger with a total exposure time of 6×300 s. We only obtained an upper limit of 22.8 mag in the r band, as mentioned in Table B1. We reported our preliminary photometry in Z. N. Wang et al. (2024a).

A.2.24. EP 241109a

EP 241109a was discovered by EP-WXT at 2024-11-09T06:01:55. An autonomous observation was also performed by the EP-Follow-up X-ray Telescope, which detected an uncataloged source at the spatial position with R.A. = 18.3599 deg and decl. = 0.0184 deg having an uncertainty of 15″ in radius (A. Li et al. 2024).

A. Li et al. (2024) indicated the presence of a close star in the GAIA DR3 database lying within the EP-Follow-up X-ray Telescope error circle of EP 241109a. Thus, they proposed EP 241109a could be a stellar flare event. Further, the observation by I. Perez-Garcia et al. (2024e) confirmed the event arising from a stellar flare as the proposed star diminished by 0.8 mag within 40 minutes of their observations. Later, spectroscopic observation by W. Zheng et al. (2024d) indicated a slight excess in flux below $\sim$4000 Å. These observations further confirmed EP 241109a being a stellar flare. Our observations from the 40 cm SLT in the r band started about 7.06 hr after the EP-WXT trigger with a total exposure time of 7×150 s. We probably missed the stellar flare as our observations were late. The flared star had a magnitude of 13.99 ± 0.03 in our observations. About 50 minutes after the first epoch of our observation, we performed further follow-up observation in the r band with a total exposure time of 12×30 s. The new magnitude (13.94 ± 0.13) was again similar to the previous one. Besides this source, the upper limits in the r band from the two epochs of observations are presented in Table B1. The right-hand panel of Figure D1 shows the FoV of the star that underwent a flaring event.

A.2.25. EP 241115a

EP-WXT discovered the EP 241115a at 2024-11-15T05:47:20 with R.A. = 19.416 deg and decl. = −17.954 deg having an uncertainty of 2.′6 in radius (J. W. Hu et al. 2024b).

The temporal and spatially localization of EP 241115a coincided significantly with GRB 241115D (SVOM/GRM team et al. 2024c). A Swift-XRT ToO follow-up observation by C. Y. Dai et al. (2024) detected an uncataloged source within the EP-WXT localization error circle, and proposed that the source be associated with EP 241115a. Followed by the EP-Follow-up X-ray Telescope detection, only a few telescopes triggered in the search for the optical counterpart of EP 241115a. V. Lipunov et al. (2024c) obtained only an upper limit. Our observations from the 40 cm SLT in the *r* band started about 30.64 hr after the EP-WXT trigger with a total exposure time of 7×300 s. We too obtained upper limits in the *r* band and *g* band as presented in Table B1. We reported our preliminary photometry in L. L. Fan et al. (2024b).

A.2.26. EP 241119a

EP 241119a was first detected by EP-WXT at 2024-11-19T17:53:20 with R.A. = 84.116 deg and decl. = 3.832 deg, having an uncertainty of 2.′3 in radius. About 9 hr after the EP-WXT discovery, EP-Follow-up X-ray Telescope follow-up observation detected an uncataloged X-ray source at R.A. = 84.1062 deg and decl = 3.8404 deg with an uncertainty of about 10″ in radius (W. J. Zhang et al. 2024b).

Followed by the EP-WXT discovery and EP-Follow-up X-ray Telescope follow-up observation, several telescopes were triggered to search for the optical/NIR counterpart of EP 241119a. None of those observations found any evidence of an optical counterpart (T. Ahumada et al. 2024; V. Lipunov et al. 2024e; G. S. H. Paek et al. 2024; A. P. Saikia et al. 2024). Our observations from the 40 cm SLT in the *r* band started about 23.22 hr after the EP-WXT trigger with a total exposure time of 24×300 s. We only obtained an upper limit as presented in Table B1. We reported our preliminary photometry in A. Aryan et al. (2024d).

A.2.27. EP 241125a

EP-WXT discovered the EP 241125a at 2024-11-25T00:06:06 with R.A.= 48.561 deg and decl. = 37.677 deg having an uncertainty of 2.′65 in radius (B. T. Wang et al. 2024d).

Besides our observations from the Lulin Observatory, no other optical observations were reported for EP 241125a. Our observations from 1 m LOT in the *r* band started about 12.09 hr after the EP-WXT trigger with a total exposure time of 15×120 s. We did not detect any evidence of any optical counterpart candidate down to 23.0 mag as presented in Table B1. We reported our preliminary photometry in C. H. Lai et al. (2024b).

A.2.28. EP 241126a

EP 241126a was first detected by EP-WXT at 2024-11-26T19:39:41 with R.A.= 33.744 deg and decl. = 11.705 deg having an uncertainty of 2.′429 in radius (D. F. Hu et al. 2024). Followed by the EP-WXT discovery, a ToO observation was performed using the EP-Follow-up X-ray Telescope about 7.5 hr later. An uncatalogued X-ray source was reported with R.A. = 33.7444 deg and decl. = 11.7013 deg, having an uncertainty of 10″ in radius (T. C. Zheng et al. 2024a).

Followed by the EP-WXT discovery and EP-Follow-up X-ray Telescope ToO observation, several telescopes were triggered to search for the optical counterpart of EP 241126a. S. Y. Fu et al. (2024e) proposed the detection of an optical counterpart with an *R*-band magnitude of ∼22.0 mag at R.A. = $02^{h}14^{m}57^{s}.96$, decl. = $+11°42'04''.76$ in their observations starting about 6.84 hr after the EP-WXT discovery. This optical counterpart was also confirmed in further observations (W. X. Li et al. 2024g; J.-J. Geng et al. 2024; SVOM/VT commissioning team et al. 2024c; D. B. Malesani et al. 2024a; J. Freeburn et al. 2024b). The observations by X. Zou et al. (2024a) only obtain upper limits about 15.8 hr after the EP-WXT discovery. Our observations from 1 m LOT in the *r* band started about 16.23 hr after the EP-WXT trigger with a total exposure time of 6×300 s. We only obtained an upper limit of 22.5 mag in the *r* band, as mentioned in Table B1. Since the FXT was detected faint and our observations were late, the FXT probably faded beyond the detection limit in our images. We reported our preliminary photometry in C. H. Lai et al. (2024c).

A.2.29. EP 241206a

EP-WXT discovered the EP 241206a at 2024-12-06T16:34:47 with R.A. = 34.702 deg and decl. = 38.914 deg having an uncertainty of 3.′78 in radius (Y. H. I. Yin et al. 2024a).

Followed by the EP-WXT discovery, only a few telescopes were triggered to search for the optical counterpart. All the optical follow-up observations only obtained upper limits (V. Lipunov et al. 2024f; A. Sota et al. 2024; D. R. Xiong et al. 2024b). Our observations from the 40 cm SLT in the *r* band started about 22.45 hr after the EP-WXT trigger with a total exposure time of 8×300 s. We did not find any evidence of any optical counterpart in our observations down to 20.9 mag. Details of our further follow-up observations are presented in Table B1.

A.2.30. EP 241208a

EP 241208a was first detected by EP-WXT at 2024-12-08T16:36:13 with R.A. = 127.812 deg and decl. = 49.082 deg having an uncertainty of 4′ in radius (Y. L. Wang et al. 2024c). A follow-up observation was also performed using the EP-Follow-up X-ray Telescope about 22 hr after the EP-WXT discovery. An uncatalogued X-ray source was reported with R.A. = 127.8303 deg and decl. = 49.0831 deg, having an uncertainty of 10″ in radius (Y. Wang et al. 2024b).

A few telescopes were triggered in the direction of EP 241208a to search for the optical counterpart. All of those observations only obtained upper limits (V. Lipunov et al. 2024g; X. Liu et al. 2024a). Our observations from the 40 cm SLT in the *r* band started about 23.62 hr after the EP-WXT trigger with a total exposure time of 24×300 s. We also did not detect any optical counterpart candidate in our observations down to 21 mag. We reported our preliminary photometry in Z. N. Wang et al. (2024b). Later, the SVOM-ECLAIRs telescope detected a coincident long and soft transient with EP 241208a (SVOM/ECLAIRS commissioning team et al. 2024).

Appendix B
Photometry Logs for Sources with Upper Limits

Table B1 presents the details of photometry logs for sources with upper limits. Both SLT and LOT have the same Astrodon photometric Sloan filters, providing excellent multiband observational capabilities. The corresponding filter transmission curves are shown in Figure B1.

Table B1
Photometric Observation Log for the Sources with an Upper Limit

FXT	$T_{start} - T_0$ (hr)	$T_{mid} - T_0$ (hr)	MJD_{start}	Telescope	Total Exposure Time	Filter	Magnitude (AB mag)	Catalog
EP 240331a	17.62	18.30	60401.656	LOT	4 × 4 × 300 s	*r*	>22.3[a]	Pan-STARRS1
	17.67	18.24	60401.658	SLT	3 × 4 × 300 s +1 × 3 × 300 s	*g*	>21.3[a]	Pan-STARRS1
EP 240408a	42.55	43.41	60410.520	LOT	24 × 180 s	*r*	>22.5	SkyMapper
	42.74	43.65	60410.528	SLT	15 × 300 s	*i*	>20.3	SkyMapper
	65.33	65.85	60411.469	LOT	20 × 300 s	*r*	>22.8	SkyMapper
EP 240413a	73.55	73.77	60416.676	LOT	6 × 300 s	*r*	>22.8	Pan-STARRS1
EP 240506a	32.10	33.56	60437.547	SLT	30 × 300 s	*r*	>22.0	SDSS
EP 240617a	30.95	31.24	60479.803	SLT	6 × 300 s	*r*	>19.8	Pan-STARRS1
	97.94	98.36	60482.594	SLT	10 × 300 s	*r*	>19.3	Pan-STARRS1
	98.87	99.30	60482.633	SLT	10 × 300 s	*i*	>19.3	Pan-STARRS1
EP 240618a	11.81	12.20	60479.731	SLT	10 × 300 s	*r*	>20.6	Pan-STARRS1
	12.67	13.06	60479.767	SLT	10 × 300 s	*i*	>20.7	Pan-STARRS1
	35.18	35.57	60480.705	SLT	10 × 300 s	*r*	>20.0	Pan-STARRS1
	36.05	36.43	60480.741	SLT	10 × 300 s	*i*	>20.5	Pan-STARRS1
	82.43	82.91	60482.673	SLT	10 × 300 s	*r*	>20.6	Pan-STARRS1
	83.47	83.86	60482.717	SLT	10 × 300 s	*i*	>20.6	Pan-STARRS1
EP 240625a	40.99	41.37	60487.783	SLT	10 × 300 s	*i*	>19.8	SDSS
	62.39	62.60	60488.675	SLT	6 × 300 s	*r*	>19.9	SDSS
EP 240626a	33.16	33.38	60488.651	SLT	6 × 300 s	*r*	>20.1	Pan-STARRS1
EP 240702a	16.05	17.70	60493.704	SLT	35 × 300 s	*r*	>22.2	SkyMapper
EP 240703a	12.43	12.52	60494.545	LOT	3 × 300 s	*r*	>21.8	Pan-STARRS1
	13.72	13.94	60494.599	LOT	6 × 300 s	*i*	>21.6	Pan-STARRS1
EP 240703c	20.61	21.27	60495.619	SLT	16 × 300 s	*r*	>21.5	Pan-STARRS1
EP 240708a	17.02	18.53	60500.687	SLT	36 × 300 s	*r*	>21.3	Pan-STARRS1
	17.16	17.38	60500.693	LOT	6 × 300 s	*r*	>22.6	Pan-STARRS1
	17.78	18.00	60500.719	LOT	6 × 300 s	*g*	>22.4	Pan-STARRS1
Blazar[b]	39.55	40.02	60509.782	SLT	12 × 300 s	*r*	18.42 ± 0.05	SDSS
	39.55	40.02	60509.782	SLT	12 × 300 s	*r*	>21.1[c]	SDSS
EP 240802a	29.22	29.50	60525.657	LOT	6 × 300 s	*r*	>21.9	Pan-STARRS1
	31.17	31.35	60525.738	LOT	5 × 300 s	*r*	>21.4	Pan-STARRS1
	54.37	55.09	60526.705	LOT	8 × 300 s	*r*	>21.9	Pan-STARRS1
	126.93	127.16	60529.728	LOT	6 × 300 s	*r*	>21.7	Pan-STARRS1
	149.04	149.22	60530.650	LOT	5 × 300 s	*r*	>22.3	Pan-STARRS1
	171.62	171.84	60531.590	LOT	6 × 300 s	*r*	>22.0	Pan-STARRS1
EP 240908a	24.22	24.69	60562.737	SLT	12 × 300 s	*r*	>21.6	SDSS
EP 240913a	26.44	26.53	60567.588	LOT	3 × 300 s	*r*	>21.3	Pan-STARRS1
	26.71	26.93	60567.599	LOT	6 × 300 s	*g*	>21.9	Pan-STARRS1
EP 240918a	2.30	2.95	60571.571	SLT	16 × 300 s	*r*	>20.5	Pan-STARRS1
	4.84	5.06	60571.677	LOT	6 × 300 s	*r*	>21.1	Pan-STARRS1
EP 240918b	22.02	22.28	60572.570	SLT	7 × 300 s	*r*	>19.0	Pan-STARRS1
EP 240918c	19.59	19.83	60572.571	LOT	5 × 300 s	*r*	>18.9	Pan-STARRS1
EP 240919a	1.17	1.60	60572.669	SLT	11 × 300 s	*r*	>19.8	Pan-STARRS1
EP 241026b	142.08	142.56	60615.680	LOT	12 × 300 s	*r*	>23.5	Pan-STARRS1
EP 241101a	17.08	17.30	60616.708	LOT	6 × 300 s	*r*	>22.9	SDSS
	17.61	17.86	60616.729	LOT	6 × 300 s	*g*	>23.0	SDSS
EP 241104a	18.68	18.93	60619.552	LOT	6 × 300 s	*r*	>22.8	SDSS
EP 241109a[d]	7.06	7.38	60623.545	SLT	7 × 150 s	*r*	13.99 ± 0.03[e]	SDSS
	7.06	7.38	60623.545	SLT	7 × 150 s	*r*	>19.9[c]	SDSS
	7.95	8.10	60623.583	SLT	12 × 30 s	*r*	13.94 ± 0.13[e]	SDSS
	7.95	8.10	60623.583	SLT	12 × 30 s	*r*	>19.1[c]	SDSS
EP 241115a	30.64	30.90	60630.518	SLT	7 × 300 s	*r*	>20.7	Pan-STARRS1
	31.27	31.75	60630.544	SLT	10 × 300 s	*g*	>20.5	Pan-STARRS1
	31.31	31.53	60630.546	LOT	6 × 300 s	*r*	>20.7	Pan-STARRS1
EP 241119a	23.22	24.33	60634.713	SLT	24 × 300 s	*r*	>20.8	SDSS
EP 241125a	12.09	12.35	60639.508	LOT	15 × 120 s	*r*	>23.0	Pan-STARRS1
EP 241126a	16.23	16.45	60641.495	LOT	6 × 300 s	*r*	>22.5	Pan-STARRS1
EP 241206a	22.45	22.75	60651.626	SLT	8 × 300 s	*r*	>20.9	Pan-STARRS1
	25.32	25.41	60651.746	LOT	3 × 300 s	*r*	>22.5	Pan-STARRS1
	46.88	47.97	60652.644	SLT	48 × 150 s	*r*	>21.1	Pan-STARRS1
EP 241208a	23.62	24.61	60653.676	SLT	24 × 300 s	*r*	>21.0	SDSS

Notes. The magnitudes in the table are not corrected for the expected foreground extinction.
[a] Deepest limiting magnitude among the four pointings. In the *r* band, each pointing has a total exposure time of 4 × 300 s, while in the *g* band, three pointings have 4 × 300 s, and one pointing has 3 × 300 s of exposure.
[b] Blazar NVSS J004348+342626 flaring event.
[c] Corresponding upper limit from the same field.
[d] Stellar flare event.
[e] Magnitude of the (flaring) star. The finding charts of the blazar NVSS J004348+342626 and the stellar flare event EP 241109a from the 40 cm SLT are shown in Figure D1.

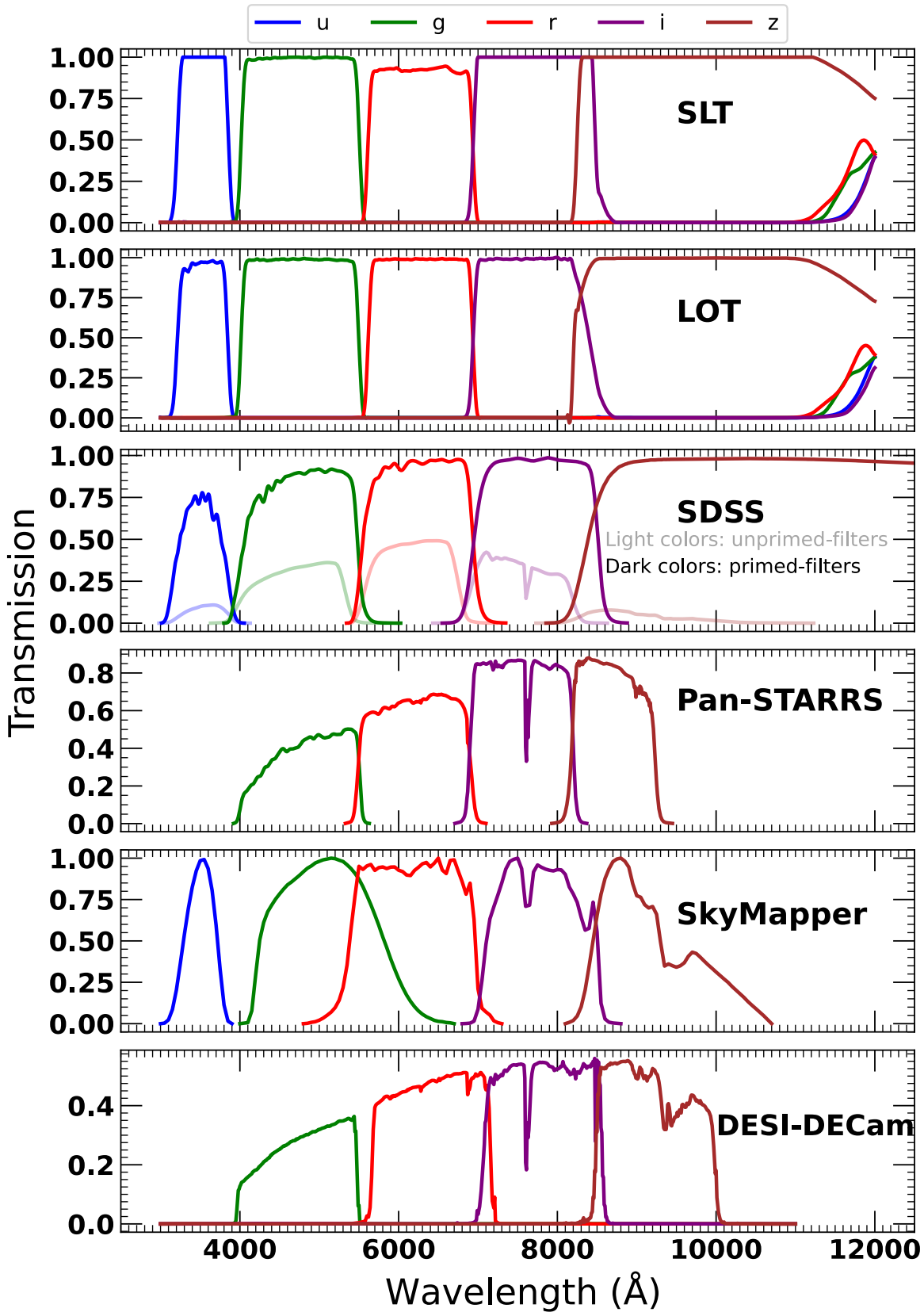

Figure B1. The comparison of the Lulin Observatory LOT and SLT filters with different sky survey filters.

Appendix C
Precursor Searches for EP Sources with Optical Counterparts

As shown in Figure C1, we utilized forced photometry from the ZTF and ATLAS surveys to search for potential precursor activity in archival difference images, spanning approximately 10 yr prior to the reported EP detection time. This analysis reveals no significant evidence of real, astrophysical excess flux in the historical data, down to the 5σ detection limit.

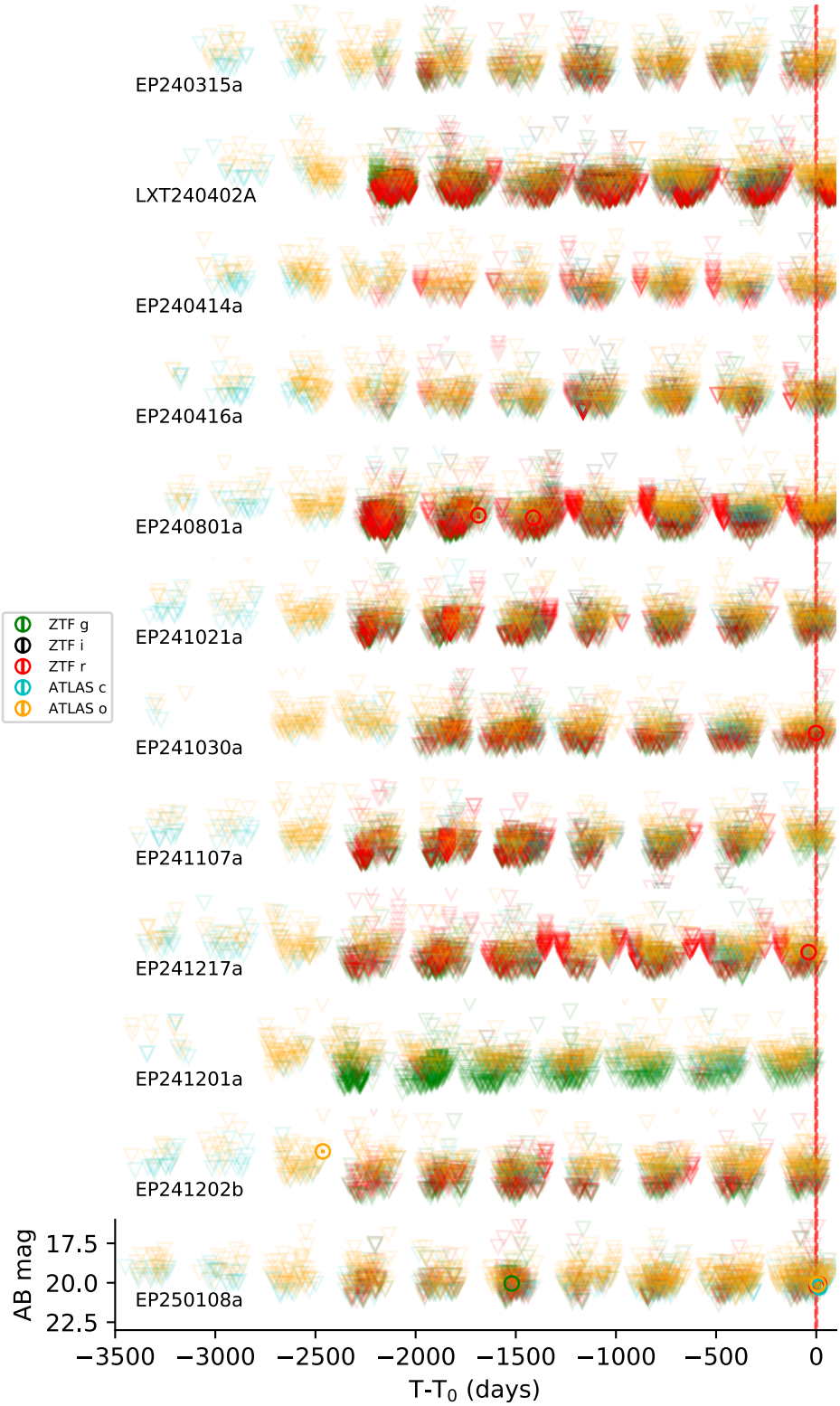

Figure C1. Search for precursor activity at the locations of FXTs discovered by EP-WXT, using archival data from the ZTF and ATLAS surveys over a ∼10 yr baseline prior to the reported EP detection time (T_0, marked as day zero on the x-axis). The y-axis shows the Milky Way extinction-corrected AB magnitudes. Both ZTF (g, r, and i bands) and ATLAS (c and o bands) forced photometry light curves are shown. 5σ detection limits are used throughout. Detections are indicated by open circles, while upper limits are marked as open inverted triangles.

Appendix D
References for the First Detections and Upper Limits

Here, we credit the first optical detections or the earliest upper limits presented in Figure 4. EPW20240219aa: A. Bochenek et al. (2024); EPW20240305aa: S. Antier et al. (2024); LXT 240402A: S. Yang et al. (2024b) and A. J. Levan et al. (2024b); EP 240315a: J. H. Gillanders et al. (2024); EP 240331a: T. W. Chen et al. (2024b); EP 240408a: W. X. Li et al. (2024l); EP 240413a: K. A. Pall'e et al. (2024); EP 240414a: A. Aryan et al. (2024g); EP 240416a: T. W. Chen et al. (2024a); EP 240417a: T.-R. Sun et al. (2024a); EP 240420a: J. An et al. (2024e); EP 240426a: B. T. Wang et al. (2024b); EP 240426b: T.-R. Sun et al. (2024c); EP 240506a: I. Perez-Garcia et al. (2024c); EP 240518a: W. X. Li et al. (2024h); EP 240617a: this work; EP 240618a: this work; EP 240625a: S. Y. Fu et al. (2024b); EP 240626a W. Zheng et al. (2024i); EP 240702a: W. X. Li et al. (2024e); EP 240703a: this work; EP 240703b: W. X. Li et al. (2024i); EP 240703c: this work; EP 240708a: S. Q. Jiang et al. (2024b); EP 240801a: S. Y. Fu et al. (2024c); EP 240802a: W. Zheng et al. (2024e); EP 240804a: J. An et al. (2024a); EP 240806a: I. Pérez-Fournon et al. (2024b) (no information of time for W. X. Li et al. 2024j, who reported the first detection); EP 240807a: V. Lipunov et al. (2024p); EP 240816a: I. Perez-Garcia et al. (2024a); EP 240816b: W. Zheng et al. (2024g); EP 240820a: J. An et al. (2024b); EP 240904a: S. Y. Fu et al. (2024a); EP 240908a: S. Y. Fu et al. (2024d); EP 240913a: Z. P. Zhu et al. (2024b); EP 240918a: this work; EP 240918b: this work; EP 240918c: this work; EP 240919a: this work; EP 240930a: V. Lipunov et al. (2024q); EP 241021a: S. Y. Fu et al. (2024h); EP 241025a: S. Q. Jiang et al. (2024c); EP 241026a: A. M. Watson et al. (2024); EP 241026b: A. Rossi et al. (2024); EP 241030a: N. J. Klingler et al. (2024); EP 241101a: I. Perez-Garcia et al. 2024h; EP 241103a: L. Izzo & D. B. Malesani (2024b); EP 241104a: V. Lipunov et al. (2024s); EP 241107a: M. Odeh et al. 2024b; EP 241113b: V. Lipunov et al. (2024h); EP 241115a: V. Lipunov et al. (2024c); EP 241119a: V. Lipunov et al. (2024e); EP 241125a: this work; EP 241126a: S. Y. Fu et al. (2024e); EP 241201a: M. H. Lee et al. (2024b); EP 241202b: C. C. Ngeow et al. (2024); EP 241206a: D. R. Xiong et al. (2024b); EP 241208a: X. Liu et al. (2024a); EP 241213a: P. Barria et al. (2024); EP 241217a: A. J. Levan et al. (2024d); EP 241217b: T. Hussenot-Desenonges et al. (2024); EP 241223a: V. Lipunov et al. (2024i); EP 241231b: A. Kumar et al. (2025b); EP 250101a: A. Bochenek & D. A. Perley (2025); EP 250108a: R. Eyles-Ferris (2025); EP 250109a: SVOM/VT commissioning team et al. (2025); EP 250109b: A. Kumar et al. (2025c); No optical follow-ups were reported for EP 240305a, EP 240309a, EP 240327a, and EP 240709a. The finding charts of the flaring-blazar and stellar-flare events are shown in Figure D1.

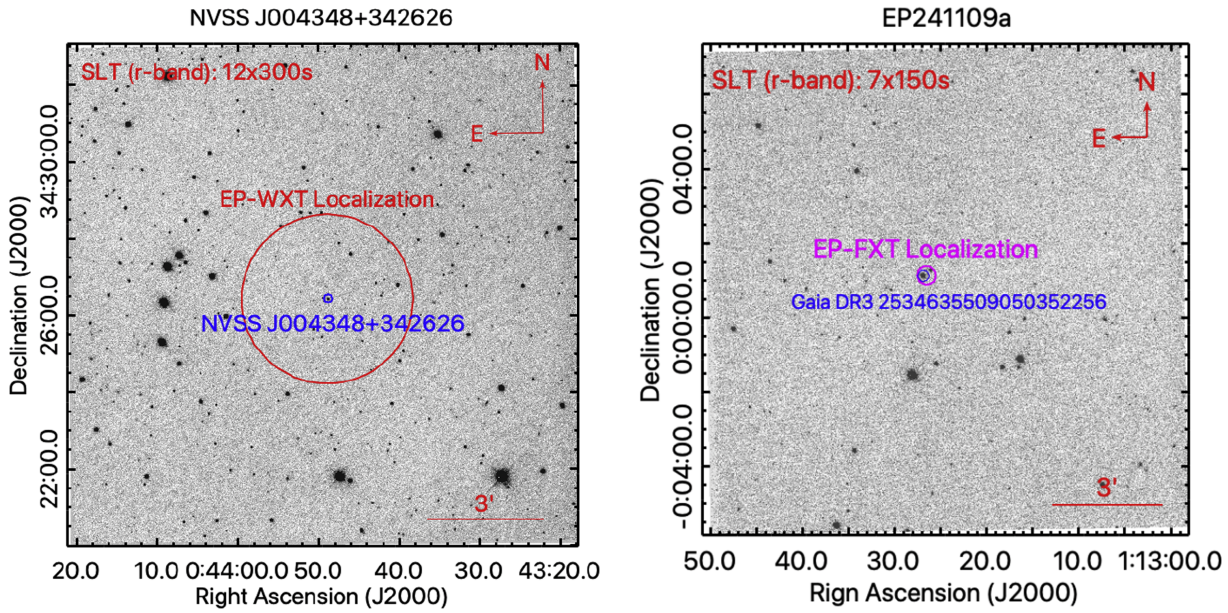

Figure D1. The finding charts of the flaring-blazar (left) and stellar-flare (right) events from the Lulin Observatory 40 cm SLT. The R.A. is in hh:mm:ss format, while decl. is in dd:mm:ss format. The EP-WXT and EP-Follow-up X-ray Telescope (if available) localizations are indicated with open red and magenta circles in the FoV, respectively.

ORCID iDs

Amar Aryan https://orcid.org/0000-0002-9928-0369
Ting-Wan Chen https://orcid.org/0000-0002-1066-6098
Sheng Yang https://orcid.org/0000-0002-2898-6532
James H. Gillanders https://orcid.org/0000-0002-8094-6108
Albert K. H. Kong https://orcid.org/0000-0002-5105-344X
S. J. Smartt https://orcid.org/0000-0002-8229-1731
Heloise F. Stevance https://orcid.org/0000-0002-0504-4323
Yi-Jung Yang https://orcid.org/0000-0001-9108-573X
Aysha Aamer https://orcid.org/0000-0002-9085-8187
Rahul Gupta https://orcid.org/0000-0003-4905-7801
Lele Fan https://orcid.org/0009-0007-4482-2101
Amit Kumar https://orcid.org/0000-0003-3164-8056
Meng-Han Lee https://orcid.org/0009-0003-0553-3340
Yu-Hsing Lee https://orcid.org/0009-0003-5139-9007
Hung-Chin Lin https://orcid.org/0009-0008-4171-0152
Chow-Choong Ngeow https://orcid.org/0000-0001-8771-7554
Matt Nicholl https://orcid.org/0000-0002-2555-3192
Yen-Chen Pan https://orcid.org/0000-0001-8415-6720
Shashi Bhushan Pandey https://orcid.org/0000-0002-1474-1980
Aiswarya Sankar.K https://orcid.org/0009-0003-2609-3591
Shubham Srivastav https://orcid.org/0000-0003-4524-6883
Guanghui Sun https://orcid.org/0009-0009-7577-1516

References

Abdollahi, S., Acero, F., Ackermann, M., et al. 2020, ApJS, 247, 33
Adami, C. 2024, GCN, 38060, 1
Adami, C., Dennefeld, M., Coleiro, A., Basa, S., & Le Floc'h, E. 2024a, GCN, 38122, 1
Adami, C., Le Floc'h, E., Fortin, F., et al. 2024b, GCN, 36702, 1
Adami, C., & Schneider, B. 2024, GCN, 38041, 1
Aguado, D. S., Ahumada, R., Almeida, A., et al. 2019, ApJS, 240, 23
Ahumada, T., Mo, G., Schneider, B., et al. 2024, GCN, 38286, 1
Ai, S., & Zhang, B. 2021, ApJL, 915, L11
Akerlof, C., Balsano, R., Barthelmy, S., et al. 1999, Natur, 398, 400
Akl, D., Le Calloch, A., Rajabov, Y., et al. 2024a, GCN, 36771, 1
Akl, D., Masek, M., Andrade, C., et al. 2024b, GCN, 36712, 1
Alp, D., & Larsson, J. 2020, ApJ, 896, 39
An, J., Fu, S. Y., Jiang, S. Q., et al. 2024a, GCN, 37035, 1
An, J., Jiang, S. Q., Tinyanont, S., et al. 2024b, GCN, 37215, 1
An, T., Liu, Y., Geng, J., & Wu, X. 2025a, GCN, 38749, 1
An, T., Liu, Y., Geng, J., et al. 2025b, GCN, 38998, 1
An, J., Tinyanont, S., Anutarawiramkul, R., et al. 2024c, GCN, 36820, 1
An, J., Xu, D., Li, W. X., et al. 2024d, GCN, 37004, 1
An, J., Zhu, Z. P., Liu, X., et al. 2024e, GCN, 36202, 1
Andreoni, I., Coughlin, M. W., Perley, D. A., et al. 2022, Natur, 612, 430
Antier, S., Wang, X., Yuan, W. M., et al. 2024, ATel, 16531, 1
Antipov, G., Lipunov, V., Balanutsa, P., et al. 2024a, GCN, 36142, 1
Antipov, G., Lipunov, V., Balanutsa, P., et al. 2024b, GCN, 36060, 1
Aryan, A., Chen, T.-W., Hou, W.-J., et al. 2024c, GCN, 38061, 1
Aryan, A., Chen, T. W., Hou, W. J., et al. 2024d, GCN, 38290, 1
Aryan, A., Chen, T. W., Yang, S., et al. 2024b, GCN, 37021, 1
Aryan, A., Kong, A. K. H., Hou, W.-J., et al. 2024a, GCN, 38042, 1
Aryan, A., Kong, A. K. H., Hsiao, H. Y., et al. 2024e, GCN, 37002, 1
Aryan, A., Kong, A. K. H., Yang, Y. J., et al. 2024f, GCN, 37575, 1
Aryan, A., Michailidis, G., Ranjan Das, S., et al. 2025, GCN, 38924, 1
Aryan, A., Yang, S., Chen, T. W., et al. 2024g, GCN, 36094, 1
Aryan, A., Yang, S., Chen, T. W., et al. 2024h, TNSTR, 2024, 1
Aryan, A., Yang, S., Chen, T. W., et al. 2024i, GCN, 36408, 1
Aryan, A., Yang, S., Chen, T. W., et al. 2024j, GCN, 36819, 1
Asquini, L., Landoni, M., D'Avanzo, P., Campana, S., & Farias, C. 2024, GCN, 37499, 1
Astropy Collaboration, Price-Whelan, A. M., Sipőcz, B. M., et al. 2018, AJ, 156, 123
Astropy Collaboration, Robitaille, T. P., Tollerud, E. J., et al. 2013, A&A, 558, A33
Balasubramanian, A., Eappachen, D., Anupama, G. C., Bhalerao, V., & Sahu, D. K. 2024, GCN, 38584, 1
Barria, P., Gianfagna, G., Rodi, J. C., et al. 2024, GCN, 38556, 1
Bauer, F. E., Treister, E., Schawinski, K., et al. 2017, MNRAS, 467, 4841
Becker, A., 2015 HOTPANTS: High Order Transform of PSF ANd Template Subtraction, Astrophysics Source Code Library, ascl:1504.004
Belkin, S., Inasaridze, R. Y., Pozanenko, A., Pankov, N. & GRB IKI FuN 2024a, GCN, 37584, 1
Belkin, S., Klunko, E., Pozanenko, A., Pankov, N. & GRB IKI FuN 2024b, GCN, 37583, 1
Belkin, S., Sokolov, I., Pozanenko, A., Pankov, N. & GRB IKI FuN 2024c, GCN, 36158, 1
Bertin, E., & Arnouts, S. 1996, A&AS, 117, 393
Bochenek, A., Hinds, K. R., & Perley, D. A. 2024, GCN, 35783, 1
Bochenek, A., & Perley, D. A. 2024a, GCN, 37869, 1
Bochenek, A., & Perley, D. A. 2024b, GCN, 38030, 1
Bochenek, A., & Perley, D. A. 2024c, GCN, 38615, 1
Bochenek, A., & Perley, D. A. 2024d, GCN, 36821, 1
Bochenek, A., & Perley, D. A. 2024e, GCN, 38018, 1
Bochenek, A., & Perley, D. A. 2025, GCN, 38801, 1
Brennan, S. J., & Fraser, M. 2022, A&A, 667, A62
Bright, J., Carotenuto, F., Jonker, P. G., Fender, R., & Smartt, S. 2024, GCN, 36362, 1
Bright, J. S., Carotenuto, F., Fender, R., et al. 2024, ApJ, 981, 48
Bright, J. S., Carotenuto, F., Fender, R., et al. 2025, ApJ, 981, 48
Brivio, R., Ferro, M., D'Avanzo, P., et al. 2024, GCN, 37579, 1
Brocato, E., Branchesi, M., Cappellaro, E., et al. 2018, MNRAS, 474, 411
Burns, E., Svinkin, D., Fenimore, E., et al. 2023, ApJL, 946, L31
Busmann, M., Gruen, D., O'Connor, B., & Palmese, A. 2024a, GCN, 38019, 1
Busmann, M., Gruen, D., O'Connor, B., & Palmese, A. 2024d, GCN, 38120, 1
Busmann, M., Gruen, D., O'Connor, B., & Palmese, A. 2024e, GCN, 38064, 1
Busmann, M., Gruen, D., O'Connor, B., Palmese, A., & Schmidt, M. 2024b, GCN, 37877, 1
Busmann, M., Gruen, D., O'Connor, B., Palmese, A., & Schmidt, M. 2024c, GCN, 37878, 1
Busmann, M., O'Connor, B., Sommer, J., et al. 2025, A&A, 701, A225
Carotenuto, F., Bright, J., & Fender, R. 2024, GCN, 38014, 1
Carotenuto, F., Bright, J., & Jonker, P. G. 2025, GCN, 38958, 1
Castro-Tirado, A. J., Gupta, R., Pandey, S. B., et al. 2024, A&A, 683, A55
Castro-Tirado, A. J., Soldán, J., Bernas, M., et al. 1999, A&AS, 138, 583
Chambers, K. C., Magnier, E. A., Metcalfe, N., et al. 2016, arXiv:1612.05560
Chang, N., Cui, L., Huang, Y., et al. 2024, GCN, 36414, 1
Chen, T. W., Aryan, A., Yang, S., et al. 2024a, GCN, 36139, 1
Chen, T. W., Yang, S., Smartt, S., et al. 2024b, GCN, 36011, 1
Chen, T.-W., Yang, S., Srivastav, S., et al. 2025, ApJ, 983, 86
Chen, W., Dai, C. Y., Wen, S. X., et al. 2024a, GCN, 36801, 1
Chen, W., Sun, H., Zhou, H., et al. 2024b, GCN, 36723, 1
Chen, W., Wang, Y. L., Hu, J. W., et al. 2024c, GCN, 36838, 1
Chen, W., Zhao, G. Y., Zhou, C., et al. 2024d, GCN, 38430, 1
Chen, W., Zhao, T., Zhou, C., et al. 2024e, GCN, 38415, 1
Cheng, H. Q., Wang, W. X., Yuan, W., et al. 2024, GCN, 36138, 1
Clocchiatti, A., Suntzeff, N. B., Covarrubias, R., & Candia, P. 2011, AJ, 141, 163
Condon, J. J., Cotton, W. D., Greisen, E. W., et al. 1998, AJ, 115, 1693
Dai, C. Y., Huang, M. Q., Liu, Z. Y., et al. 2024, GCN, 38251, 1
Dainotti, M. G., De Simone, B., Mohideen Malik, R. F., et al. 2024, MNRAS, 533, 4023
Dasgupta, A., Srijan, S., Waratkar, G., et al. 2024, GCN, 37505, 1
Dey, A., Schlegel, D. J., Lang, D., et al. 2019, AJ, 157, 168
Djorgovski, S. G., Frail, D. A., Kulkarni, S. R., et al. 2001, ApJ, 562, 654
Du, G., Zhang, J., Zhong, S., et al. 2024, GCN, 38446, 1
Eappachen, D., Jonker, P. G., Quirola-Vásquez, J., et al. 2024, MNRAS, 527, 11823
Eyles-Ferris, R. 2025, GCN, 38878, 1
Eyles-Ferris, R. A. J., Jonker, P. G., Levan, A. J., et al. 2025a, ApJL, 988, L14
Eyles-Ferris, R. A. J., Malesani, D. B., O'Brien, P. T., et al. 2025b, GCN, 38983, 1
Fan, L. L., Aryan, A., Chen, T. W., et al. 2024a, GCN, 38592, 1
Fan, L. L., Aryan, A., Chen, T. W., et al. 2024b, GCN, 38254, 1
Fermi-GBM team 2024a, GCN, 37955, 1
Fermi-GBM team 2024b, GCN, 38075, 1
Fernandez-Garcia, E., Perez-Garcia, I., Wu, S. Y., et al. 2024, GCN, 36822, 1
Ferrero, P., Kann, D. A., Zeh, A., et al. 2006, A&A, 457, 857
Frederiks, D., Lysenko, A., Ridnaia, A., et al. 2024, GCN, 36809, 1

Freeberg, M., Antier, S., Wang, X., et al. 2024, GCN, 36010, 1
Freeburn, J., & Andreoni, I. 2024, GCN, 38062, 1
Freeburn, J., Andreoni, I., & Carney, J. 2024a, GCN, 37942, 1
Freeburn, J., Andreoni, I., & Carney, J. 2024b, GCN, 38409, 1
Freeburn, J., Andreoni, I., Quirola-Vasquez, J., et al. 2024c, GCN, 37911, 1
Fu, S. Y., An, J., Jiang, S. Q., et al. 2024a, ATel, 16807, 1
Fu, S. Y., An, J., Jiang, S. Q., et al. 2024b, GCN, 36761, 1
Fu, S. Y., An, J., Tinyanont, S., et al. 2024c, GCN, 36998, 1
Fu, S. Y., Jiang, S. Q., Tinyanont, S., et al. 2024d, GCN, 37434, 1
Fu, S. Y., Jiang, S. Q., Tinyanont, S., et al. 2024e, GCN, 38337, 1
Fu, S. Y., Liu, X., Jiang, S. Q., et al. 2024f, GCN, 37547, 1
Fu, S. Y., Tinyanont, S., Anutarawiramkul, R., et al. 2024g, GCN, 37842, 1
Fu, S. Y., Zhu, Z. P., An, J., et al. 2024h, GCN, 37840, 1
Fynbo, J. U., Jensen, B. L., Gorosabel, J., et al. 2001, A&A, 369, 373
Galama, T. J., Vreeswijk, P. M., van Paradijs, J., et al. 1998, Natur, 395, 670
Garrappa, S., Konno, R., Ofek, E. O., et al. 2024, ATel, 16729, 1
Geng, J.-J., Jiang, J.-A., Jiang, N., et al. 2024, GCN, 38357, 1
Gianfagna, G., Bruni, G., Piro, L., & Thakur, A. L. 2024, GCN, 37906, 1
Gianfagna, G., Piro, L., Bruni, G., et al. 2025, arXiv:2505.05444
Gillanders, J. H., Rhodes, L., Srivastav, S., et al. 2024, ApJL, 969, L14
Glennie, A., Jonker, P. G., Fender, R. P., Nagayama, T., & Pretorius, M. L. 2015, MNRAS, 450, 3765
Gompertz, B. P., Kumar, A., Ramsay, G., et al. 2024, GCN, 37835, 1
Greiner, J., Krühler, T., Klose, S., et al. 2011, A&A, 526, A30
Groot, P., Jonker, P., Levan, A., et al. 2024, GCN, 36007, 1
Grossan, B., Maksut, Z., Krugov, M., et al. 2024, GCN, 38079, 1
Grove, J. E., Cheung, C. C., Kerr, M., et al. 2020, Yamada Conf. LXXI: Gamma-ray Bursts in the Gravitational Wave Era 2019, ed. T. Sakamoto, M. Serino, & S. Sugta,, 57, https://yokohamagrb2019.wdfiles.com/local–files/proceedings:files-1/47.pdf
Guan, J., Li, C. K., Chen, Y., et al. 2024, GCN, 36129, 1
Gulati, A., Castro-Tirado, A. J., & Murphy, T. 2024, GCN, 37952, 1
Gupta, R. 2023, arXiv:2312.16265
Gupta, R., Kumar, A., Pandey, S. B., et al. 2022, JApA, 43, 11
Gupta, R., Oates, S. R., Pandey, S. B., et al. 2021a, MNRAS, 505, 4086
Gupta, R., Pandey, S. B., Castro-Tirado, A. J., et al. 2021b, RMxAC, 53, 113
Gupta, R., Racusin, J., Lipunov, V., et al. 2024, arXiv:2412.18152
Hale, C. L., McConnell, D., Thomson, A. J. M., et al. 2021, PASA, 38, e058
Hamidani, H., Sato, Y., Kashiyama, K., et al. 2025a, ApJL, 986, L4
Hamidani, H., Sato, Y., Kashiyama, K., et al. 2025b, ApJL, 986, L4
Harris, C. R., Millman, K. J., van der Walt, S. J., et al. 2020, Natur, 585, 357
Hjorth, J., Levan, A. J., Tanvir, N. R., et al. 2017, ApJL, 848, L31
Ho, A. Y. Q., Perley, D. A., Kulkarni, S. R., et al. 2020, ApJ, 895, 49
Ho, A. Y. Q., Perley, D. A., Gal-Yam, A., et al. 2023, ApJ, 949, 120
Hu, D. F., Zheng, T. C., Wang, B. T., et al. 2024, GCN, 38335, 1
Hu, J. W., Chen, W., Wang, Y. L., et al. 2024a, GCN, 36840, 1
Hu, J. W., Huang, M. Q., Liu, Z. Y., et al. 2024b, GCN, 38239, 1
Hu, J. W., Wang, Y., He, H., et al. 2024c, GCN, 37834, 1
Hu, J. W., Zhao, D. H., Liu, Y., et al. 2024d, GCN, 36053, 1
Hu, J. W., Zhao, D. H., Liu, Y., et al. 2024e, GCN, 36057, 1
Hu, L., Wang, L., Chen, X., & Yang, J. 2022, ApJ, 936, 157
Hunter, J. D. 2007, CSE, 9, 90
Hussenot-Desenonges, T., de Almeida, L., Corradi, W., et al. 2024, GCN, 38597, 1
Irwin, J. A., Maksym, W. P., Sivakoff, G. R., et al. 2016, Natur, 538, 356
Izzo, L. 2025, GCN, 38912, 1
Izzo, L., & Malesani, D. B. 2024a, GCN, 38588, 1
Izzo, L., & Malesani, D. B. 2024b, GCN, 38053, 1
J-Jin, J., Mu, H. Y. F. Z., Sun, Y. G., & Mao, R. W. Y. M. 2024, GCN, 37892, 1
Jakobsson, P., Hjorth, J., Fynbo, J. P. U., et al. 2004, ApJL, 617, L21
Jia, S. M., Sun, H., Li, C. K., et al. 2024, GCN, 36022, 1
Jiang, S. Q., An, J., Liu, X., et al. 2024a, GCN, 37565, 1
Jiang, S. Q., Liu, X., Zhu, Z. P., et al. 2024b, GCN, 36842, 1
Jiang, S. Q., Tinyanont, S., Anutarawiramkul, R., et al. 2024c, GCN, 37862, 1
Jiang, S. Q., Wang, Y., Shui, Q. C., et al. 2024d, ATel, 16725, 1
Jiang, S.-Q., Xu, D., van Hoof, A. P. C., et al. 2025, ApJL, 988, L34
Jiang, S. Q., Zhu, Z. P., Li, D. Y., et al. 2024e, GCN, 37497, 1
Jin, J. J., Mu, H. Y., Fan, Z., et al. 2024, GCN, 36419, 1
Jonker, P. G., Glennie, A., Heida, M., et al. 2013, ApJ, 779, 14
Jonker, P. G., Levan, A. J., Malesani, D. B., et al. 2024, GCN, 36110, 1
Jordana-Mitjans, N., Mundell, C. G., Kobayashi, S., et al. 2020, ApJ, 892, 97
Jin, J., Mao, Y., Zheng, J., et al. 2024, GCN, 38607, 1
Karambelkar, V., Tinyanont, K., Rose, S., et al. 2024, GCN, 36189, 1
Klingler, N., Oates, S. R., Eyles-Ferris, R., & Team, S.-U. 2024, GCN, 37990, 1
Klingler, N. J., Dichiara, S., Gupta, R., et al. 2024, GCN, 37956, 1
Kong, A. K. H., Aryan, A., Chen, T. W., et al. 2024a, GCN, 38131, 1
Kong, A. K. H., Aryan, A., Chen, T. W., et al. 2024b, GCN, 37545, 1
Kozyrev, A. S., Golovin, D. V., Litvak, M. L., et al. 2024a, GCN, 37538, 1
Kozyrev, A. S., Golovin, D. V., Litvak, M. L., et al. 2024b, GCN, 37078, 1
Kumar, A., Maund, J. R., Sun, N. C., et al. 2024a, GCN, 37875, 1
Kumar, A., Maund, J. R., Sun, N. C., et al. 2025a, GCN, 38907, 1
Kumar, A., Maund, J. R., Sun, N. C., et al. 2025b, GCN, 38788, 1
Kumar, A., Sun, N. C., Maund, J. R., et al. 2025c, GCN, 38921, 1
Kumar, A., Gompertz, B. P., Kennedy, M., et al. 2024b, GCN, 37566, 1
Lai, C. H., Aryan, A., Chen, T. W., et al. 2024a, GCN, 36839, 1
Lai, C. H., Aryan, A., Chen, T. W., et al. 2024b, GCN, 38319, 1
Lai, C. H., Aryan, A., Chen, T. W., et al. 2024c, GCN, 38344, 1
Lai, C. H., Aryan, A., Kong, A. K. H., et al. 2024d, GCN, 37577, 1
Lee, M. H., Aryan, A., Yang, Y. J., et al. 2024a, ATel, 16726, 1
Lee, M. H., Yang, S., Aryan, A., et al. 2024b, GCN, 38418, 1
Leonini, S., Conti, M., Rosi, P., et al. 2024a, GCN, 36774, 1
Leonini, S., Conti, M., Rosi, P., et al. 2024b, GCN, 37029, 1
Levan, A. J., Cotter, L., Malesani, D. B., Martin-Carrillo, A., & Jonker, P. G. 2025a, GCN, 38909, 1
Levan, A. J., Jonker, P. G., Saccardi, A., et al. 2024a, arXiv:2404.16350
Levan, A. J., Malesani, D. B., Jonker, P. G., et al. 2024b, GCN, 36025, 1
Levan, A. J., Quirola-Vasquez, J. A., Rastinejad, J. C., et al. 2024c, GCN, 38593, 1
Levan, A. J., Rastinejad, J. C., Malesani, D. B., Jonker, P. G., & Quirola-Vasquez, J. A. 2024d, GCN, 38587, 1
Levan, A. J., Rastinejad, J. C., Malesani, D. B., et al. 2025b, GCN, 38987, 1
Levan, A. J., van Dalen, J., Jonker, P., et al. 2024e, GCN, 36355, 1
Li, A., Wang, C. Y., Liu, H. Y., et al. 2024, GCN, 38140, 1
Li, C. K., Jia, S. M., Chen, Y., et al. 2024, GCN, 36092, 1
Li, D. Y., Xu, X. P., Wang, B. T., et al. 2024a, GCN, 37492, 1
Li, D. Y., Yang, J., Li, A., et al. 2024b, GCN, 36405, 1
Li, L.-X. 2008, MNRAS, 388, 603
Li, R. Z., Chen, X. L., Chatterjee, K., et al. 2025a, GCN, 38861, 1
Li, R. Z., Chen, X. L., Chatterjee, K., et al. 2025b, GCN, 38888, 1
Li, R. Z., Lin, H., Li, S. S., et al. 2024a, GCN, 38027, 1
Li, R. Z., Wang, B. T., Mao, J., Zhang, X. L., & Bai, J. M. 2024b, GCN, 36999, 1
Li, W. X., Sun, N. C., Maund, J., Wang, Y. N., & Wiersema, K. 2024a, GCN, 37846, 1
Li, W. X., Xue, S. J., Andrews, M., et al. 2024b, GCN, 37844, 1
Li, W. X., Xue, S. J., Andrews, M., et al. 2024c, GCN, 38127, 1
Li, W. X., Xue, S. J., Andrews, M., et al. 2024d, GCN, 36731, 1
Li, W. X., Xue, S. J., Andrews, M., et al. 2024e, GCN, 36806, 1
Li, W. X., Xue, S. J., Andrews, M., et al. 2024f, GCN, 36852, 1
Li, W. X., Xue, S. J., Andrews, M., et al. 2024g, GCN, 38338, 1
Li, W. X., Xue, S. J., Andrews, M., et al. 2024h, GCN, 36529, 1
Li, W. X., Xue, S. J., Andrews, M., et al. 2024i, GCN, 36836, 1
Li, W. X., Xue, S. J., Andrews, M., et al. 2024j, GCN, 37064, 1
Li, W. X., Xue, S. J., Sun, H., et al. 2024k, GCN, 36154, 1
Li, W. X., Xue, S. J., Xu, D., et al. 2024l, GCN, 36079, 1
Li, W. X., Zhu, Z. P., Zou, X. Z., et al. 2025, arXiv:2504.17034
Lian, T. Y., Li, D. Y., Wang, Y. L., Yuan, S. X. W. W. & Einstein Probe team 2024a, GCN, 37902, 1
Lian, T. Y., Pan, X., Ling, Z. X., et al. 2024b, GCN, 36091, 1
Lian, T. Y., Pan, X., Ling, Z. X., et al. 2024c, GCN, 36086, 1
Liang, Y. F., Cheng, H. Q., Liu, M. J., et al. 2024a, GCN, 37561, 1
Liang, Y. F., Jiang, S. Q., Wu, H. Z., et al. 2024f, GCN, 38040, 1
Liang, Y. F., Liu, M. J., Cheng, H. Q., et al. 2024b, GCN, 37585, 1
Liang, Y. F., Liu, Q. C., Wu, Q. Y., et al. 2024e, GCN, 38039, 1
Liang, Y.-F., Yang, J., Yin, Y.-H. I., et al. 2024c, GCN, 37563, 1
Liang, Y. F., Zhang, Z. J., Liu, M. J., et al. 2024d, GCN, 37555, 1
Lin, D., Irwin, J. A., Berger, E., & Nguyen, R. 2022, ApJ, 927, 211
Ling, Z. X., Sun, X. J., Zhang, C., et al. 2023, RAA, 23, 095007
Lipunov, V., Balanutsa, P., Buckley, D., et al. 2024a, GCN, 36009, 1
Lipunov, V., Gorbovskoy, E., Tiurina, N., et al. 2024b, GCN, 38428, 1
Lipunov, V., Gorbovskoy, E., Tiurina, N., et al. 2024c, GCN, 38242, 1
Lipunov, V., Gorbovskoy, E., Tiurina, N., et al. 2024d, GCN, 38416, 1
Lipunov, V., Gorbovskoy, E., Tiurina, N., et al. 2024e, GCN, 38282, 1
Lipunov, V., Gorbovskoy, E., Tiurina, N., et al. 2024f, GCN, 38458, 1
Lipunov, V., Gorbovskoy, E., Tiurina, N., et al. 2024g, GCN, 38514, 1
Lipunov, V., Gorbovskoy, E., Tiurina, N., et al. 2024h, GCN, 38215, 1
Lipunov, V., Gorbovskoy, E., Tiurina, N., et al. 2024i, GCN, 38661, 1
Lipunov, V., Gorbovskoy, E., Tiurina, N., et al. 2024s, GCN, 38076, 1
Lipunov, V., Kornilov, V., Gorbovskoy, E., et al. 2024j, GCN, 37839, 1
Lipunov, V., Kornilov, V., Gorbovskoy, E., et al. 2024k, GCN, 37437, 1

Lipunov, V., Kornilov, V., Gorbovskoy, E., et al. 2024l, GCN, 37521, 1
Lipunov, V., Kornilov, V., Gorbovskoy, E., et al. 2024m, GCN, 37548, 1
Lipunov, V., Kornilov, V., Gorbovskoy, E., et al. 2024n, GCN, 37570, 1
Lipunov, V., Kornilov, V., Gorbovskoy, E., et al. 2024o, GCN, 37905, 1
Lipunov, V., Kornilov, V., Gorbovskoy, E., et al. 2024p, GCN, 37105, 1
Lipunov, V., Kornilov, V., Gorbovskoy, E., et al. 2024q, GCN, 37649, 1
Lipunov, V., Kornilov, V., Gorbovskoy, E., et al. 2024r, GCN, 38049, 1
Liu, D., Pan, Y., Liu, X., et al. 2024, GCN, 38636, 1
Liu, M. J., Liang, Y. F., Zhang, Z. J., et al. 2024, GCN, 37608, 1
Liu, X., An, J., Jiang, S. Q., et al. 2024a, GCN, 38560, 1
Liu, X., Fu, S. Y., An, J., et al. 2024b, GCN, 36736, 1
Liu, X., Fu, S. Y., An, J., et al. 2024c, GCN, 36741, 1
Liu, X., Jiang, S. Q., Fu, S. Y., et al. 2024d, GCN, 38425, 1
Liu, Y., Sun, H., Xu, D., et al. 2024, NatAs, 9, 546
Liu, Y., Sun, H., Xu, D., et al. 2025, NatAs, 9, 564
Malesani, D. B., Jonker, P. G., Bauer, F. E., et al. 2024a, GCN, 38385, 1
Malesani, D. B., Levan, A. J., van Hoof, A., Jonker, P. G., & Xu, D. 2025, GCN, 38902, 1
Malesani, D. B., Martin-Carrillo, A., An, J., et al. 2024b, GCN, 37567, 1
Malesani, D. B., Quirola-Vásquez, J., van Dalen, J., et al. 2024c, GCN, 37008, 1
Malesani, D. B., Rossi, A., Kuhn, O., & Cusano, F. 2024d, GCN, 37907, 1
Mao, X., Hu, J. W., Peng, J. Q., et al. 2024a, GCN, 37443, 1
Mao, X., Peng, J. Q., Yang, S. K., et al. 2024b, GCN, 37432, 1
Mazzali, P. A., Valenti, S., Della Valle, M., et al. 2008, Sci, 321, 1185
Metzger, B. D., Martínez-Pinedo, G., Darbha, S., et al. 2010, MNRAS, 406, 2650
Mo, G., Karambelkar, V., Frostig, D., et al. 2024, GCN, 36172, 1
Modjaz, M., Liu, Y. Q., Bianco, F. B., & Graur, O. 2016, ApJ, 832, 108
Mohan, T., Swain, V., Kumar, R., et al. 2024a, GCN, 37920, 1
Mohan, T., Swain, V., Kumar, R., et al. 2024b, GCN, 38612, 1
Mohan, T., Swain, V., Saikia, A. P., et al. 2024c, GCN, 38118, 1
Moretti, L., Pavoni, E., Dainotti, M. G., et al. 2024, GCN, 37014, 1
Moskvitin, A., & Goranskij, V. P. 2024, GCN, 38032, 1
Moskvitin, A., Oparin, D., Pankov, N., & Pozanenko, A. 2024, GCN, 37049, 1
Moskvitin, A. S., Spiridonova, O. I. & GRB follow-up team 2024a, GCN, 37951, 1
Moskvitin, A. S., Spiridonova, O. I. & GRB follow-up team 2024b, GCN, 37012, 1
Moskvitin, A. S., Spiridonova, O. I. & GRB follow-up team 2024c, GCN, 37017, 1
Moskvitin, A. S., Spiridonova, O. I. & GRB follow-up team 2024d, GCN, 37850, 1
Moskvitin, A. S., Spiridonova, O. I. & GRB follow-up team 2024e, GCN, 37910, 1
Moskvitin, A. S., Spiridonova, O. I. & GRB follow-up team 2025, GCN, 38925, 1
Ngeow, C. C., Yang, S., Aryan, A., et al. 2024, GCN, 38433, 1
Novara, G., Esposito, P., Tiengo, A., et al. 2020, ApJ, 898, 37
Odeh, M., Alshamsi, S., Manal Pattani, N., & Guessoum, N. 2024a, GCN, 38128, 1
Odeh, M., Alshamsi, S., Manal Pattani, N., & Guessoum, N. 2024b, GCN, 38115, 1
Oganesyan, G., Karpov, S., Salafia, O. S., et al. 2023, NatAs, 7, 843
Paek, G. S. H., Im, M., Choi, H., et al. 2024, GCN, 38610, 1
Pall'e, K. A., Gompertz, B. P., O'Brien, P., et al. 2024, GCN, 36098, 1
Pan, X., Liu, M. J., Liu, Y., et al. 2024a, ATel, 16564, 1
Pan, X., Lv, Z. Z., Fu, Y. C., et al. 2024b, GCN, 36757, 1
Pan, X., Lv, Z. Z., Fu, Y. C., et al. 2024c, GCN, 36760, 1
Pan, Y., Kumar, B., Lin, W., et al. 2024, GCN, 37968, 1
Pankov, N., Elenin, L., Pozanenko, A., et al. 2024a, GCN, 36157, 1
Pankov, N., Kim, V., Krugov, M., et al. 2024b, GCN, 37146, 1
Pankov, N., Pozanenko, A., Inasaridze, R. Y. & GRB IKI FuN 2024c, GCN, 36714, 1
Pankov, N., Pozanenko, A., Klunko, E., et al. 2024d, GCN, 37444, 1
Pankov, N., Pozanenko, A., Rumyantsev, V., Belkin, S. & GRB IKI FuN 2024e, GCN, 36417, 1
Pankov, N., Pozanenko, A., Rumyantsev, V., Inasaridze, R. Y. & GRB IKI FuN 2024f, GCN, 37016, 1
Pankov, N., Pozanenko, A., Rumyantsev, V. & GRB-IKI-FuN Collaboration 2024h, GCN, 38109, 1
Pankov, N., Rumyantsev, V., Pozanenko, A. & GRB IKI FuN 2024g, GCN, 37040, 1
Pawar, D. 2024, GCN, 37510, 1
Peng, Z.-K., Yang, Y.-S., Shen, R.-F., et al. 2019, ApJL, 884, L34
Pérez-Fournon, I., Poidevin, F., Aguado, D. S., et al. 2024a, GCN, 37007, 1
Pérez-Fournon, I., Poidevin, F., Aguado, D. S., et al. 2024b, GCN, 37080, 1
Pérez-Fournon, I., Sun, N. C., Li, W., et al. 2024c, GCN, 37858, 1
Perez-Garcia, I., Fernandez-Garcia, E., Caballero-Garcia, M. D., et al. 2024a, GCN, 37199, 1
Perez-Garcia, I., Fernandez-Garcia, E., Caballero-Garcia, M. D., et al. 2024b, GCN, 36056, 1
Perez-Garcia, I., Fernandez-Garcia, E., Caballero-Garcia, M. D., et al. 2024c, GCN, 36412, 1
Perez-Garcia, I., Fernandez-Garcia, E., Caballero-Garcia, M. D., et al. 2024d, GCN, 36693, 1
Perez-Garcia, I., Wu, S. Y., Castro-Tirado, A. J., et al. 2024e, GCN, 38141, 1
Perez-Garcia, I., Wu, S. Y., Fernandez-Garcia, E., et al. 2024f, GCN, 36767, 1
Perez-Garcia, I., Wu, S. Y., Fernandez-Garcia, E., et al. 2024g, GCN, 38427, 1
Perez-Garcia, I., Wu, S.-Y., Fernandez-Garcia, E., et al. 2024h, GCN, 38047, 1
Perley, D. A., Ho, A. Y. Q., Yao, Y., et al. 2021, MNRAS, 508, 5138
Pian, E., D'Avanzo, P., Benetti, S., et al. 2017, Natur, 551, 67
Planck Collaboration, Ade, P. A. R., Aghanim, N., et al. 2016, A&A, 594, A13
Polzin, A., Margutti, R., Coppejans, D. L., et al. 2023, ApJ, 959, 75
Prentice, S. J., Maguire, K., Smartt, S. J., et al. 2018, ApJL, 865, L3
Pugliese, G., Xu, D., Izzo, L., et al. 2024, GCN, 37852, 1
Quadri, U., Strabla, L., Madurini, P., et al. 2024, GCN, 37023, 1
Quirola-Vásquez, J., Bauer, F. E., Jonker, P. G., et al. 2022, A&A, 663, A168
Quirola-Vásquez, J., Bauer, F. E., Jonker, P. G., et al. 2023, A&A, 675, A44
Quirola-Vasquez, J., Bauer, F., Jonker, P., Malesani, D., & Levan, A. 2024a, GCN, 38126, 1
Quirola-Vasquez, J., Jonker, P. G., Malesani, D. B., et al. 2024b, GCN, 37551, 1
Quirola-Vásquez, J., Jonker, P. G., van Dalen, J., et al. 2024c, GCN, 36888, 1
Quirola-Vasquez, J., Malesani, D. B., Levan, A. J., et al. 2024d, GCN, 37438, 1
Quirola-Vasquez, J., Malesani, D. B., Levan, A. J., et al. 2024e, GCN, 37458, 1
Quirola-Vasquez, J. A., Malesani, D. B., Levan, A. J., Bauer, F. E., & Jonker, P. G. 2024f, GCN, 37930, 1
Quirola-Vásquez, J., van Dalen, J., Malesani, D. B., et al. 2024g, GCN, 37013, 1
Racusin, J. L., Karpov, S. V., Sokolowski, M., et al. 2008, Natur, 455, 183
Rastinejad, J. C., Levan, A. J., Jonker, P. G., et al. 2025, ApJL, 988, L13
Rau, A. 2024, GCN, 36059, 1
Ravasio, M. E., & Jonker, P. G. 2024, GCN, 36725, 1
Reguitti, A., Hu, Y.-D., Ferro, M., et al. 2024, GCN, 38107, 1
Ricci, R., Bruni, G., Carotenuto, F., Gianfagna, G., & Yao, Y. 2024a, GCN, 37949, 1
Ricci, R., Troja, E., & Yadav, M. 2024b, GCN, 38652, 1
Ricci, R., Troja, E., Yang, Y., et al. 2025, ApJL, 979, L28
Ridnaia, A., Frederiks, D., Lysenko, A., et al. 2024, GCN, 36028, 1
Roberts, O. J., Wood, J., Goldstein, A., et al. 2024, GCN, 37580, 1
Rodi, J., Linesh Thakur, A., Piro, L., Natalucci, L., & Gianfagna, G. 2024, GCN, 37573, 1
Ror, A. K., Gupta, R., Jelínek, M., et al. 2023, ApJ, 942, 34
Ror, A. K., Gupta, A., Kiran, Pandey, S. B., & Mishra, K. 2025, GCN, 39002, 1
Ror, A. K., Gupta, A., Tripathi, T., Pandey, S. B., & Mishra, K. 2024, GCN, 37845, 1
Rossi, A., Malesani, D. B., & Maiorano, E. 2024, GCN, 37938, 1
Ruocco, N., Dainotti, M. G., Niino, Y., Kalinowski, K., & De Simone, B. 2024, GCN, 37024, 1
Ryan, G., van Eerten, H., Piro, L., & Troja, E. 2020, ApJ, 896, 166
Saccardi, A., Levan, A. J., Zhu, Z., et al. 2024, GCN, 35936, 1
Saikia, A. P., Mohan, T., Swain, V., et al. 2024, GCN, 38288, 1
Santos, A., Bom, C. R., Kilpatrick, C. D., et al. 2024, GCN, 36707, 1
Sari, R., Piran, T., & Halpern, J. P. 1999, ApJL, 519, L17
Sari, R., Piran, T., & Narayan, R. 1998, ApJL, 497, L17
Sarin, N., Hübner, M., Omand, C. M. B., Setzer, C. N., et al. 2024, MNRAS, 531, 1203
Schlafly, E. F., & Finkbeiner, D. P. 2011, ApJ, 737, 103
Schneider, B., & Adami, C. 2024a, GCN, 38022, 1
Schneider, B., & Adami, C. 2024b, GCN, 38071, 1
Schneider, B., Zhu, Z. P., Levan, A. J., et al. 2024, GCN, 37515, 1
Schroeder, G., Ho, A., & Perley, D. 2025, GCN, 38970, 1
Schroeder, G., Srinivasaragavan, G., Ho, A., et al. 2024, GCN, 38640, 1
Shui, Q. C., Peng, J. Q., Dai, C. Y., et al. 2024, GCN, 36827, 1
Smartt, S. J., Chen, T. W., Jerkstrand, A., et al. 2017, Natur, 551, 75
Soderberg, A. M., Berger, E., Page, K. L., et al. 2008, Natur, 453, 469
Song, F. F., Li, R. Z., Wang, B. T., et al. 2025, GCN, 38972, 1

Sota, A., Calle, D., Flores, L. A., et al. 2024, GCN, 38480, 1
Srinivasaragavan, G. P., Hamidani, H., Schroeder, G., et al. 2025, ApJL, 988, L60
Srivastav, S., Chen, T. W., Gillanders, J. H., et al. 2025, ApJL, 978, L21
Srivastav, S., Gillanders, J. H., Rhodes, L., et al. 2024a, GCN, 36150, 1
Srivastav, S., Smartt, S. J., Fulton, M. D., et al. 2024b, GCN, 35932, 1
Stetson, P. B. 1987, PASP, 99, 191
Sun, H., Chen, W., Zhou, H., et al. 2024a, GCN, 36690, 1
Sun, H., Chen, W., Zhou, H., et al. 2024b, GCN, 36722, 1
Sun, H., Li, W. X., Liu, L. D., et al. 2025, NatAs, 9, 1073
Sun, T.-R., Geng, J.-J., Chen, J., et al. 2024a, GCN, 36178, 1
Sun, T.-R., Geng, J.-J., Chen, J., et al. 2024b, GCN, 37546, 1
Sun, T.-R., Hua, Y.-L., Geng, J.-J., et al. 2024c, GCN, 36335, 1
SVOM/C-GFT Team, Kang, Z., Wu, C., et al. 2024, GCN, 38116, 1
SVOM/ECLAIRS commissioning team, Atteia, J.-L., Bouchet, L., et al. 2024, GCN, 38557, 1
SVOM/GRM team, Tan, W.-J., Dong, Y.-W., et al. 2024a, GCN, 37022, 1
SVOM/GRM team, Wang, C.-W., Dong, Y.-W., et al. 2024b, GCN, 37574, 1
SVOM/GRM team, Wang, C.-W., Zheng, S.-J., et al. 2024c, GCN, 38250, 1
SVOM/VT commissioning team, Qiu, Y. L., Li, H. L., et al. 2025, GCN, 38872, 1
SVOM/VT commissioning team, Qiu, Y. L., Xin, L. P., et al. 2024a, GCN, 37581, 1
SVOM/VT commissioning team, Qiu, Y. L., Xin, L. P., et al. 2024b, GCN, 37610, 1
SVOM/VT commissioning team, Qiu, Y. L., Xin, L. P., et al. 2024c, GCN, 38378, 1
Tanvir, N. R., Palmerio, J., Malesani, D. B., et al. 2024, GCN, 36385, 1
Tinyanont, S., Anutarawiramkul, R., Butpan, P., et al. 2024a, GCN, 36413, 1
Tinyanont, S., Anutarawiramkul, R., Butpan, P., et al. 2024b, GCN, 36710, 1
Tinyanont, S., Anutarawiramkul, R., Butpan, P., et al. 2024c, GCN, 36831, 1
Tinyanont, S., Anutarawiramkul, R., Butpan, P., et al. 2024d, GCN, 36832, 1
Tody, D. 1986, Proc. SPIE, 627, 733
Tody, D. 1993, in ASP Conf. Ser. 52, Astronomical Data Analysis Software and Systems II, ed. R. J. Hanisch, R. J. V. Brissenden, & J. Barnes (San Francisco, CA: ASP), 173
Turpin, D., Aghayeva, S., Vidadi, Z., et al. 2024, GCN, 37015, 1
van Dalen, J. N. D., Levan, A. J., Jonker, P. G., et al. 2025, ApJL, 982, L47
Virtanen, P., Gommers, R., Oliphant, T. E., et al. 2020, NatMe, 17, 261
Volnova, A., Moskvitin, A., Pozanenko, A., et al. 2024, GCN, 36824, 1
Wang, B. T., Li, R. Z., Mao, J., Feng, H. C., & Bai, J. M. 2024a, GCN, 36171, 1
Wang, B. T., Li, R. Z., Mao, J., et al. 2024b, GCN, 36315, 1
Wang, B. T., Li, R. Z., Song, F. F., et al. 2024c, GCN, 37544, 1
Wang, B. T., Zheng, T. C., Zhang, W. J., et al. 2024d, GCN, 38318, 1
Wang, Y., He, H., Yang, S. K., et al. 2024a, GCN, 37848, 1
Wang, Y., Wang, Y. L., Peng, H. L., Zhang, W. D. & Einstein Probe team 2024b, GCN, 38513, 1
Wang, Y. L., Dai, C. Y., Peng, J. Q., et al. 2024a, GCN, 36807, 1
Wang, Y. L., Li, A., Wang, W. X., et al. 2024b, GCN, 37019, 1
Wang, Y. L., Wang, Y., Peng, H. L., Zhang, W. D. & Einstein Probe team 2024c, GCN, 38477, 1
Wang, Z. N., Aryan, A., Chen, T.-W., et al. 2024a, GCN, 38084, 1
Wang, Z. N., Yang, S., Aryan, A., et al. 2024b, GCN, 38520, 1
Waratkar, G., Dasgupta, A., Joshi, J., et al. 2024, GCN, 37018, 1
Watson, A. M., Basa, S., Lee, W. H., et al. 2024, GCN, 37900, 1
Williams, M. A., Siegel, M. H., Kennea, J. A., et al. 2024, GCN, 38596, 1
Wolf, C., Onken, C. A., Luvaul, L. C., et al. 2018, PASA, 35, e010
Woolf, R. S., Grove, J. E., Briggs, M. S., et al. 2022, Proc. SPIE, 12181, 121811O
Wu, C., Han, X., Kang, Z., et al. 2024, GCN, 36841, 1
Wu, G.-L., Yu, Y.-W., Liu, L.-D., et al. 2025, ApJ, 991, 115
Wu, H. Z., Wang, B. T., Hu, D. F., et al. 2024, GCN, 37997, 1
Wu, Q. Y., Jia, S. M., Chen, Y., et al. 2024c, GCN, 38073, 1
Wu, Q. Y., Lv, Z. Z., Shui, Q. C., et al. 2024b, GCN, 36770, 1
Wu, Q. Y., Shui, Q. C., Lv, Z. Z., et al. 2024a, GCN, 36766, 1
Wu, S., Pérez-García, I., Castro-Tirado, A. J., et al. 2025, Galax, 13, 62
Wu, S. Y., Perez-Garcia, I., Fernandez-Garcia, E., et al. 2024, GCN, 36701, 1
Xinwen, S., Lei, Y., Haonan, Y., et al. 2025, ApJL, 990, L29
Xiong, D. R., Bai, J. M., Mao, J. R., et al. 2024a, GCN, 36155, 1
Xiong, D. R., Perez-Garcia, I., Fernandez-Garcia, E., et al. 2024b, GCN, 38466, 1
Xu, D., Malesani, D. B., Jonker, P., et al. 2024, GCN, 36105, 1
Xu, D., Zhu, Z. P., Liu, X., et al. 2025, GCN, 38984, 1
Xu, X. P., Ling, Z. X., Liu, Y., et al. 2024, GCN, 36016, 1
Xue, W.-C., Xiong, S.-L., Zheng, C., et al. 2024, GCN, 36017, 1
Xue, Y. Q., Zheng, X. C., Li, Y., et al. 2019, Natur, 568, 198
Yadav, M., Troja, E., Ricci, R., et al. 2025, arXiv:2505.08781
Yadav, M., Troja, E., Yang, Y. H., & Becerra, R. L. 2024, GCN, 36253, 1
Yan, Y. S., Wang, L. T., Wang, X. F., et al. 2024, GCN, 38035, 1
Yang, J., Yin, Y.-H. I., Zhang, B., et al. 2024, GCN, 36692, 1
Yang, S., Aryan, A., Chen, T. W., et al. 2024a, GCN, 37843, 1
Yang, S., Chen, T. W., Hsiao, H. Y., et al. 2024b, GCN, 36027, 1
Yang, S., Sollerman, J., Chen, T. W., et al. 2021, A&A, 646, A22
Yang, Y. J., Aryan, A., Chen, T. W., et al. 2024a, GCN, 37178, 1
Yang, Y. J., Aryan, A., Yang, S., et al. 2024b, GCN, 36823, 1
Yin, Y. H. I., Wang, C. Y., Zhao, D. H., Pan, H. W. & Einstein Probe team 2024a, GCN, 38457, 1
Yin, Y.-H. I., Yang, J., Zhang, B.-B., Sun, H., & Wu, X. 2024b, GCN, 37493, 1
York, D. G., Adelman, J., Anderson Jr., J. E., et al. 2000, AJ, 120, 1579
Yuan, W., Zhang, C., Chen, Y., & Ling, Z. 2022, in Handbook of X-Ray and Gamma-Ray Astrophysics, ed. C. Bambi & A. Sangangelo (Singapore: Springer), 86, doi:10.1007/978-981-16-4544-0_151-1
Yuan, W., Zhang, C., Ling, Z., et al. 2018, Proc. SPIE, 10699, 1069925
Zackay, B., Ofek, E. O., & Gal-Yam, A. 2016, ApJ, 830, 27
Zhang, C., Ling, Z. X., Sun, X. J., et al. 2022, ApJL, 941, L2
Zhang, J., Zou, X., Du, G., et al. 2024, GCN, 37568, 1
Zhang, W. J., Mao, X., Zhang, W. D., et al. 2024a, GCN, 35931, 1
Zhang, W. J., Shui, Q. C., Wu, H. Z., et al. 2024b, GCN, 38281, 1
Zhang, Y., Zhang, Y., Xiong, S., et al. 2024, GCN, 37507, 1
Zhang, Y. J., Liu, M. J., Jiang, S. Q., et al. 2024a, GCN, 36818, 1
Zhang, Z. J., Liang, Y. F., Liu, H. Y., et al. 2024b, GCN, 37541, 1
Zheng, J.-H., Zhu, J.-P., Lu, W., & Zhang, B. 2025, ApJ, 985, 21
Zheng, T. C., Hu, D. F., Wang, B. T., et al. 2024a, GCN, 38339, 1
Zheng, W., Brink, T. G., Filippenko, A. V., et al. 2024a, GCN, 37228, 1
Zheng, W., Brink, T. G., Filippenko, A. V., Yang, Y. & KAIT GRB team 2024b, GCN, 37959, 1
Zheng, W., Brink, T. G., Filippenko, A. V., Yang, Y. & KAIT GRB team 2024c, GCN, 38294, 1
Zheng, W., Chornock, R., LeBaron, N., et al. 2024d, GCN, 38150, 1
Zheng, W., Han, X., Zhang, P., Filippenko, A. & KAIT GRB team 2024e, GCN, 37094, 1
Zheng, W., Han, X., Zhang, P., Filippenko, A. V. & KAIT GRB team 2024f, GCN, 37578, 1
Zheng, W., Han, X., Zhang, P., Filippenko, A. V. & KAIT GRB team 2024g, GCN, 37191, 1
Zheng, W., Han, X., Zhang, P., Filippenko, A. V. & KAIT GRB team 2024h, GCN, 38444, 1
Zheng, W., Han, X., Zhang, P., Filippenko, A. V. & KAIT GRB team 2024i, GCN, 36773, 1
Zheng, W., Han, X., Zhang, P., Filippenko, A. V. & KAIT GRB team 2024j, GCN, 37000, 1
Zheng, W., Han, X., Zhang, P., Filippenko, A. V. & KAIT GRB team 2024k, GCN, 38136, 1
Zheng, W., Han, X., Zhang, P., Filippenko, A. V. & KAIT GRB team 2024l, GCN, 36825, 1
Zheng, W., Han, X., Zhang, P., Filippenko, A. V. & KAIT GRB team 2024m, GCN, 36845, 1
Zheng, W., Han, X., Zhang, P., Filippenko, A. V. & KAIT GRB team 2024n, GCN, 37511, 1
Zheng, W., Han, X., Zhang, P., Filippenko, V. A. & KAIT GRB team 2024o, GCN, 37849, 1
Zhou, C., Zhao, G. Y., Mao, X., et al. 2024, GCN, 38426, 1
Zhou, H., Chen, W., Sun, H., et al. 2024a, GCN, 36691, 1
Zhou, H., Li, R.-Z., Chen, W., et al. 2024d, GCN, 38112, 1
Zhou, H., Li, R.-Z., Liu, Q. C., et al. 2024e, GCN, 38081, 1
Zhou, H., Liang, R. D., Zhu, S. F., Ling, Z. X. & Einstein Probe team 2024b, GCN, 38586, 1
Zhou, H., Wang, W. X., Hu, J. W., et al. 2024c, GCN, 36997, 1
Zhu, Z. P., Corcoran, G., Levan, A. J., et al. 2025a, GCN, 38908, 1
Zhu, Z. P., Fu, S. Y., Jiang, S. Q., et al. 2024a, GCN, 37501, 1
Zhu, Z. P., Fu, S. Y., Jiang, S. Q., et al. 2024b, GCN, 37500, 1
Zhu, Z. P., Liu, X., An, J., et al. 2024c, GCN, 37010, 1
Zhu, Z. P., Liu, X., Fu, S. Y., et al. 2025b, GCN, 38885, 1
Zhu, Z. P., Liu, X., Xu, D., Fynbo, J. P. U., & Djupvik, A. A. 2024d, GCN, 38613, 1
Zou, X., Guo, H., Chen, X., et al. 2024a, GCN, 38404, 1
Zou, X., Liu, C., Kumar, B., et al. 2025, GCN, 38914, 1
Zou, X., Liu, X., Zhang, Y., et al. 2024b, GCN, 37582, 1